Puerto Rico Distributed Energy Resource Integration Study

Achieving a Renewable, Reliable, and Resilient Distributed Grid

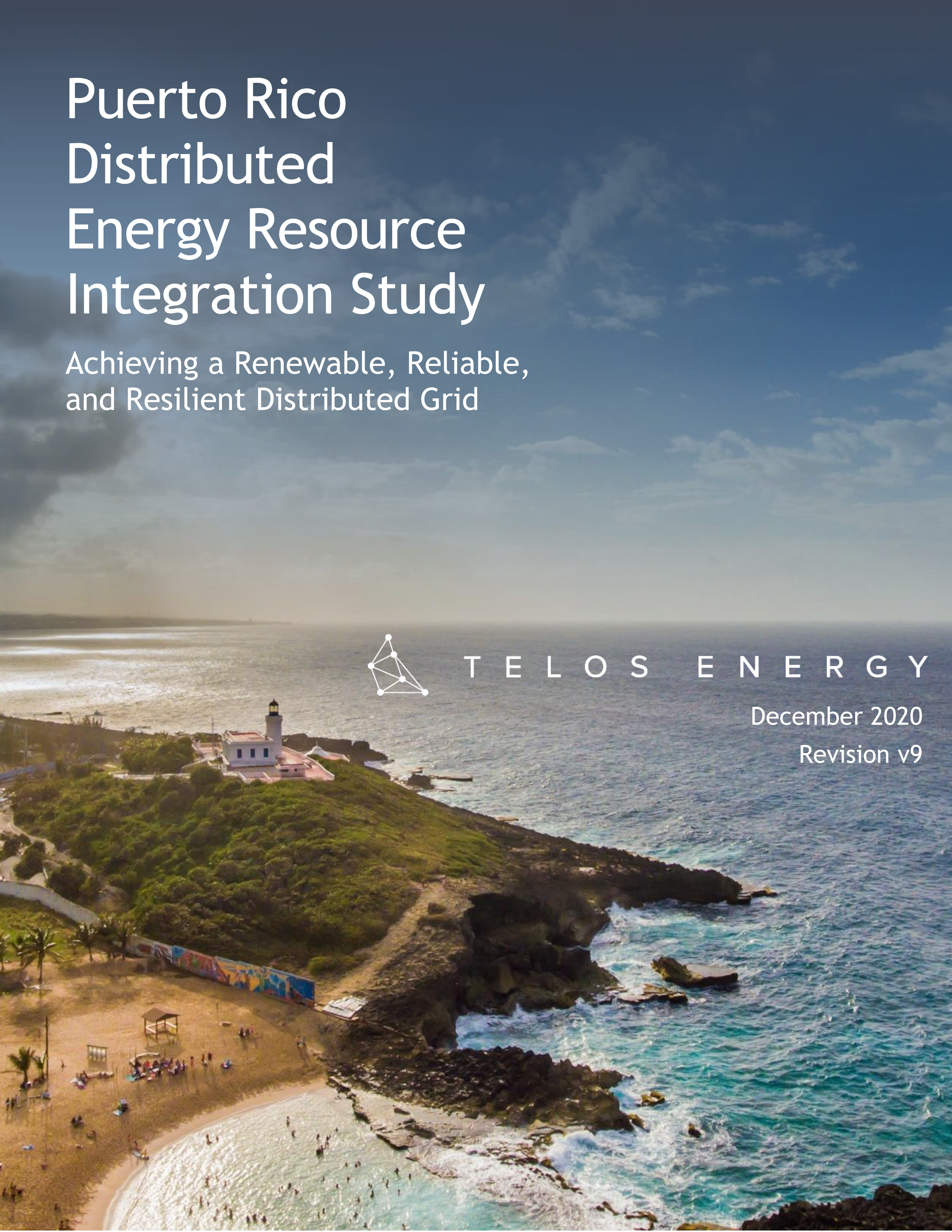

TELOS ENERGY

December 2020

Revision v9

Puerto Rico Distributed Energy Resource Integration Study

Achieving a Renewable, Reliable, and Resilient Distributed Grid

Contact Information

Derek Stenclik
Founding Partner
Telos Energy, Inc.
518-290-0032

Revision History

Revision	Date	Author	Comment
Rev01	10/1/2020	D. Stenclik	Initial draft
Rev06	10/30/2020	D. Stenclik	Initial draft submitted to CAMBIO for review
Rev07	11/30/2020	D. Stenclik	Final draft incorporated CAMBIO comments
Rev08	12/18/2020	D. Stenclik	Final draft submission
Rev09	2/23/2021	D. Stenclik	Minor adjustments
Rev10	3/2/2021	D. Stenclik	Minor adjustments
Rev11	3/4/2021	D. Stenclik	Minor adjustments

Table of Contents

`

List of Figures

`

`

List of Tables

List of Abbreviations

AC	Alternating Current
BCF	Billion Cubic Feet
BESS	Battery Energy Storage System
CC	Combined Cycle
DC	Direct Current
DER	Distributed Energy Resource
DPV	Distributed Photovoltaic
DR	Demand Response
EE	Energy Efficiency
EIA	US Energy Information Agency
EMT	Electromagnetic Transient
ES	Energy Storage
FFR	Fast Frequency Response
FO&M	Fixed Operations and Maintenance
GADS	NERC Generating Availability Data System
GIS	Geographic Information System Mapping
GT	Gas Turbine (aka Combustion Turbine)
GW	Gigawatt (1,000 megawatts)
IBR	Inverter Based Resource
IRP	Integrated Resource Plan
LNG	Liquified Natural Gas
MVA	Million Volt Amperes
MW	Megawatt (1,000 kilowatts)
NEPR	Negociado de Energía de Puerto Rico
NREL	National Renewable Energy Laboratory
NSRDB	NREL National Solar Radiation Database
OE	Oeste (West)
PREB	Puerto Rico Energy Bureau
PREPA	Puerto Rico Electric Power Authority
PSSE	Siemens Power System Simulator for Engineering tool
PV	Photovoltaic
RPS	Renewable Portfolio Standard
SAM	NREL System Advisor Model
ST	Steam Turbine
STG	Steam Turbine Generator
TC	Tap Changer
UFLS	Under-Frequency Load Shedding
VO&M	Variable Operations and Maintenance

Executive Summary

The aftermath of Hurricane Maria led PREPA to propose several new plans to rebuild the island's infrastructure and make investments to strengthen the island's power grid. In 2019, PREPA completed the Integrated Resource Plan, outlining potential new investments to meet current and future system needs. Many of these investments were large-scale, centralized fossil generation.

As an alternative to PREPA's plans, a multisectoral coalition comprised of community and labor groups, as well as environmental and energy experts presented Queremos Sol in 2018[1] as a holistic path to modernize Puerto Rico's energy sector to attain a more sustainable, resilient and equitable electric system. Queremos Sol's grid transformation is driven by: (1) efficiency, conservation and demand management; (2) distributed renewable generation with storage emphasizing roof top solar; and (3) accelerated phase-out of fossil-fuel generation. Queremos Sol seeks to achieve 25% energy efficiency and a minimum 50% renewable generation by 2035 to attain 100% renewable generation by 2050.

The objectives of this study are to provide a detailed economic and technical analysis evaluating a radically different energy mix than Puerto Rico has today as proposed by Queremos Sol. Specifically, it will utilize detailed grid planning for the following:

- Illustrate a future grid integrating with high levels of distributed energy resources, prioritizing rooftop solar and storage, following the Queremos Sol proposal,
- Evaluate a future grid designed to meet Puerto Rico's renewable, resiliency, reliability, and economic goals,
- Understand the operational, transmission, and distribution opportunities, and challenges associated with DER integration to evaluate possible mitigations to ensure stable and reliable growth of DER,
- Quantify the effects of DER integration, including changes to renewable generation, avoided fuel consumption, reduced CO_2 emissions, potential curtailment, unit cycling, and grid stability, and
- Present a possible schedule for fossil fuel generation phase out following DER integration increase.

To evaluate the changes to power system operations and grid stability with increasing DER, this analysis leveraged detailed power system simulation and modeling software. Four scenarios were selected to represent potential future power systems with increased DER. Grid configurations were evaluated with increasing installations of DER, corresponding to residential PV, commercial PV, and behind-the-meter battery energy storage, as well as corresponding fossil generator retirements.

The study levered detailed modeling and power system simulation to quantify the operational and grid stability challenges associated with high DER integration. A diagram of the modeling process is provided in the figure below.

[1] For additional details please refer to the Queremos Sol proposal (www.queremossolpr.com)

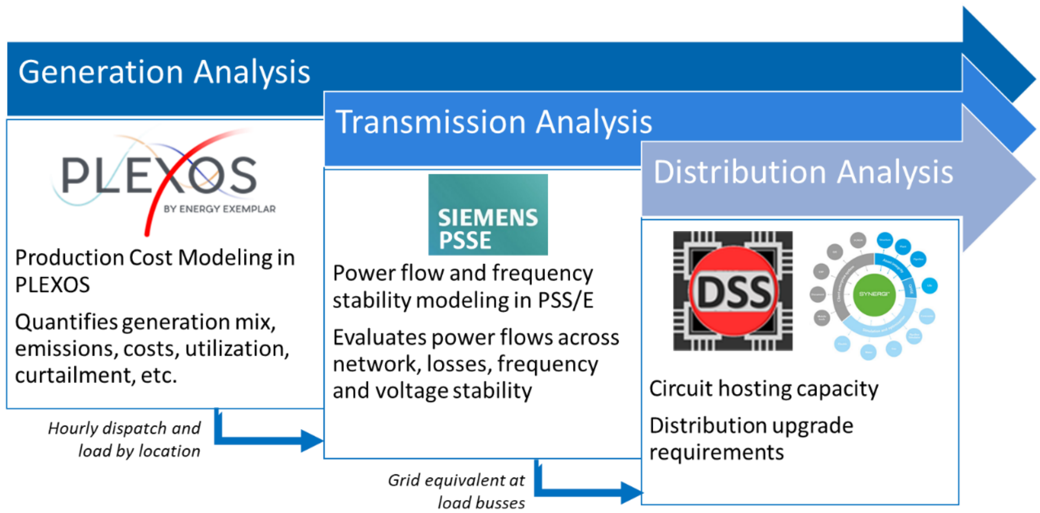

Overview of Software Tools and Methods

This study evaluated three scenarios for Puerto Rico's future electric generation mix, reaching 25%, 50%, and 75% of annual energy from renewable sources and a 25% reduction in load due to energy efficiency. These scenarios provide a pathway to meet and exceed the Queremos Sol 2035 RPS objectives and put the system on a trajectory to achieve the 100% clean energy by 2050.

The study scenarios met these renewable goals using DER exclusively. This translates to between 50% and 100% of single-family homes in Puerto Rico integrating rooftop solar. Residential systems were assumed based on installations in Puerto Rico, ranging between 1.8 kW to 4.2 kW of PV and 7.2 to 21.6 kWh of behind-the-meter battery storage. The remaining PV necessary to reach the RPS targets was assumed to be distributed across commercial and industrial customers, solar carports, and repurposed landfills or brownfields.

Assuming gross energy sales after energy efficiency of 11,700 GWh, and an annual rooftop solar capacity factors of approximately 19%$_{ac}$, these renewable targets equate to approximately 1500 MW (25% DER), 3200 MW (50% DER), and 5000 MW (75% DER) of installed distributed PV. The scenarios also included a large buildout of behind-the-meter battery energy storage, with all residential PV systems including battery storage, assuming each residential PV system was paired with, on average, 4.5 hours of storage. For example, a 2.7 kW rooftop PV system paired with a 12.6 kWh behind-the-meter battery. An overview of the renewable goals and DER capacities by scenarios is provided in the following table.

Scenario Overview

		25% DPV	50% DPV	75% DPV
Renewable Share	% of Total Sales	25%	50%	75%
Resilient Homes	% of Resilient Homes	50%	75%	100%
Distributed PV Capacity (MW)	Residential	1,350	2,025	2,700
	Commercial	143	1,212	2,282
	Total	1,493	3,237	4,982
Distributed BESS Capacity	Power Rating (MW)	1,178	1,853	2,528
	Energy Rating (MWh)	5,301	8,339	11,376
	Duration (hrs)	4.5	4.5	4.5

`

The study also outlined and evaluated a potential phase-out of fossil generation and included fossil retirements that could be achieved based on the amount of DER integration. To determine the sequence of fossil-fired unit retirement for each scenario, a weighted a combination of seven factors was developed, which included: age, emissions, flexibility, dependence on long-distance transmission (south to north), fixed operations and maintenance costs, generation costs (fuel costs, variable costs, etc.), and reliability (forced outage rates). The result included 2,300 MW of fossil generator retirements and included the AES coal plant, Palo Seco Power Plant, and the Aguirre Power Plant. By replacing legacy coal and oil-fired steam generating units with state of the art solar and battery energy storage systems, Puerto Rico's grid would become cleaner, more flexible, and more reliable.

The combination of solar PV, battery additions, and fossil generator retirements creates a resource mix that is fundamentally different than the one Puerto Rico has today and would take time to develop. For the purposes of long-term planning, the transition is spread across a 20-year horizon as shown in the figure below. On an installed capacity basis, solar and storage (inverter based resources) become the largest form of capacity by the 50% DER scenario and total installed capacity in Puerto Rico increases to over 10 GW by the 75% DER scenario, nearly double today's capacity despite increased energy efficiency.

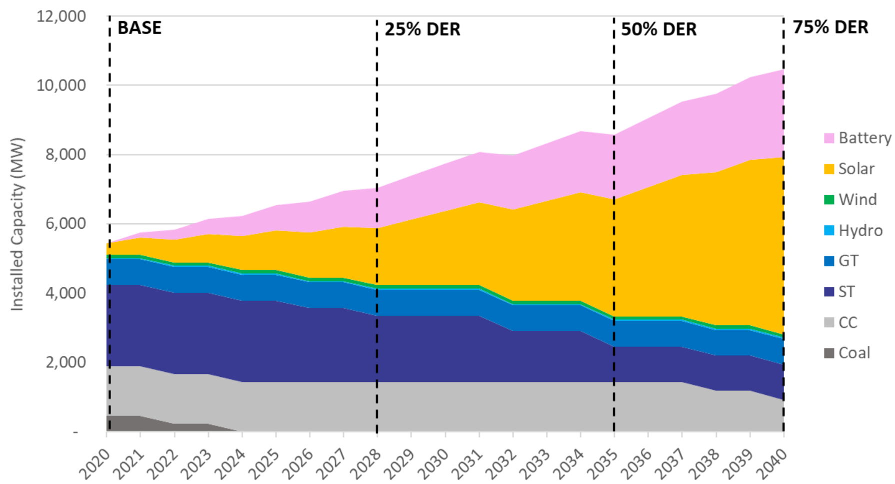

Installed Capacity by Resource Type

For this analysis, 96 solar sites were selected across Puerto Rico to represent the distributed rooftop PV. Sites were concentrated in developed areas where residential and commercial PV systems would be most prevalent. Twelve sites were selected in each of the eight regions of the island, where the installed capacity was weighted based on the density of urban development and existing transmission and distribution infrastructure. In general, capacity factors are highest along the coast and at lower elevations away from the mountainous interior.

For each of the 96 sites identified, a full year of chronological, 5-minute resolution weather data was downloaded from the NREL Puerto Rico Simulated High Resolution Dataset and converted into power production profiles. This generated over 10 million data points of chronological solar data that were modeled for the study to ensure adequate geographic diversity and granular chronology of variability. The data was then aggregated for each region by averaging the twelve sites into a single composite regional profile for use in the production cost modeling.

`

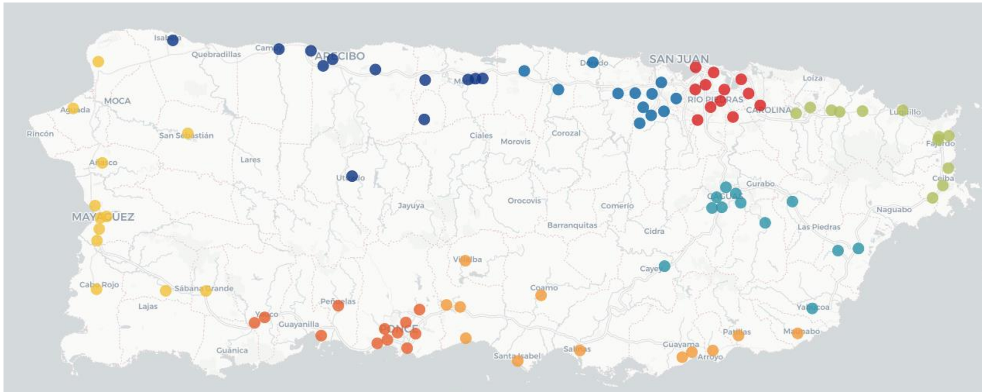

Map of Simulated Solar Locations Across Puerto Rico
(colored by region)

Results of the analysis show that grid operations change markedly as the system moves towards a higher penetration of DER. Figure 15 highlights how annual generation by unit type changes over the four scenarios studied. As solar generation increases, it displaces fossil fuels on the grid. The types and amount of fossil fuel displacement depends on the costs, flexibility, and physical characteristics of each generating unit. The retirement of AES in all but the Base Case stands out with the coal unit type denoted by a dark gray. The immediate result of a system without AES and a 25% integration of DER is an increased role for existing combined cycle (CC) plants. The 25% DER case shows much of the generation once provided by AES is instead produced by existing combined cycle plants, which operate on either LNG or oil fuels.

As the penetration of DER increases in the 50% and 75% DER cases, solar takes on a much larger role and begins to displace steam turbine (ST) units and later CC units. While simple-cycle gas turbines (GT), also referred to as "peakers," generate a relatively low amount of generation in the base case, their role in total generation is reduced further in the 50% and 75% scenarios as battery energy storage effectively reduces peak loads. The figures below show the annual generation mix (top) and representative daily generation profile (bottom) across each of the scenarios evaluated.

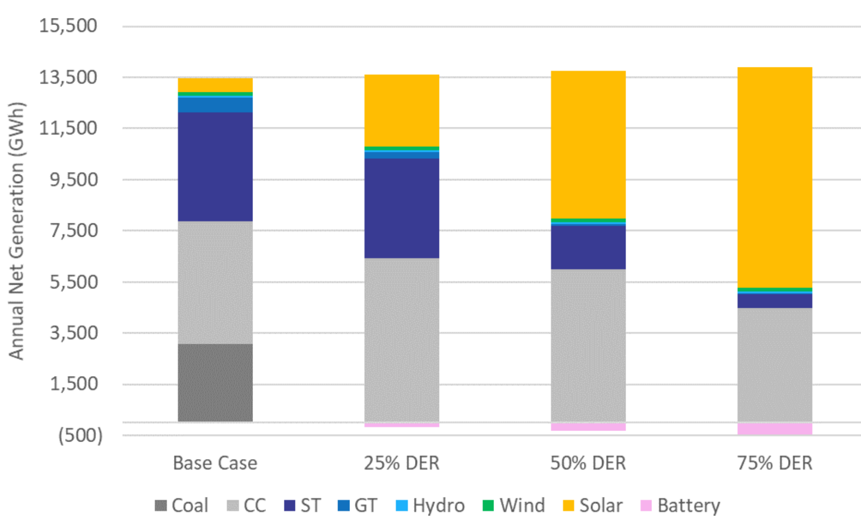

Annual Net Generation by Unit Type

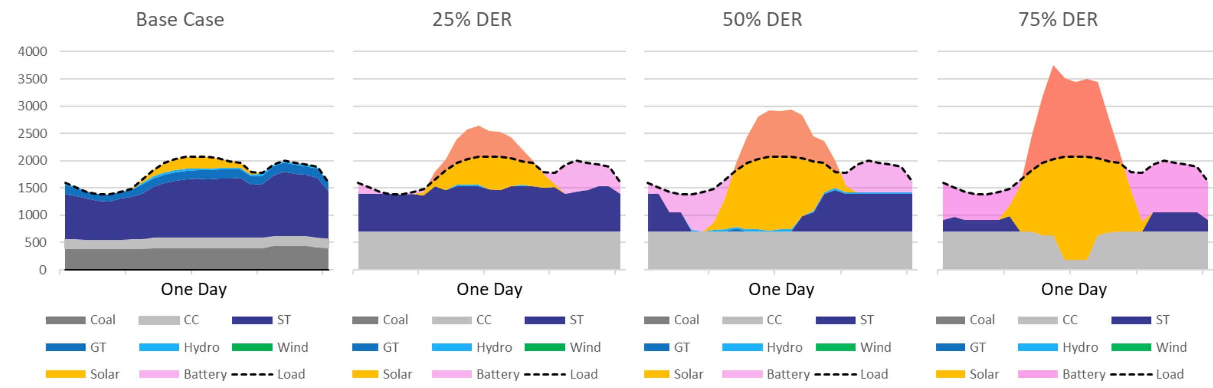

Dispatch Diagrams for a "Normal" Day

The study also quantified changes of power flows across the transmission network, provided in the figure below. Positive numbers represent net exports and negative numbers represent net imports. In the Base Case, both Ponce ES and Ponce OE are the only net exporters among the eight regions. The overarching trend from the Base Case to the 75% DER case is that net flows decrease as each individual region becomes more self-sufficient with the increase in DER as generation is sited directly at the point of consumption. The reduced flows across the network has several benefits, including reduced transmission losses and increased reliability because the system becomes less susceptible of transmission outages, failures, and storm related damage.

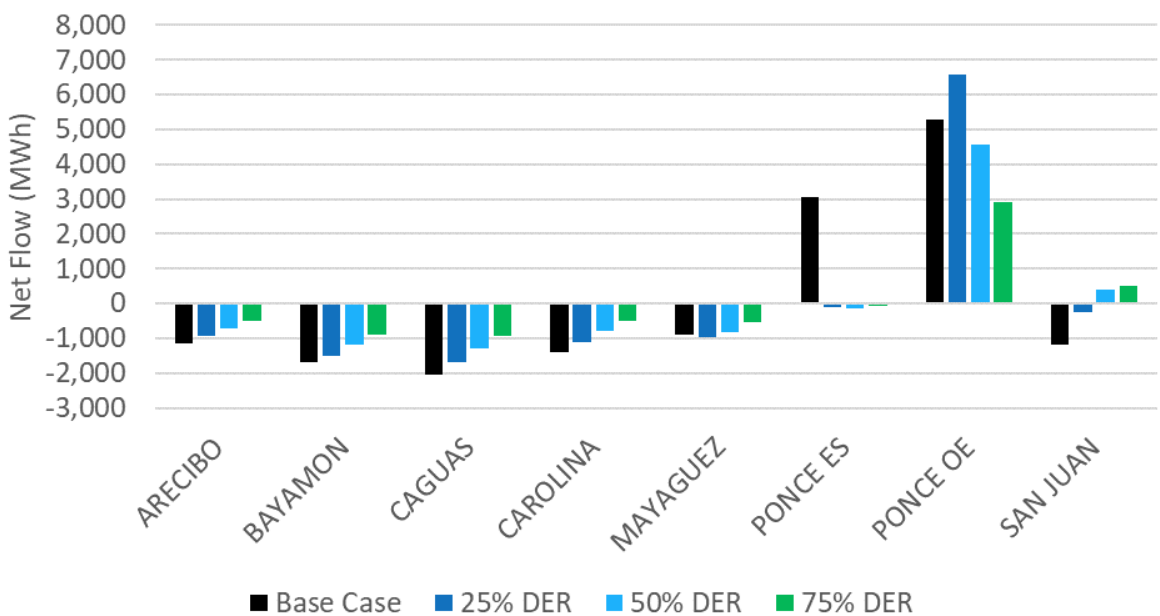

Annual Net Flows by Regions

The study also evaluated the instantaneous operation of these resources across the entire year. This is important because both solar and batteries (as well as wind) resources are inverter-based resources (IBR). IBRs connect to the grid through a power electronic interface, called an inverter, whose software-defined controls determine the behavior, performance, and stability of these resources on the grid. As

IBRs take on a larger role in the grid, there will be operational and grid stability challenges given inherent limitations of current inverter technology. It is important to note that because solar and wind resources are variable, there are hours of the course of a year when IBRs will dominate the behavior of the grid by reaching very high levels of penetration (as a percentage of the grid's total resource mix) even if their annual generation levels are relatively modest.

In the scenarios evaluated, there are times when inverter-based generation exceed 50% of instantaneous load even in the 25% DER scenario, and periods reaching 100% instantaneous penetration in the 50% and 75% DER scenarios. These periods require close attention and detailed grid stability evaluations the electric power industry has little to no experience with inverter-dominant island grids at the scale of Puerto Rico's grid.

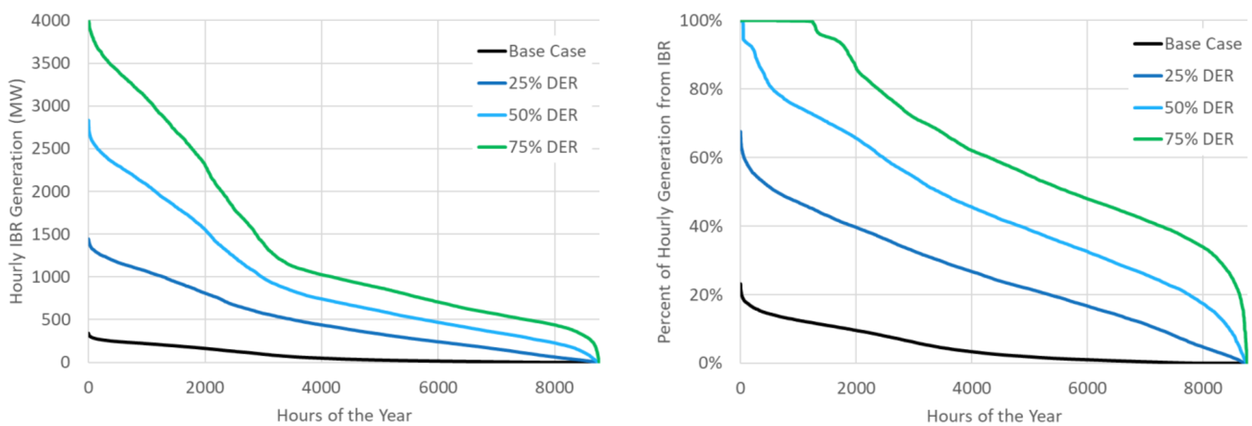

Duration Curves of IBR Generation (left) and Percent of Total Generation (right)

All electric power grids must be analyzed to ensure stable operation under a large variety of operating conditions, environments, and grid disturbance events. This is true regardless of the level of renewables on the grid. However, grids with very high levels of renewables face more acute technical challenges because of the high-levels of IBR like PV and battery systems and the displacement of conventional power plants with synchronous machine technology. However, these new resources also offer new benefits for supporting the grid in ways that were not previously available with conventional power plant technology.

These benefits are primarily due to the flexibility and speed of the inverters that form the interface between the resource (solar or battery) and the grid. The flexibility is because of a programmable response of inverters to different grid conditions and grid events. The speed refers to the faster rate at which IBRs are capable of responding to changing grid conditions. While a fast or faster response is not always desirable, it can be useful in certain circumstances. These advantages, coupled with an energy reservoir as in the case of battery storage, makes for a powerful combination (as shown through simulated response of the grid to challenging events) that can help support a future grid with a dramatically different generation mix than the one that exists today.

To assess the stability of the grid under the proposed high-renewable scenarios, the frequency stability, fault recovery, and inverter control stability were evaluated by simulating the response of the grid to disruptive events or grid disturbances.

- **Frequency Stability:** Grid frequency is held close to 60Hz by maintaining a balance between generation and load. If generation exceeds load (for instance, due to a sudden loss of load), then grid frequency rises and generation must be reduced to bring frequency back to nominal. If generation drops below load (for instance, due to a sudden loss of generation), then grid frequency decreases and additional power must be injected to the grid, or load must be reduced or shed, in order to restore grid frequency.
- **Fault Recovery:** The ability of the grid to recover from a fault event, or a short-circuit on the grid is termed fault recovery. Grid faults may be causes by obstructions like trees falling on transmission lines, lightning strikes of lines or towers, the collapse of transmission towers, etc. When such a fault occurs, the grid is designed to quickly remove the faulted transmission line from service, thereby “clearing” the fault from the grid. The desired intent is that the grid continues to operate without the line in-service until a crew can be dispatched to repair the line.
- **Inverter control stability**: refers generally to the behavior of an inverter to respond in a stable manner to grid events like the loss-of-generation events and fault events described. Examples of unstable behavior includes oscillatory behavior to a failure to ride-through and recover from the disturbance without causing voltages or currents that are damaging to the inverter or other equipment. While oscillatory behavior may be acceptable for brief periods of time (well-damped behavior), sustained or growing oscillations are not acceptable.

The grid stability simulations capture the dynamic response of the grid over the course of 10 to 20 seconds following a grid event like a loss of generation or a fault event. Because it is impractical to simulate the dynamic response of the grid over the course of an entire year, as was evaluated in the production cost analysis, a selection of “snapshots” in time from each of the scenarios was selected for simulation of dynamic grid stability. The selection of these “snapshots” is very important as they must be chosen to be representative of a range of grid operations and not “cherry-picked” as worst-case or best-case operations, which would skew the conclusions drawn from the results.

Results of these simulations show that as IBRs increase on the grid and conventional generation is displaced, the grid spends more time operating in periods of low system inertia. If no mitigations were applied, it would be expected that blackouts would occur more frequently for loss of generation events. However, if FFR (note this is only one of many types of mitigation) is applied, it can not only enable the grid to survive loss-of-generation events, but also reduce or eliminate the need for load shedding. It is important to note that correctly applying FFR is not trivial. If the FFR is tuned to be too slow, it will not be effective and the grid may fail to survive the event. However, if the FFR is tuned to be too fast, it may over-react and/or result in oscillatory behavior and participate in adverse interactions with other grid equipment, destabilizing the grid and ultimately leading to a failure to survive the event. However, it must be noted that for extremely low levels of inertia, FFR loses its efficacy.

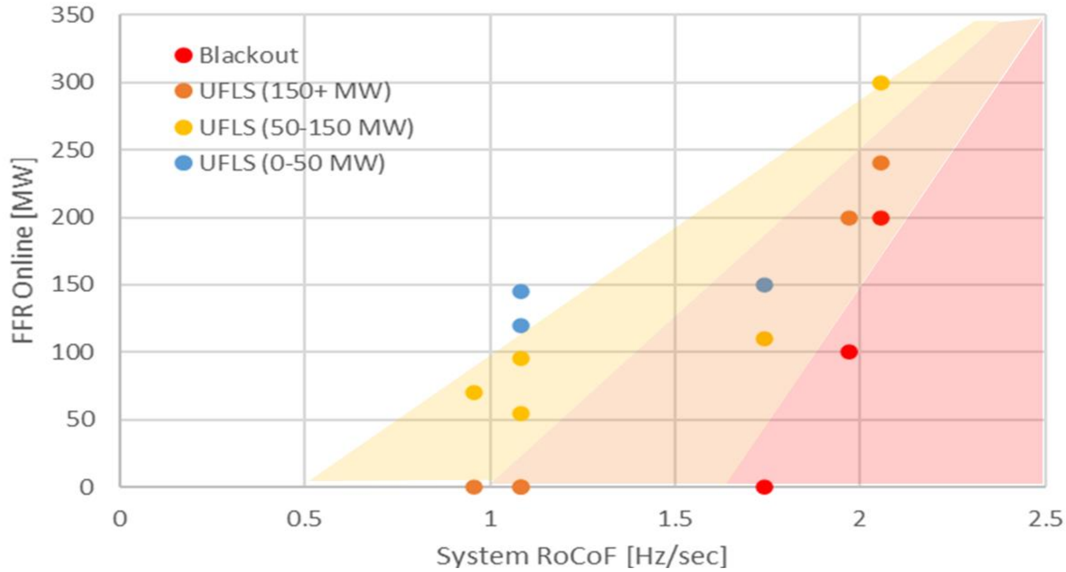

Summary and Trends Identified from Loss-of-Generation Events

In addition, the grid stability simulations show the evolution of DER controls and the resulting improvement in performance of the grid in response to transmission fault events. Beginning with basic implementation of "smart-inverter" functions and ending with tuned smart-inverter functions and reasonably expanded inverter protection settings, the performance of the grid can be greatly improved. The results are simplified and summarized in the following figures, which are color-coded as follows: green cells for in cases where performance is considered good, similar to that shown in the current scenario, orange is used for marginal performance where the grid survives but with some loss of DER and/or loss of load. Red is used for cases in which the system does not survive the fault event. Brown is used for cases in which there is evidence that the simulation tool is not capable of accurately simulating the event.

Line | Scenario	Current	25%	50%	75%
Costa Sur-Manati 230kV				
Costa Sur-Mayaguez 230kV				
Costa Sur-Dbocas Fase 230kV				
Aguirre-Agubuena 230kV				
Cayey-Caguas 115kV				
Guanica-San German 115kV				

Performance Summary for Grid Faults with Basic DER Functionality

Line | Scenario	Current	25%	50%	75%
Costa Sur-Manati 230kV				
Costa Sur-Mayaguez 230kV				
Costa Sur-Dbocas Fase 230kV				
Aguirre-Agubuena 230kV				
Cayey-Caguas 115kV				
Guanica-San German 115kV				

Performance Summary for Grid Faults with FFR and Improved Volt-Var DER Functionality

Line | Scenario	Current	25%	50%	75%
Costa Sur-Manati 230kV				
Costa Sur-Mayaguez 230kV				
Costa Sur-Dbocas Fase 230kV				
Aguirre-Agubuena 230kV				
Cayey-Caguas 115kV				
Guanica-San German 115kV				

Performance Summary for Grid Faults with FFR and Improved Volt-Var and Expanded Over-Voltage Protection from DER

The results of this study are significant and clearly illustrate that Puerto Rico can radically shift its power system to one that is based on local, renewable, and resilient distributed energy resources. This can be done in a way that improves system reliability, grid stability, and resiliency for Puerto Rico's ratepayers. This transition will yield environmental benefits with reduced CO_2 emissions and other environmental pollutants and will considerably decrease fossil fuel consumption in Puerto Rico. This will make the power system and the economy less susceptible to the fuel price volatility of oil markets and more energy independent. In addition, the study results produced the following key findings:

- DER can be used as a tool to accelerate the retirement of Puerto Rico's aging fossil fleet replacing that capacity with more flexible, clean, and resilient technology. The AES coal plant, for example, could be retired by 2024 with investment in DERs and energy efficiency.
- Increased flexibility will be required of the fossil fleet, especially for the CC units, which will be expected to cycle on and offline more often and run for fewer hours per year. This may change the maintenance requirements, cycling costs, and reliability of these generators in the future.
- Renewable curtailment is quite low across all scenarios and is highest (on a relative basis) in the Base Case before any storage is added. Total renewable energy perspective, curtailment is limited to 1% even in the highest DER scenarios.
- Oil and gas fuels both experience more than a 50% decline in consumption by the 75% DER scenario. As a result, Puerto Rico would be less susceptible to fuel price volatility and would become more energy independent with increased DER adoption. This reduction in fuel consumption also translates to a more than 70% reduction (over 6 million tons) in carbon dioxide emissions by the 75% DER case.

`

- The production cost savings (not accounting for capital cost of new resources) from introducing more DER onto the grid while also retiring fossil fuel-based generation are considerable, with savings range anywhere from roughly $144 million (25% DER) to $703 million per year (75% DER). This equates to an avoided energy cost of $64 to $86/MWh of additional solar energy.
- Another benefit of DER integration is that the resources are sited directly at the loads, reducing the total amount of energy that flows across the transmission network. This yields reliability, resiliency, and avoided transmission loss benefits. Across the scenarios analyzed, DER reduced net flows across the network as each individual region becomes more self-sufficient with the increase in DERs located within that respective region.
- In the 50% DER and 75% DER case there are hours with 100% of generation coming from IBR, even after using storage to shift much of the surplus generation. With current inverter technologies and the absence of synchronous condensers, this level of operation would not be reliable, but changes to operations can be made to ensure reliability if those mitigations are not available.

DER inverter controls for grid-response is critical to achieving stable grid operation up through the 50% scenario. The use of DER inverter functions like frequency-watt response (FFR) and volt-var response that are tuned for fast-response are effective in stabilizing the grid for significant disturbances. About 300MW of FFR is needed to enable the grid to survive generation-loss events through the 50% scenario.

1 Introduction

1.1 Study Objectives

Puerto Rico's power system is at a pivotal transition point. Hurricane Maria, which hit Puerto Rico in September of 2017, created catastrophic damage across the island including much of the power grid. Many regions and residents were left without power for months. In addition, the aging infrastructure of the Puerto Rico power grid and financial stress of the island's utility and grid operator Puerto Rico Electric Power Authority (PREPA), have severely eroded system reliability.

These events have led PREPA to propose several new plans to rebuild the island's infrastructure and make investments to strengthen the island's power grid. In 2019, PREPA completed the Integrated Resource Plan, outlining potential new investments to meet current and future system needs. Many of these investments were large-scale, centralized fossil generation.

As an alternative to PREPA's plans, a multisectoral coalition conformed of community and labor groups, as well as environmental and energy experts presented Queremos Sol in 2018[2] as a holistic path to modernize Puerto Rico's energy sector to attain a more sustainable, resilient and equitable electric system. Queremos Sol's grid transformation is driven by: (1) efficiency, conservation and demand management; (2) distributed renewable generation with storage emphasizing roof top solar; and (3) accelerated phase-out of fossil-fuel generation. Queremos Sol seeks to achieve 25% energy efficiency and a minimum 50% renewable generation by 2035 to attain 100% renewable generation by 2050.

Concurrent to these events two significant shifts have taken place in Puerto Rico's energy sector. First, there has been a prioritization of residents towards resiliency, with many residents investing in behind-the-meter backup generation. Second, the economics of distributed generation - specifically solar photovoltaic (PV) and battery energy storage systems (BESS) - have become increasingly favorable. As a result, distributed energy resource (DER) adoption across Puerto Rico has increased significantly and growth is expected to continue as long as the regulatory structure and power grid allows for it.

The objectives of this study are to provide a detailed economic and technical analysis evaluating a radically different energy mix than Puerto Rico has today as proposed by Queremos Sol. Specifically, it will utilize detailed grid planning for the following:

- Illustrate a future grid integrating with high levels of distributed energy resources, prioritizing rooftop solar and storage, following the Queremos Sol proposal,
- Evaluate a future grid designed to meet Puerto Rico's renewable, resiliency, reliability, and economic goals,
- Understand the operational, transmission, and distribution opportunities and challenges associated with DER integration and possible mitigations to ensure reliable growth of DER,
- Quantify the effects of DER integration, including changes to renewable generation, avoided fuel consumption, reduced CO_2 emissions, potential curtailment, unit cycling, and grid stability.
- Present a possible schedule for fossil fuel generation phase out following DER integration increase.

[2] For additional details please refer to the Queremos Sol proposal (www.queremossolpr.com)

The results of this study will quantify the effects of high DER integration, with solar energy becoming the primary source of electricity across Puerto Rico and integration of battery storage to meet reliability and resiliency needs.

The results will also provide an alternative future scenario for Puerto Rico that puts the island on a path towards 100% renewable energy. While a 100% renewable energy system is the Queremos Sol end goal, this study is meant to provide a roadmap to higher renewable energy and thus focus attention on intermediate renewable goals of 25%, 50% and 75% of annual sales. This is intended to convince key stakeholders – including PREPA engineers and executive management, the Puerto Rico Energy Bureau (PREB), US Department of Energy (DOE), among others - that a high solar future can be operated with a high degree of reliability and grid stability. At the same time the study will contribute to Queremos Sol's continued effort for public engagement and capacity building regarding a more sustainable and equitable energy sector transformation.

1.2 Data Collection

Information and data used for the study were provided by PREPA during the month of April 2020. (Please refer to Section 3 for more detailed information on data input). Furthermore, as part of the development of the model two virtual sessions were held with PREPA personnel to clarify information and calibrate progress.

Although data used was provided by PREPA the model has been independently developed by Telos on behalf of CAMBIO PR and in no way represents any proposal, projection or representation of the Puerto Rico Electric Power Authority.

1.3 Queremos Sol Feedback

During the course of the study's model and scenario development, two meetings were conducted with the Queremos Sol group. These meetings covered the objectives, methodologies, and preliminary results of the study in order to solicit feedback from the group on the methodology and assumptions used in the study so that the scenarios reflected the goals and objectives of the Queremos Sol group. This feedback was instrumental in determining the amount of PV and battery storage assumed in each scenario, the timing and prioritization of assumed fossil retirements, assumptions related to new unit installations and energy efficiency targets.

1.4 Methodology & Process

To evaluate the changes to power system operations and grid stability with increasing DER, this analysis leveraged detailed power system simulation and modeling software. Four scenarios were selected, identified in Section 2, to represent potential future power systems with increased DER. Grid configurations were evaluated with increasing installations of DER, corresponding to residential PV, commercial PV, and behind-the-meter battery energy storage, as well as corresponding fossil generator retirements. All other assumptions were held constant across the scenarios to isolate the effects of the additional DER.

The software tools used in this analysis are available from third-party software vendors, heavily used throughout the industry, and are the same ones leveraged by PREPA and other global utilities. These grid planning tools allow for an evaluation and simulation of a future power system using the same methods and processes used to operate and control today's grid to isolate the effects of integrating DER, new technology, and operational changes.

When it comes to power system modeling, no one tool can provide a comprehensive analysis across the generation, transmission, and distribution segments of utility planning. In addition, no one tool can properly evaluate all the timescales of planning, which range from sub-seconds to an entire year, or years, of operation. To overcome this limitation, this study leveraged multiple power system planning tools with tight coupling between the different stages. This allows for each tool to properly evaluate its domain, while linking inputs, assumptions, and outputs between the tools to ensure the study overcomes seams in the analysis typically found between the generation, transmission, and distribution analyses.

- **Generation Analysis**: utilized Energy Exemplar's PLEXOS production cost model to quantify hour-to-hour, and sub-hourly operation of the grid to match load and generation in a least cost manner. The outputs of this model provide generator dispatch levels and load allocation by location for subsequent transmission modeling.
- **Transmission Stability Analysis**: utilized Siemens' PSS/E power flow modeling software to evaluate dynamic stability on the transmission network (from 38kV to 230kV voltage levels), including frequency and voltage stability. The transmission model was also used to calculate the grid representation (Thevenin equivalent) at each load bus for subsequent distribution system modeling.
- **Distribution Analysis**: utilized EPRI's OpenDSS distribution tool (and validated output against DNVGL's Synergi model) to identify circuit hosting capacity and necessary distribution upgrades due to DER integration.

A diagram illustrating the linkages between the software tool can be found in Figure 1. While this diagram illustrates a unidirectional flow of information, there was also information passed in the reverse direction. For example, after the transmission analysis evaluated dynamic stability, it identified a potential mitigation to frequency instability (due to low synchronous inertia) and thus developed a new constraint that could be input into the generation analysis to ensure grid stability in commitment and dispatch decisions.

Note that the analysis presented in this report, and conducted by Telos Energy, is limited to the generation and transmission analysis. This work was coordinated with the distribution analysis, the results of which can be found in the report authored by EE+.

`

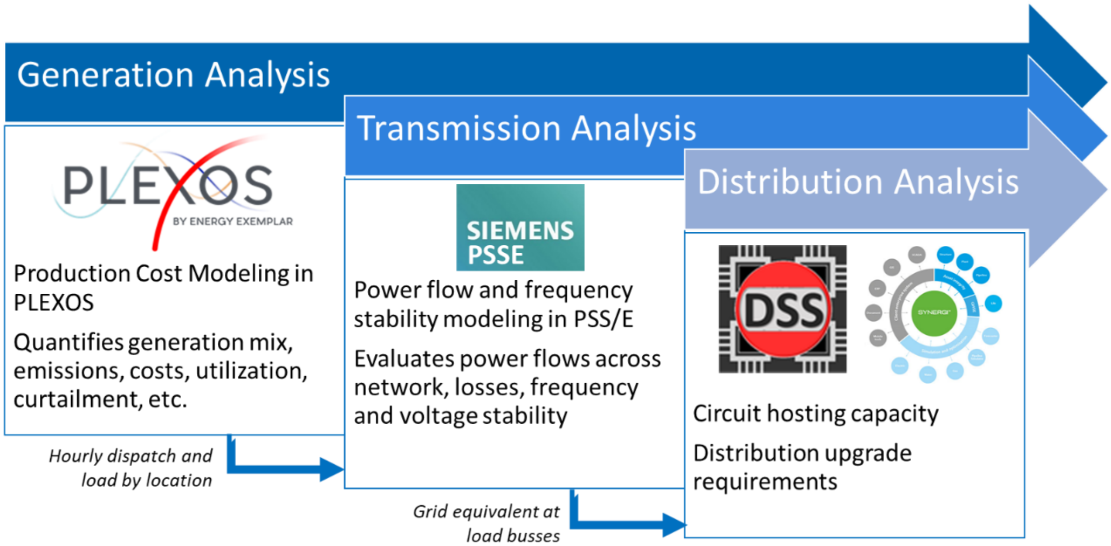

Figure 1: Overview of Software Tools and Methods

1.5 Study Limitations

The forward projections provided in this report are based on fundamentals analysis. While the authors took great care to ensure accurate and robust modeling, any forecast has uncertainty. As such, there are several limitations that should be identified, including:

- The model's representation of the grid's supply and demand is exogenously determined and is an input into the model. The starting point demand was assumed based on PREPA's 2020 forecasted energy load, reduced by the Queremos Sol 25% energy efficiency goal. The supply was based on PREPA's current installed generating fleet, with increasing additions of DER to evaluate the effects of increased solar adoption. The modeling did not evaluate an optimal least-cost capacity expansion and retirement plan, but rather evaluated grid operations and reliability across specific scenarios with costs and benefits calculated as a result of the study.
- DER was integrated with some level of coordination and control. This would allow the system operator to take into account expected generation from DER resources to commit and dispatch the system and schedule battery energy storage, at least in part, based on system needs. This study was a system-level analysis and did not evaluate the use of behind-the-meter solar and battery energy storage optimized for individual use.
- Distributed battery storage in this analysis is able to provide grid spinning reserve requirements through an aggregator that coordinates the output of many DER assets to provide controllable grid services. If this is not technically achievable in the short-term due to technology limitations of broad communications and coordination challenges, there may be a need for increased spinning reserves, which were not evaluated for this study.
- Because the residential solar PV was integrated as hybrid systems with coupled battery energy storage, this study also did not include an increase in reserves, above current requirements, due to either the variability or uncertainty of solar resources. The study used the reasonable assumption that the solar and battery resources could "self-regulate" and manage net-to-grid variability via ramp rate limits or other inverter controls.

- The grid stability analysis used fundamental-frequency positive-sequence simulation tools that represent a balanced system. Unbalance and asymmetric faults were not analyzed for dynamic stability.
- Each inverter is different, and the specific control loops used can make a difference on system stability. Without knowing the specific inverters that will be deployed in the future, this study made reasonable assumptions on their likely grid-interactive behavior. The dynamic models of the DER were represented with generic models, which are widely used as a best practice, but also do not capture all of the nuances of response present in real equipment. This limitation becomes more pronounced as the power rating of DER represented on the grid rises with respect to the online MVA rating of synchronous machines, particularly in the 75% penetration scenario.
- The dynamic stability model included representation of “grid-following” distributed inverter technology, which is widely in use as of this publication. This analysis does not contain representation of “grid-forming” inverter technology, a promising but not yet commercially available technology, but which may provide benefits to operating island power systems with few to no synchronous machines online.

2 Study Scenarios

2.1 Evaluating a Future Puerto Rico Energy Mix

Currently Puerto Rico generates less than 3% of its annual electricity from renewable sources, about half of which is from variable renewables like wind and solar. In October 2018, Queremos Sol – multisector clean energy and solar power advocacy group - released a report titled, "Queremos Sol: Sostenible, Local, Limpio."[3] In the report, Queremos Sol set an ambitious goal to achieve a Renewable Portfolio Standard (RPS) of 50% by 2035 and 100% by 2050, and an Energy Efficiency and Conservation Policy Objective of 25% by 2035. In addition, it advocated for a clear public policy for the following:

- Efficiency, conservation, and demand management.
- Renewable distributed generation with storage, prioritizing rooftop solar.
- Accelerated phase-out of fossil fuels.

Underpinning all of these goals is the importance of reliability and resilience. When Hurricane Maria hit the island in 2017 it took several months for complete restoration of power. The blackout represents the largest grid reliability event in US history, with 3.4 billion lost customer hours.[4] Since that time, there have been multiple recent island wide blackout events due to earthquakes, storms, and generator failures. This has made reliability and resilience a new priority in Puerto Rico, with most electricity users investing in backup generation. In addition, many of the new rooftop PV systems installed across the island include battery storage for reliability purposes.

In addition to the renewable policy objectives of Queremos Sol and the reliability needs of the system, there is also clear economic justification for distributed energy resources. According to the EIA, residential and commercial electricity rates in Puerto Rico in 2019 were above 23 cents/kWh, double the US average.[5] This provides strong economic incentives for the adoption of rooftop PV and other distributed energy resources.

2.2 Solar and Storage Additions

Based on the drivers identified in the previous section, this study evaluated three scenarios for Puerto Rico's future electric generation mix, reaching 25%, 50%, and 75% of annual energy from renewable sources and a 25% reduction in load due to energy efficiency. These scenarios provide a pathway to meet and exceed the Queremos Sol 2035 RPS objectives and put the system on a trajectory to achieve the 100% clean energy by 2050. The study also includes a fourth reference case that represents the system as it is today, with estimate of current levels of distributed rooftop PV and utility-scale solar, which was also included in the other scenarios. These four scenarios are referred to as the Base Case, 25% DER, 50% DER, and 75% throughout this report.

The study scenarios met these renewable goals using DER exclusively. This translates to between 50% and 100% of single-family homes in Puerto Rico integrating rooftop solar. Residential systems were assumed based on installations in Puerto Rico, ranging between 1.8 kW to 4.2 kW of PV and 7.2 to 21.6

[3] Queremos Sol, https://www.queremossolpr.com/
[4] Rhodium Group, "The World's Second Largest Blackout," https://rhg.com/research/puerto-rico-hurricane-maria-worlds-second-largest-blackout/, April 2018.
[5] U.S. Energy Information Agency, "Puerto Rico Territory Energy Profile," Last Update: March 2020.

kWh of behind-the-meter battery storage. The remaining PV necessary to reach the RPS targets was assumed to be distributed across commercial and industrial customers, solar carports, and repurposed landfills or brownfields.

Assuming gross energy sales after energy efficiency of 11,700 GWh, and an annual rooftop solar capacity factors of approximately 19%$_{ac}$,[6] these renewable targets equate to approximately 1500 MW (25% DER), 3200 MW (50% DER), and 5000 MW (75% DER) of installed distributed PV. The scenarios also included a large buildout of behind-the-meter battery energy storage, with all residential PV systems including battery storage, assuming each residential PV system was paired with, on average, 4.5 hours of storage. For example, a 2.7 kW rooftop PV system paired with a 12.6 kWh behind-the-meter battery. An overview of the renewable goals and DER capacities by scenarios is provided in Table 1 and Figure 2. Detailed assumptions on the calculations used to develop these values is provided in the Appendix, Table 17.

Table 1: Scenario Overview

		25% DPV	50% DPV	75% DPV
Renewable Share	% of Total Sales	25%	50%	75%
Resilient Homes	% of Resilient Homes	50%	75%	100%
Distributed PV Capacity (MW)*	Residential	1,350	2,025	2,700
	Commercial	143	1,212	2,282
	Total	1,493	3,237	4,982
Distributed BESS Capacity	Power Rating (MW)	1,178	1,853	2,528
	Energy Rating (MWh)	5,301	8,339	11,376
	Duration (hrs)	4.5	4.5	4.5

*Includes existing distributed PV

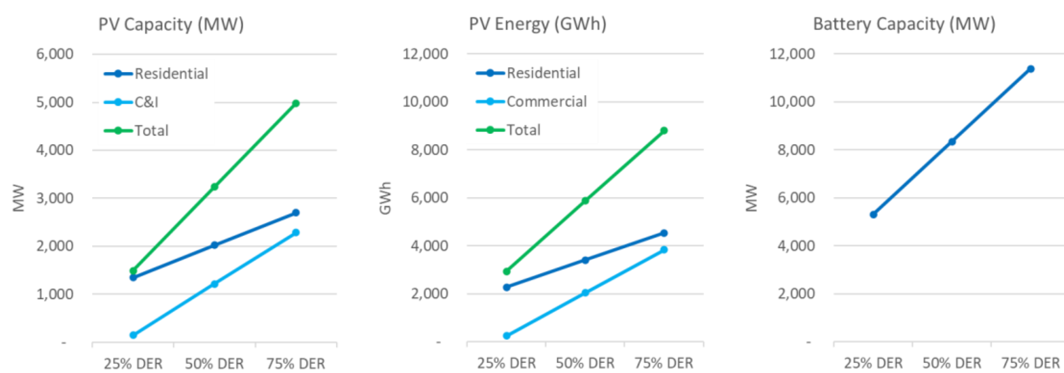

Figure 2: PV Capacity, PV Energy, and Battery Capacity by Scenario

[6] Annual capacity factors based on the National Renewable Energy Laboratory's National Solar Radiation Database (NREL NSRDB) and Puerto Rico specific locations. See Section 4.1 for more information.

2.3 Generator Retirements

The integration of solar PV and battery energy storage provides a path to initiate the retirement of Puerto Rico's fossil generation fleet. The fossil fleet is aging, with an average age of 41 years and some units exceeding 60 years of operations. This leads to high likelihood of generator failures, with an assumed weighted forced outage rate of 14.2% across the fleet, and low flexibility. The fixed operations and maintenance (FO&M) costs of keeping these systems in place is also high, with a weighted average FO&M of $32.73/kW-yr. This is significantly higher than the FO&M cost of new gas turbine or combined cycle technologies (~$11-13/kW-yr).[7] As a result, the scenarios also evaluated fossil retirements that could be achieved based on the amount of DER integration.

All generators included in the PREPA 2019 Plan Integrado de Recursos (IRP 2019)[8] were modeled and included for the purposes of this study unless otherwise specified in each scenario based on assumed retirements discussed in this section. Units specifically not included in the IRP due to maintenance or emission issues are excluded from this analysis and all scenarios.

To determine the order of retirement of fossil fired units, for all scenarios, weighted a combination of seven factors was developed, which included: Age, Emissions, Flexibility, Dependence on long-distance transmission (South to North), Fixed Operations and Maintenance Costs, Generation Costs (fuel costs, variable costs, etc.), and Reliability (forced outage rates). These factors, shown in Figure 3 were weighted based on the likelihood to help integrate additional renewable energy.

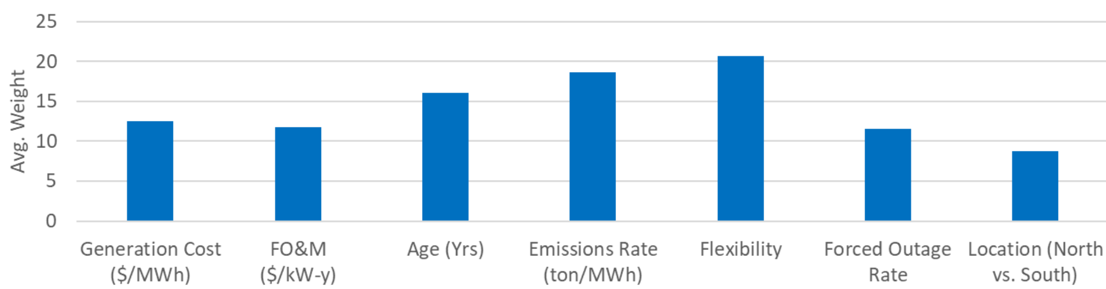

Figure 3: Retirement Analysis Weighting Factors

To determine the amount of retirements in each scenario, a screening resource adequacy analysis was conducted by randomly drawing sixty random outages for each generator and calculating the expected unserved energy. After solar and storage resources were added to each scenario, capacity was removed from the model based on the retirement order determined above until the Base Case reliability level (after accounting for reduced load from energy efficiency) was achieved. It should be noted that this was a screening analysis only and should not replace the required reliability analysis necessary to make retirement decisions.

However, the approach taken was conservative. It did not assume growth in PREPA's demand response program to 250 MW as required by PREB Order Number NEPR-AP-2020-0001. Based on this analysis, a retirement schedule was developed for each scenario and is shown in Table 2. By the 75% DER scenario,

---

[7] National Renewable Energy Laboratory, 2020 Annual Technology Baseline, https://atb.nrel.gov/.
[8] PREPA, Plan Integrado de Recursos (Integrated Resource Plan) 2019, https://aeepr.com/es-pr/QuienesSomos/Paginas/ley57/Plan-Integrado-de-Recursos.aspx

2,300 MW of fossil generation is retired relative to nearly 5,000 MW of PV and 2,700 MW of battery energy storage added to the system. In addition, the solar and storage additions defer the need for any further new capacity despite the retirement of the above units.

Table 2: Scenario Retirement Schedule

Case	Units Retired	Incremental Capacity (MW)	Cumulative Capacity (MW)
Base Case	Not Applicable	0	0
25% DER	AES 1 & 2 and Palo Seco Steam 3 & 4	886	886
50% DER	Aguirre Steam 1 & 2	900	1,786
75% DER	Aguirre CC 1 & 2	520	2,306

2.4 A New Resource Mix for Puerto Rico

The combination of solar PV and battery additions and fossil generator retirements creates a resource mix that is fundamentally different than the one Puerto Rico has today. The total installed capacity by scenario is provided in Figure 4, which for the purposes of long-term planning is spread across a 20-year horizon as shown in Figure 5. On an installed capacity basis, solar and storage (inverter based resources) become the largest form of capacity by the 50% DER scenario and total installed capacity in Puerto Rico increases to over 10 GW by the 75% DER scenario, nearly double today's capacity despite increased energy efficiency.

This is a radically different resource mix and power system than what Puerto Rico has today, or the one proposed by PREPA in the 2019 IRP. From an engineering standpoint, such a fundamental change in the grid's resource mix can be achieved with current technology, but it requires detailed planning and grid simulation modeling like the work conducted in this study.

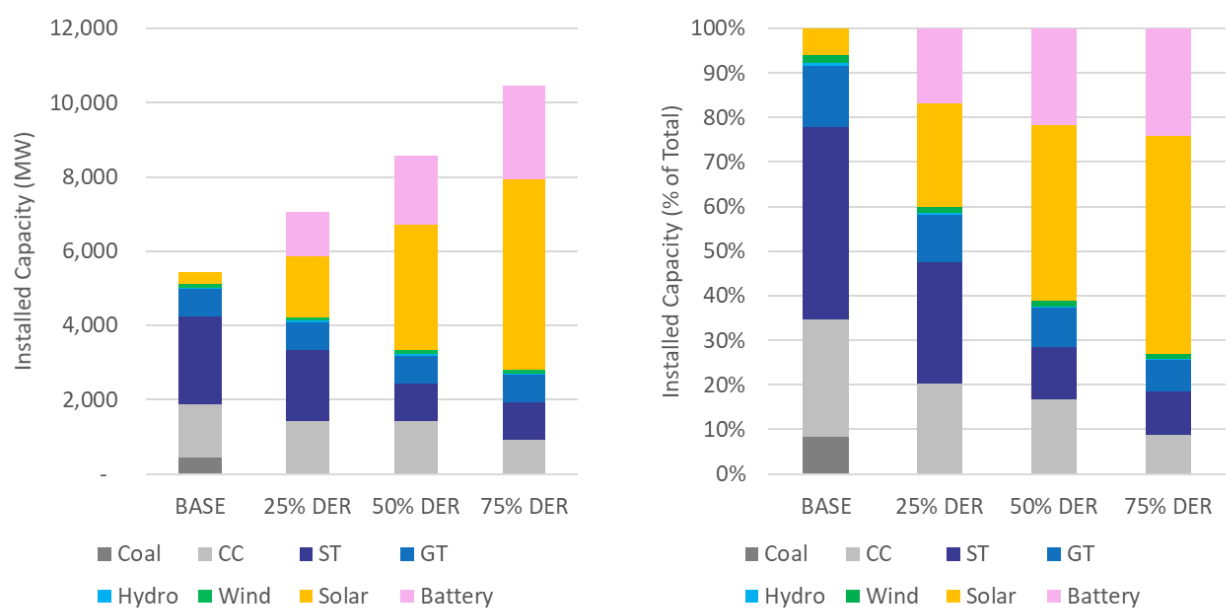

Figure 4: Installed Capacity by Scenario, MW (left) and % of Total (right)

`

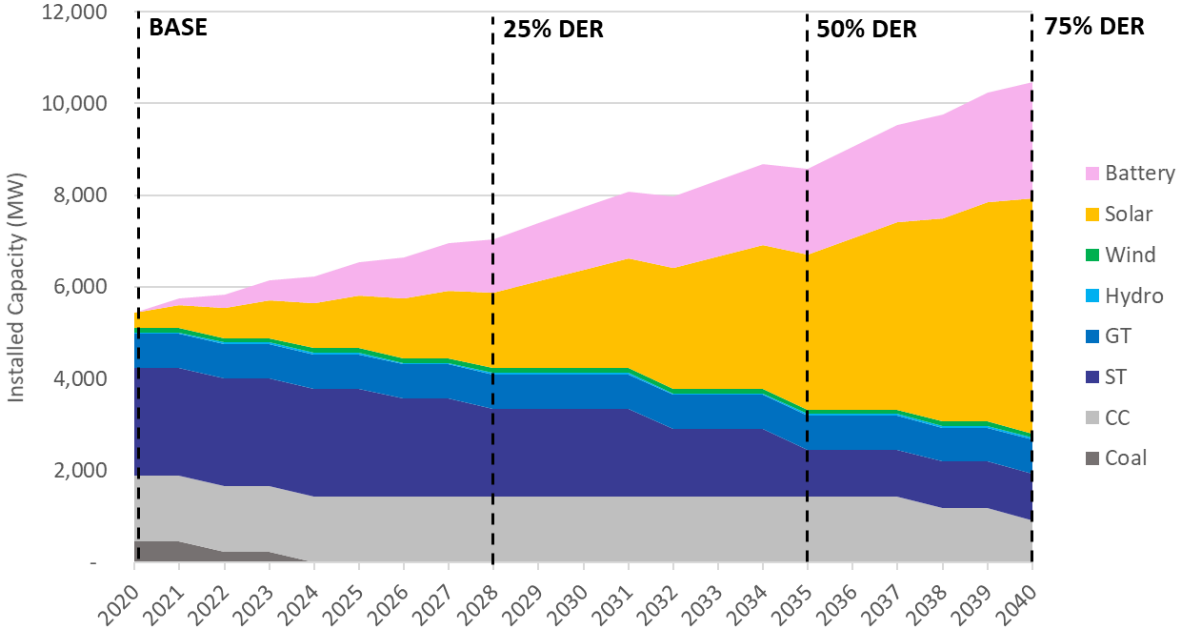

Figure 5: Installed Capacity by Forecast Year

3 Inputs & Assumptions

3.1 Network Topology

This study relied on a detailed representation of Puerto Rico's transmission network based on network data provided by PREPA. Specifically, PREPA provided transmission models in Siemen's PSS/E v33 format, and the Day Peak 2018 model was used. This model represents a snapshot in time, of what load, generator dispatch, and transmission flows look like during a mid-day peak load event. The Day Peak case was selected because it aligns with the period of solar generation analyzed throughout this study. This included a detailed representation of the transmission network topology, which include 8 regions, 1,234 transmission line branches, 181 transformers, and 860 load busses. The PSS/E power flow data included line impedances, line ratings, load allocation by bus, dynamic generator models, and other detailed network data.

The PLEXOS production cost model incorporated a full nodal transmission topology and monitored all transmission lines at the 38kV and higher level and load was allocated across the network on an hourly basis following the proportional allocation of load in the power flow data.

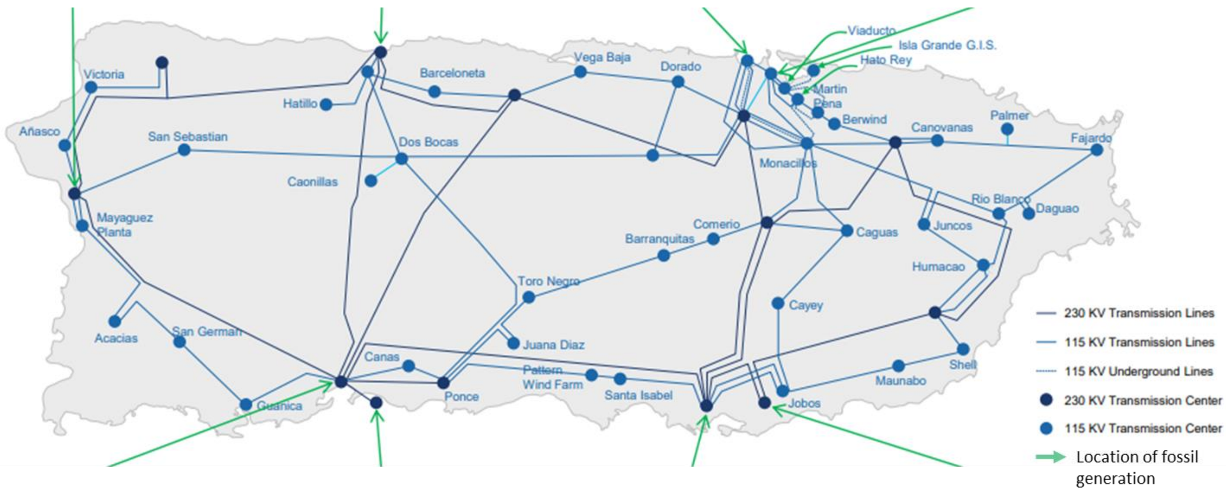

Figure 6: Puerto Rico High Voltage Transmission Topology

For planning and reporting purposes, the Puerto Rico power system is divided into nine planning regions used by PREPA and PREB. These include Arecibo, San Juan and surrounding Bayamón regions in the north, Carolina and Caguas in the east, Ponce OE (west) and Ponce E (east) in the south, and Mayagüez in the west. These divide the island based on location of major load busses and transmission interfaces between the regions. A map of the planning regions is provided in Figure 7.

Figure 7: Map of Puerto Rico Grid Planning Regions

3.2 Load & Energy Efficiency

Load and energy efficiency assumptions were crafted jointly with Energy Futures Group (EFG). EFG conducted the analysis to identify the necessary components of an energy efficiency program over the next 15 years to achieve the desired 25% reduction in load. However, for the purposes of this analysis the final energy efficiency value is most important, not the application of programs over time. For more information on the path and application of energy efficiency programs please refer to the companion report from EFG. The application of EFG's analysis in how it relates to this analysis will be covered in more detail below.

As for many of this study's inputs and assumptions, PREPA's 2019 IRP acted as the original data source and the project team utilized the base assumptions to the extent feasible. The 2020 gross energy demand for generation (Exhibit 3-11) from PREPA's 2019 IRP was used as the starting point for this study's own forecast. However, there is one change that was incorporated into the Gross Energy Sales (GWh) for 2020. The generation served by existing DPV installations was added back into the Gross Energy Sales amount this way the existing DPV capacity could be modeled as a generator instead of being imbedded in a lower load figure. Appendix 4 (Exhibit 3-1) of the IRP[9] along with the PREB Module[10] PV Approval List served as guidance for the level of existing DPV on the system. With the many economic and demographic changes Puerto Rico is undergoing load growth between 2020 and 2035 was assumed to be 0% or flat.

This means that the 25% energy efficiency target from EFG's analysis was simply applied to the total energy demand and peak load from 2020 to calculate the 2035 values. The breakdown of the load forecast and energy efficiency assumptions is found in Table 3. It is assumed that PREPA's own use will

[9] Puerto Rico Integrated Resource Plan 2018-2019, Appendix 4: Demand Side Resources, Exhibit 3-1
[10] Puerto Rico Energy Bureau, PV Modules approved by the Energy Bureau, https://energia.pr.gov/modulos-pv/

`

not be as affected by overall energy efficiency programs, so it was held constant across time. Even if it is reduced it is already a small component of the total energy and should not significantly change results.

Table 3: Total Energy Demand & Peak Load with 25% Energy Efficiency Reduction by 2035

Year	2020	2035
Gross Energy Sales w/ Existing DPV (GWh)	15,648	11,736
Technical Losses (GWh)	1,444	1,083
Non-Technical Losses (GWh)	830	623
PREPA Own Use (GWh)	34	34
Total Energy Demand w/ Existing DPV (GWh)	17,956	13,476
Peak Load (MW)	2,826	2,120

The total energy and peak load for 2035 were divided across the 8 study regions proportionally based on the regions respective total energy for 2020 from the 2019 IRP. This breakdown is shown in Table 4.

Table 4: Regional Breakdown of Total Energy (GWh) and Peak Load (MW)

	2035	
	Total Energy (GWh)	Peak Load (MW)
ARECIBO	1,338	211
BAYAMON	1,959	308
CAGUAS	2,158	339
CAROLINA	1,498	236
MAYAGÜEZ	1,502	236
PONCE ES	551	87
PONCE OE	1,089	171
SAN JUAN	3,382	532
TOTAL	**13,476**	**2,120**

Using the above total energy and peak load by region combined with a load profile that was shared by PREPA via their PROMOD database the Build function within PLEXOS was used to create a respective 8760 hours per year load profile for each region that matched the total energy and peak load inputs. The resulting profiles were then used across all simulations. Load was then allocated at each individual load bus based on the proportional allocation in the PSS/E power flow data.

3.3 Generator Characteristics

All major generator characteristics and parameters were modeled to match what is used in the 2019 IRP. This includes assumptions for max capacity, fuel type, ramp up, ramp down, forced outage rates, fixed operation and maintenance costs, and variable operation and maintenance costs.

Although the IRP also specified minimum up and down times along with minimum stable levels, some of these figures were conservative and not in line with what is common in other grids. Based on this some units have more flexible min up and down time parameters and min stable levels than the IRP outlines. This assumes that over the next 15 years these units will receive the required investment to keep them running and bring their operation up to the level other similar units already have in 2020.

Additionally, only the full load heat rate was shared in the IRP. Using the minimum stable level, maximum capacity, and full load heat rate for each respective unit and a default heat rate curve that differed for each unit type (i.e. CC, ST, GT) a polynomial heat rate curve was calculated for each unit (Appendix, Table 19, Figure 63). The polynomial heat rate curve was used within the production cost modeling simulations. This allows for a more accurate representation of a unit's dispatch as opposed to simply modeling the full load heat rate.

Lastly, while the IRP reported forced outage rates, it did not report maintenance rates. The maintenance rate for all units were based off the NERC Generating Availability Data System (GADS) dataset.[11] The NERC GADS dataset includes average generator reliability by unit type and fuel type.

No new unit additions have been added outside of the solar and battery installments discussed in Section 2.2. But 50 MW of utility scale solar projects were added to the model that were not included in the IRP because they were built or started construction in the interim period.

3.4 Fuel Prices

Fuel prices are taken directly from what the IRP used for its fuel forecast. These can be found Table 5.

Table 5: Fuel Prices (real 2020 $/MMBtu)

Year	Coal	Diesel	Fuel Oil	Natural Gas
2035	2.65	17.42	12.92	7.84

3.5 DER Representation & Characteristics

The DER represented on the power system included distributed PV (DPV), distributed BESS (dBESS), and distributed demand response (DR). These were captured in the model at 288 different 38kV buses throughout all PREPA areas of the power system. The distribution at each bus was chosen to be proportional to the distribution of load across the buses for a given PREPA area, as provided in the original PREPA base case. This allowed the levels of DER to vary by PREPA area while still be distributed across individual buses in a reasonable and consistent manner.

[11] PJM, 2018 PJM Reserve Requirement Study, https://www.pjm.com/-/media/planning/res-adeq/2018-pjm-reserve-requirement-study.ashx?la=en

Demand Response and Load Representation

The demand response service is considered to be relatively long-duration (hours) and slow-acting (minutes to hours of advanced notification) such that it is represented in the transmission model as a reduction in load.

The load across the system was originally provided from the power flow model as static loads with constant P and constant Q values. For representation in the dynamic model, the load was represented as 75% static load and 25% dynamic load by MW. The static portion of the load was represented as a constant active current and constant reactive impedance. The constant active current representation is a compromise that captures a mix of constant power and constant impedance loads that are assumed to physically be on the system, while a constant reactive impedance is a reasonable representation of the majority of physical loads.

The dynamic portion of the load was represented by a composite load model (CMLDBLU1) that contains representation of a feeder transformer, feeder impedance, power-electronic loads, and four different types of aggregate motor loads, as shown in Figure 8. This model was developed by power system stakeholders in the Western US to better capture the impact of induction motor-driven compressor loads like those found in three-phase and single-phase air-conditioning systems. The composite load model is parameterized for typical residential and light commercial loads. For further improving the diversity of the load representation, four different sets of parameters were developed with slight variations to important settings like contactor opening and reclosing voltage thresholds and timers. The behavior of motor-driven loads is particularly important when assessing the stability of the grid for fault events, and it cannot be reasonably neglected. However, it is acknowledged that accurate dynamic load modeling is very difficult to achieve and continues to be a work-in-progress by the industry, as it has been for decades.

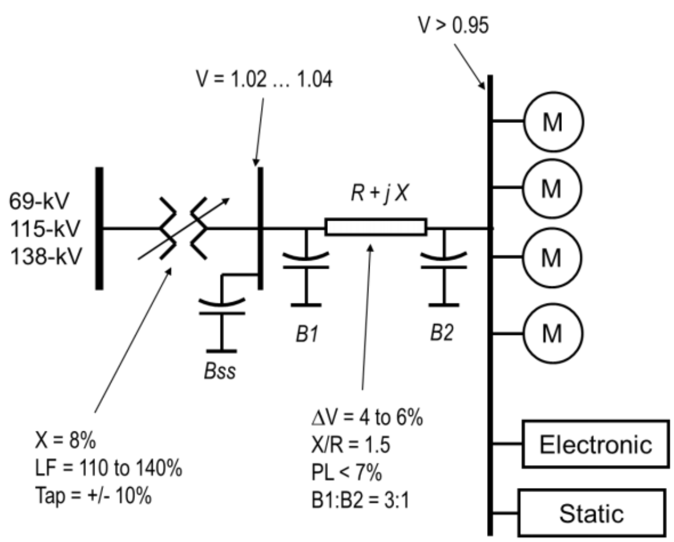

Figure 8: Composite Load Model Overview

Distributed PV and BESS Representation

The DPV and dBESS are both represented by a generic renewable energy model for distributed resources (DER_A). This model was developed in recent years and has gained increasing use across the US for representing distributed inverter-based renewables like solar PV and battery systems, which are capable of both sourcing and absorbing active and reactive power. This dynamic model also contains frequency-response and volt-var response functions (often referred to as "smart inverter" features), which can be enabled and adjusted to allow the DER to provide essential reliability services to support the grid.

The inverters for PV and BESS are extremely similar in reality, and therefore, the PV and BESS is represented as a single DER_A model at each of the 288 38kV buses. The active power of the model is set to be the sum of the DPV and dBESS contributions as specified by PLEXOS, where positive values for dBESS are for discharging operation and negative values are for dBESS charging. Therefore, it is possible that for some hours in the high-penetration scenarios, the DER will have a net negative power, indicating that the BESS charging rate exceeds the PV generation at that time.

Model Linkage – Production Cost, Transmission, and Distribution

The grid is represented and analyzed at the transmission level by PSSE and at the distribution level by OpenDSS. To align these models, both are fed data from the production cost simulation model, which specifies the level of active power for the load, DR, DPV, and dBESS for each hour of each scenario evaluated. This is shown by the large blue arrow in Figure 9. The distribution model contains detailed feeder topologies and a simple equivalent representation of the grid beyond the 38kV bus. To ensure consistency between the transmission and distribution models, the Thevenin Equivalent source for grid representation at the distribution level was calculated for each load bus in PSSE. Finally, the voltage at the 38kV buses forming the interface between transmission and distribution models is considered decoupled by the on-load-tap-changer at each feeder transformer, where the voltages in steady-state are regulated by the feeder transformer to achieve a desired low-side voltage given the power flows on the feeder at the time.

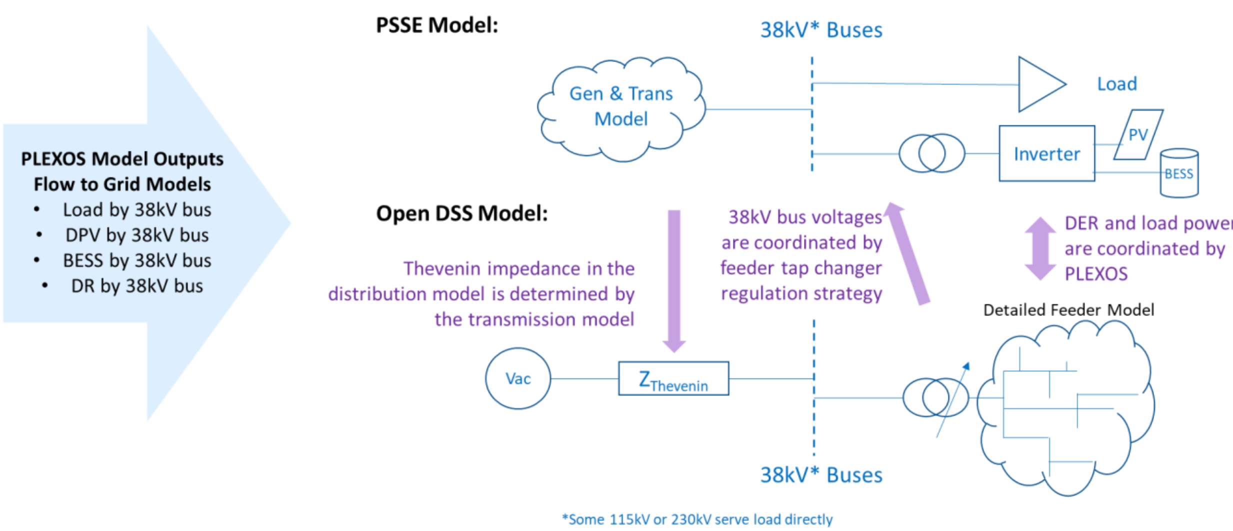

Figure 9: Linkages of Models Representing the Puerto Rican Grid

DER Aggregation and Control

In addition, it was assumed that the DER was integrated with some level of coordination and control. This would allow the system operator could take into account expected generation from DER resources to commit and dispatch the system and schedule battery energy storage, at least in part, based on system needs. This study was a system-level analysis and did not evaluate the potential for conflicting needs of behind-the-meter solar and battery energy storage optimized for both individual and system use. This is a reasonable assumption because while it would be impossible to simulate each individual system, when viewed at the system-level there will be surplus capacity available to use for grid services.

It was also assumed that distributed battery storage in this analysis is able to provide grid spinning reserve requirements through an aggregator that coordinates the output of many DER assets to provide controllable grid services. If this is not technically achievable in the short-term due to technology limitations of broad communications and coordination challenges, there may be a need for increased spinning reserves, which were not evaluated for this study.

In addition, because the residential solar PV was integrated as hybrid systems with coupled battery energy storage, this study also did not include an increase in reserves, above current requirements, due to either the variability or uncertainty of solar resources. The study used the reasonable assumption that the solar and battery resources could "self-regulate" and manage net-to-grid variability via ramp rate limits or other inverter controls. For example, if the solar is back-feeding onto the distribution circuit during mid-day operations, a drop in the solar output would be mitigated by a short term increase in battery storage output to minimize any rapid change in rooftop PV output.

4 Characterizing Puerto Rico's Solar Resource

4.1 Solar Irradiance Data and Power Production Profiles

To accurately simulate a power grid with high distributed solar integration, it is important to properly characterize solar variability across timescales that vary from sub-hourly to seasonally. While using actual measured data at existing solar plants can be useful to characterize solar variability at an individual plant, it is inadequate for full system evaluations and high solar integration studies. This is because it is important to accurately capture geographic diversity. As solar integration increases across Puerto Rico it will be spread out across the island. While any individual solar site may have a large amount of variability due to cloud cover, the island-wide variability will be significantly reduced. For this reason, this study utilized simulated historical solar data instead of actual measured plant output.

The data source for the chronological solar irradiance data was the National Solar Radiation Database (NSRDB) from the National Renewable Energy Laboratory (NREL). The NSRDB is a serially complete collection of hourly and half-hourly values of meteorological data and the three most common measurements of solar radiation: global horizontal, direct normal and diffuse horizontal irradiance spanning 21-years of historical weather.[12] The NSRDB also has a specialized dataset for Puerto Rico – the Puerto Rico Simulated High Resolution Dataset[13] – that was utilized for this study to also include weather data at 5-minute resolution.

The irradiance data was then converted to power production profiles using the NREL System Advisor Model (SAM). The System Advisor Model (SAM) is a free techno-economic software model that can simulate a wide variety of renewable energy systems. For this project, SAM was used to model the power production of distributed rooftop and utility-scale photovoltaic systems. Using the weather data collected from the NSRDB and plant characteristics - like DC:AC ratios, tilt, azimuth, etc. – chronological power production profiles were developed for use in the PLEXOS model. Assumptions used to develop power production profiles are provided in Table 6 for distributed rooftop PV systems. While each PV system will have unique attributes, these assumptions are meant to represent the weighted average of all systems in Puerto Rico. Existing utility-scale projects utilized similar properties, but assumed a DC to AC ratio of 1.3, and a specific plant capacity and location.

Table 6: Photovoltaic System Design

Property	Assumption
DC:AC ratio	1.1
Inverter Efficiency	96%
System Losses	14%
Racking	Fixed-axis roof mount
Tilt	18 degrees
Azimuth	180 degrees

[12] National Renewable Energy Laboratory, National Solar Radiation Database, https://nsrdb.nrel.gov/
[13] National Renewable Energy Laboratory, Puerto Rico Simulated High Resolution Dataset, https://developer.nrel.gov/docs/solar/nsrdb/puerto-rico-download/

4.2 Geographic Diversity & Site Selection

One of the benefits of DERs over utility-scale projects is the geographic diversity benefits gained through thousands of distributed systems across the island. While this study did not attempt to simulate the chronological solar power production of each individual rooftop PV system, it did incorporate a large dataset of solar locations spread across Puerto Rico's population centers.

For this analysis, 96 sites were selected across Puerto Rico, concentrated in developed areas where residential and commercial PV systems would be most prevalent. For the initial site selection PREPA's transmission busses were mapped using GIS data provided by PREPA. This provided locations of existing transmission and distribution infrastructure. Twelve sites were then selected for each of the eight regions (Figure 7) based on the density of urban development and existing transmission and distribution infrastructure. This created 96 sites total (8 regions and 12 sites per region) across the island, which were clustered around urban and suburban load centers to weight solar generation to those regions. A map of the 96 selected solar sites, colored by region, is provided in Figure 10 and annual capacity factors by site are provided in Figure 11. In general, capacity factors are highest along the coast and at lower elevations away from the mountainous interior.

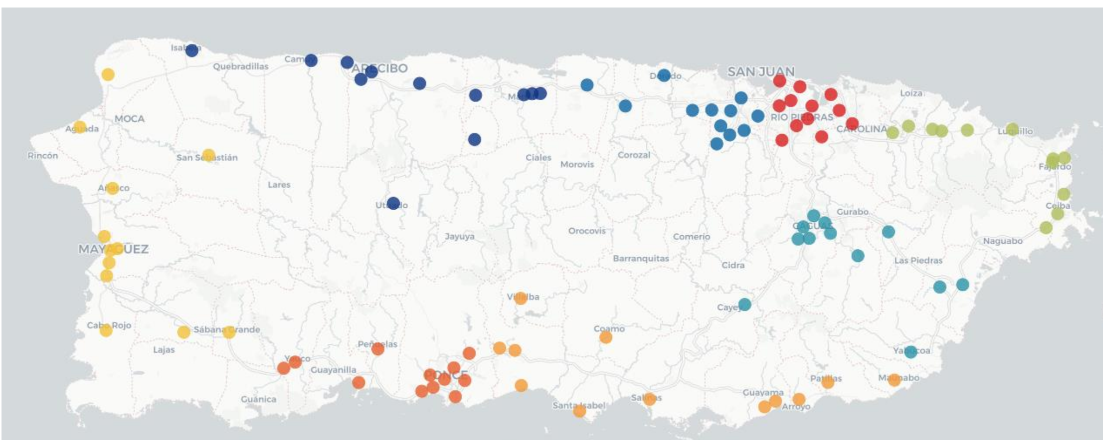

Figure 10: Map of Simulated Solar Locations Across Puerto Rico
(colored by region)

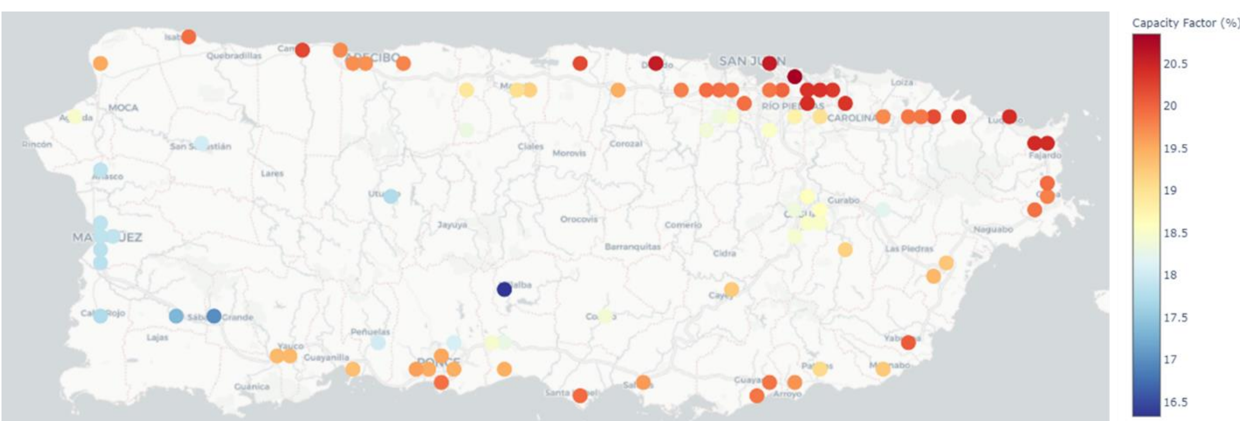

Figure 11: Map of Solar Capacity Factors Across Puerto Rico
(colored by annual capacity factors)

For each of the 96 sites identified a full year of chronological, 5-minute resolution weather data was downloaded from the NREL Puerto Rico Simulated High Resolution Dataset and converted into power production profiles. This generated over 10 million data points of chronological solar data that were modeled for the study to ensure adequate geographic diversity and granular chronology of variability. The data was then aggregated for each region by averaging the twelve sites into a single composite regional profile for use in the production cost modeling.

An example of the geographic variability is provided in Figure 12 which shows the five-minute solar capacity factors for three regions across one day of operation, as well as the island-wide average. The two regions in close proximity, Caguas and Ponce ES, both are characterized as cloudy days with solar PV decreasing availability in the afternoon hours. Mayagüez, which is in the westernmost side of the island is experiencing a relatively sunny day. The average of all eight regions (dotted line) shows a somewhat smoother profile. This data is quantified in the correlation matrix in Figure 13, which is a measure of alignment in the chronological profile. This plot shows that regions in close proximity have higher solar profile correlations.

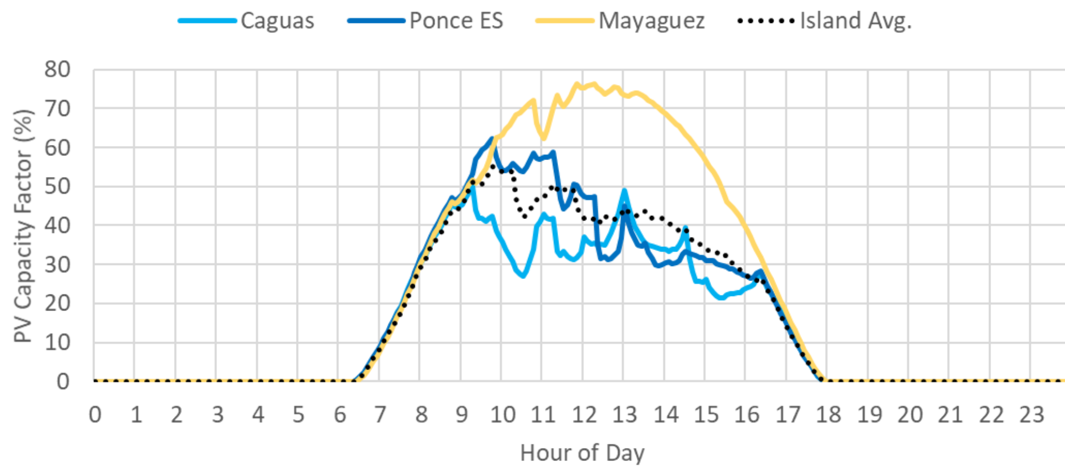

Figure 12: Sample Day of Solar Variability by Region

West → East

	Mayaguez	Arecibo	Ponce OE	Ponce ES	Bayamon	San Juan	Caguas	Carolina
Mayaguez	1.00							
Arecibo	0.87	1.00						
Ponce OE	0.86	0.86	1.00					
Ponce ES	0.85	0.88	0.94	1.00				
Bayamon	0.81	0.91	0.83	0.88	1.00			
San Juan	0.81	0.89	0.83	0.89	0.95	1.00		
Caguas	0.80	0.87	0.86	0.92	0.90	0.91	1.00	
Carolina	0.80	0.89	0.84	0.89	0.91	0.93	0.93	1.00

Figure 13: Correlation Matrix of 5-Minute Chronological Solar Profiles

While the previous maps show the locations selected for simulated weather data, the installed PV capacity were sited based on existing residential and commercial load locations. The data source for the load was the PSS/E power flow network data, which provided the load at each load bus across the system. Load busses were classified by type (residential, commercial, industrial, agriculture, etc.) and assigned to each of the load regions. For the purposes of this study, it was assumed that current and future residential and commercial distributed PV was sited proportional to the load of that type. The PV capacity was then distributed across the system, interconnecting at 289 distinct transmission busses.

The breakdown of load and DER capacity by region is shown in Table 7 and Figure 14. Because San Juan has the largest amount of commercial and residential load, it was also assumed to have the most installed DER capacity. A complete breakdown of the DER capacity, both solar PV and battery, by region, customer class, and scenario is provided in the Appendix, Table 20.

Table 7: Allocation of Residential and Commercial Load & DER by Region and Customer Class

Region	Residential Load (MW)	Commercial Load (MW)	Other Load (MW)	Residential DER (%)	Commercial DER (%)
Arecibo	124	63	83	10%	8%
Bayamón	237	66	77	19%	9%
Caguas	205	101	109	16%	13%
Carolina	157	69	58	12%	9%
Mayagüez	140	113	39	11%	15%
Ponce ES	49	25	105	4%	3%
Ponce OE	109	43	83	9%	6%
San Juan	245	277	129	19%	37%
Total	**1267**	**756**	**682**	100%	100%

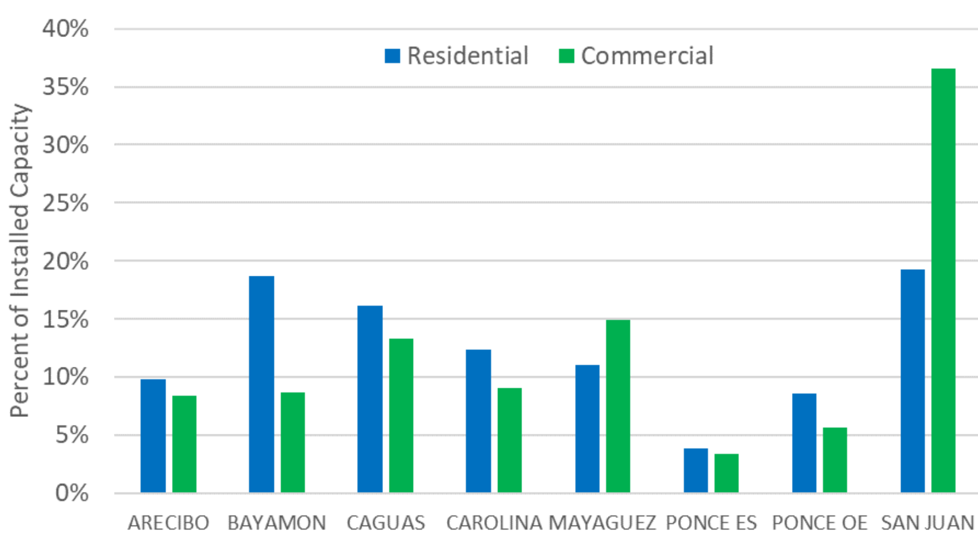

Figure 14: Allocation of Residential and Commercial DER by Region and Customer Class

`

5 Generation & Production Cost Modeling Results

5.1 Grid Operations with High DER

Grid operations change markedly as the system moves towards a higher penetration of DER. Figure 15 highlights how annual generation by unit type changes over the four reference results. As solar generation increases it displaces fossil fuels on the grid. The types and amount of fossil fuel displacement depends on the costs, flexibility, and physical characteristics of each generating unit. The retirement of AES in all but the Base Case stands out with the coal unit type denoted by a dark gray. The immediate result of a system without AES and a 25% integration of DER is an increased role for existing combined cycle (CC) plants. The 25% DER case shows much of the generation once provided by AES is instead produced by existing combined cycle plants, which operate on either LNG or oil fuels. These existing combined cycle plants include both EcóElectrica and the two San Juan CC units, all of which can increase generation from what is dispatched in the Base Case.

As the penetration of DER increases in the 50% and 75% DER cases, solar takes on a much larger role and begins to displace steam turbine (ST) units and later CC units. While simple-cycle gas turbines (GT), also referred to as "peakers," generate a relatively low amount of generation in the base case, their role in total generation is reduced further in the 50% and 75% scenarios as battery energy storage effectively reduces peak loads.

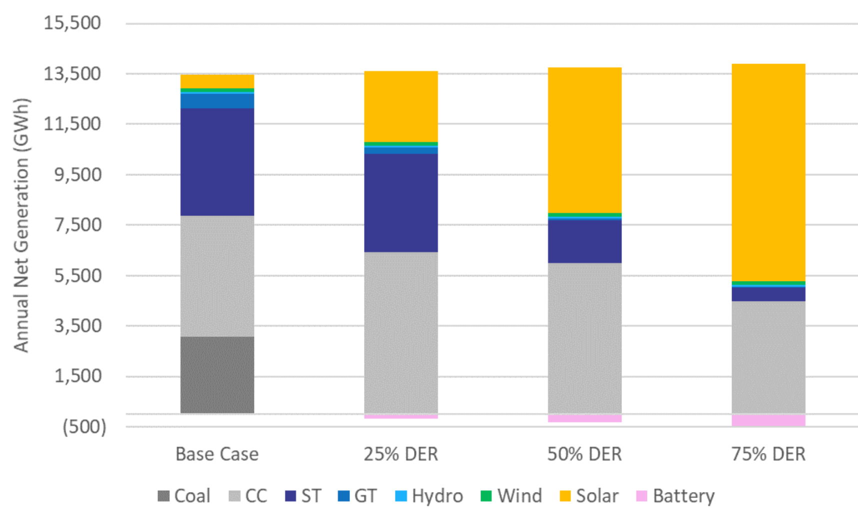

Figure 15: Annual Net Generation by Unit Type

It should be noted in this chart that the 25%, 50%, and 75% values do not necessarily equate to the percentage of total generation. This is because the scenarios were developed based on energy *sales*, which does not take into account transmission losses, distribution losses, non-technical losses (theft), PREPA self-use, round-trip energy losses associated with battery storage utilization, or curtailment. These components of total energy demand are included in Table 3.

Another way to highlight the change across the cases is to compare the displacement of generation (Figure 16) which represents the net *change in generation* in each scenario, relative to the Base Case. Resources that are increasing the amount of generation they contribute are on the positive side (or right side of x-axis) and those that are being displaced by the new resources are shown on the negative side (or left side of x-axis). It is important to note that battery resources are on the left side due to the round-trip efficiency losses inherent with the technology. As the battery buildout increases with increased penetration of DERs the amount of round-trip losses increases as a result of their increased usage.

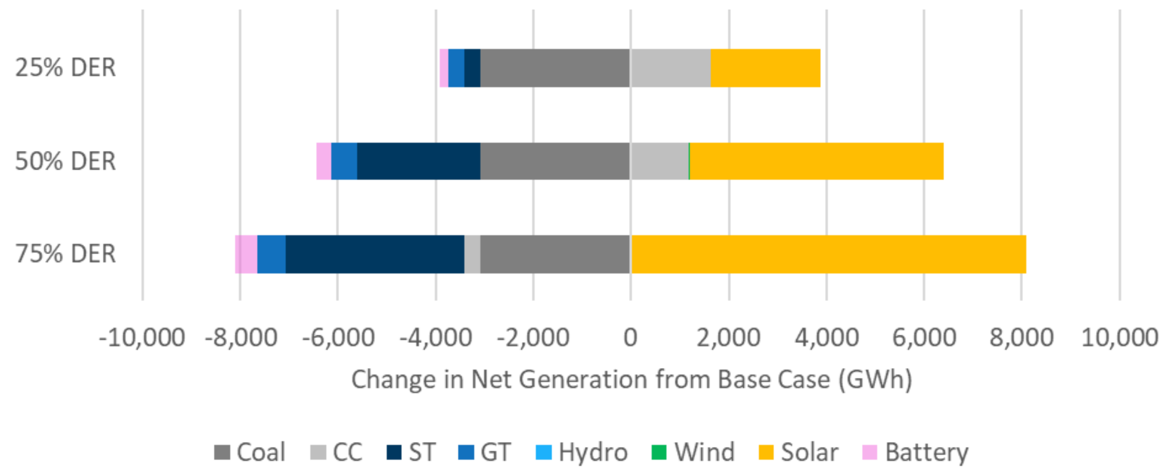

Figure 16: Displacement of Generation by New Resources when compared against Base Case

While annual generation and displacement values are important for public policy and long-term system planning, it provides little information on day-to-day, hourly, or sub-hourly operations. Because system load changes from hour-to-hour, and solar resources are variable, understanding *chronological* generation by unit and resource type is critical. The production cost analysis performs a chronological commitment and dispatch of the power grid to minimize system cost – in a similar fashion as the grid operator (PREPA). The commitment determines which units should be online while dispatch determines the MW output from each generator.

The below dispatch diagrams in Figure 17 show a relatively “normal” day of operation for each respective case. The dashed black line shows the load level for each given hour. Battery storage is depicted as two shades; when the battery storage (dark pink) is above the black line it is charging, and when it is directly below the black line (light pink) the battery storage is discharging.

There is no storage installed in the Base Case, but as storage is added in the 25% DER scenario the use of GT units drops as their generation is now mostly covered by battery storage. The role of conventional “baseload” generation shifts from the AES coal plant in the Base Case to the combined cycle units in all the following cases. Because these resources represent the least cost form of fossil generation, they are utilized as much as possible to avoid generation from higher cost resources.

As DER penetration increases along with the buildout of battery storage, battery storage fulfills a larger portion of load during the morning and evening hours. As mentioned above by first displacing GT unit generation but by the 75% DER case most of the generation formerly provided by ST units is also replaced by Storage.

With this increase in DER, solar and storage becomes the largest resource on the system in most hours of the day, with CC – and to a lesser extent ST – fossil units dispatching in the morning and evening hours when solar generation is reduced. The peak solar hours of the day are not only the prime hours

`

for charging the battery storage resources but also the hours where most fossil fuel-based generation is either reduced to lower loading levels or turned off entirely. This is most noticeable in the 75% DER case where all generation, save a small portion of combined cycle generation, is displaced during the middle of the day by solar. It is important to note that this is happening even with a large amount of solar generation being directly charged by battery storage for use at a later time.

The decision to turn down a generator or entirely turn off a generator is based on several variables, including the resource's start-up and shutdown costs, minimum loading level, spinning reserve requirements, and expected amount of time the generator can be turned off for.

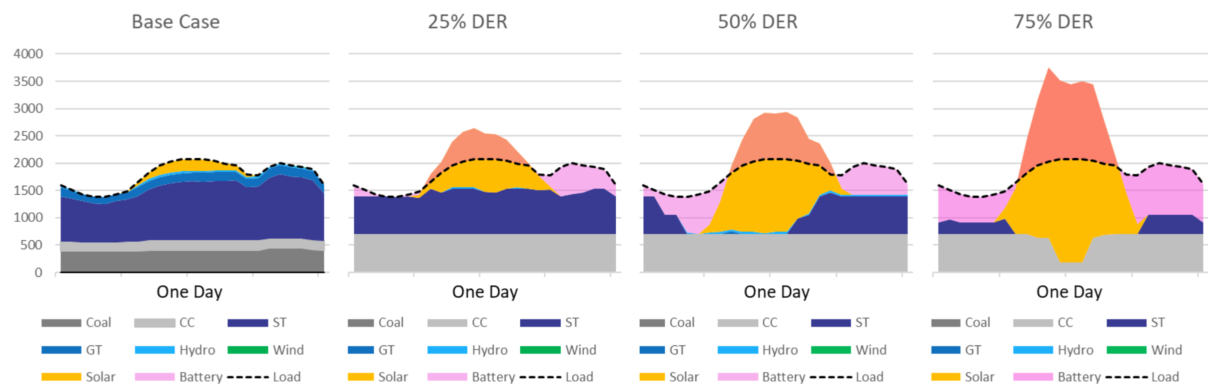

Figure 17: Dispatch Diagrams for "Normal" Day

While Figure 17 shows a single day of operation across the four scenarios, commitment and dispatch decisions must be made taking into account what occurred previously, and what will occur afterwards. To illustrate this, dispatch diagrams showing weeklong periods are provided in Figure 18 and Figure 19. These two weeks were selected to highlight how the system operates during the period of peak load and during the week with the most amount of renewables generation. In Figure 18 the Base Case heavily commits ST and GT units to meet load even with the presence of the AES coal unit providing a fixed output. While in the 75% DER case, which has retired AES and other thermal units, the ST and GT units are rarely operated despite this representing the week with the highest demand. Instead solar combined with batteries can sufficiently meet load with selective use of ST and GT units in evening hours – even on lower solar days.

The trends in chronological generation are even more apparent during the week of highest renewable generation, as shown in Figure 19. The Base Case relies on ST units every hour of the week, but as DER penetration increases this reliance declines. By the 75% DER case ST units are only dispatched two evenings of the week and GT units are barely called on at all. Overall, each of these weeks show that solar in combination with batteries can supplant an array of thermal generation, from oil-fired peakers like GT units to units that more traditionally provide baseload power like ST and CC units. These two samples highlight how DER is able to operate the system during its peak demand periods and how the system can fully take advantage of renewable generation. For additional weekly dispatch illustrations please see the Appendix.

`

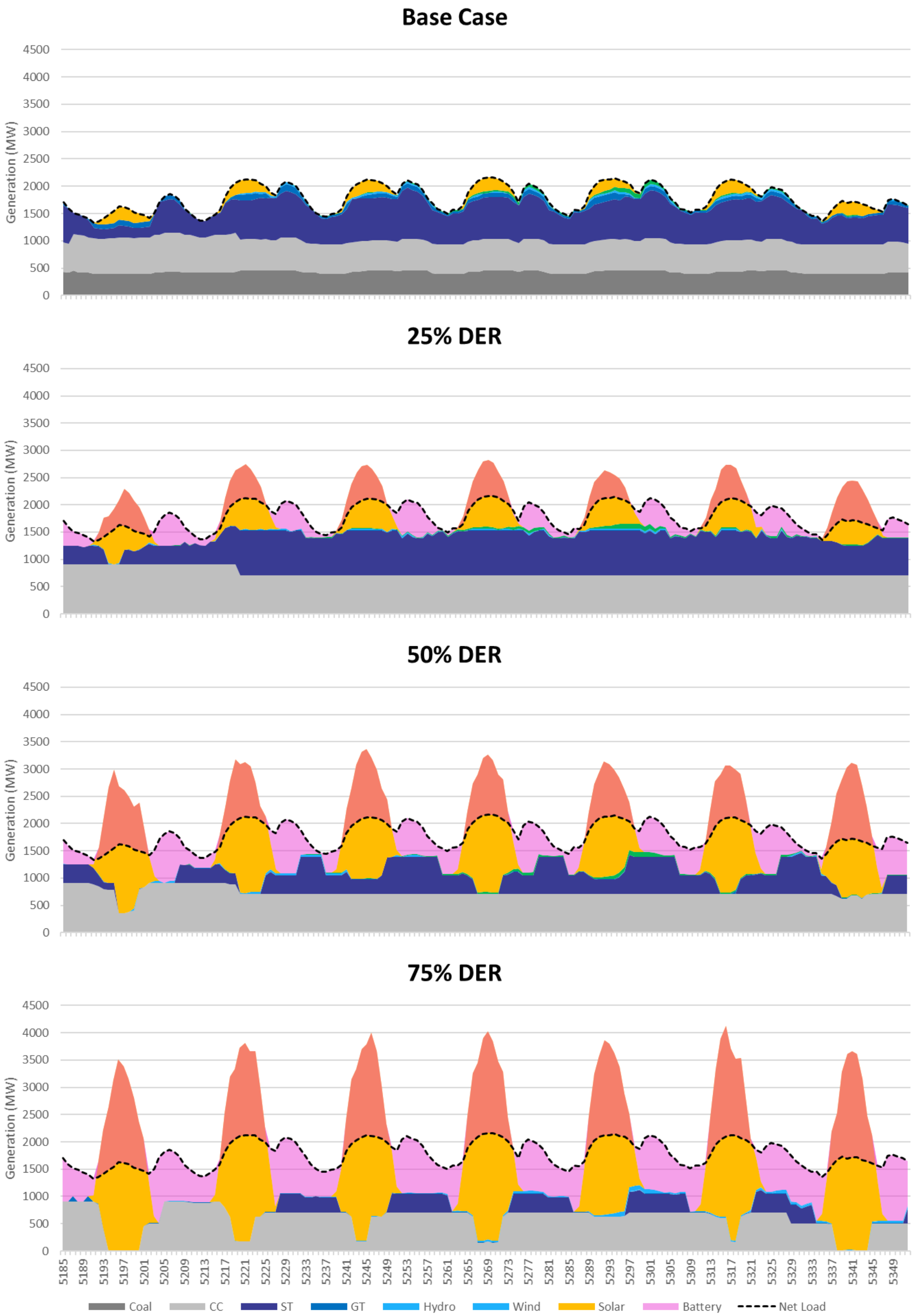

Figure 18: Dispatch Diagrams, Peak Load Week (Aug 5)

`

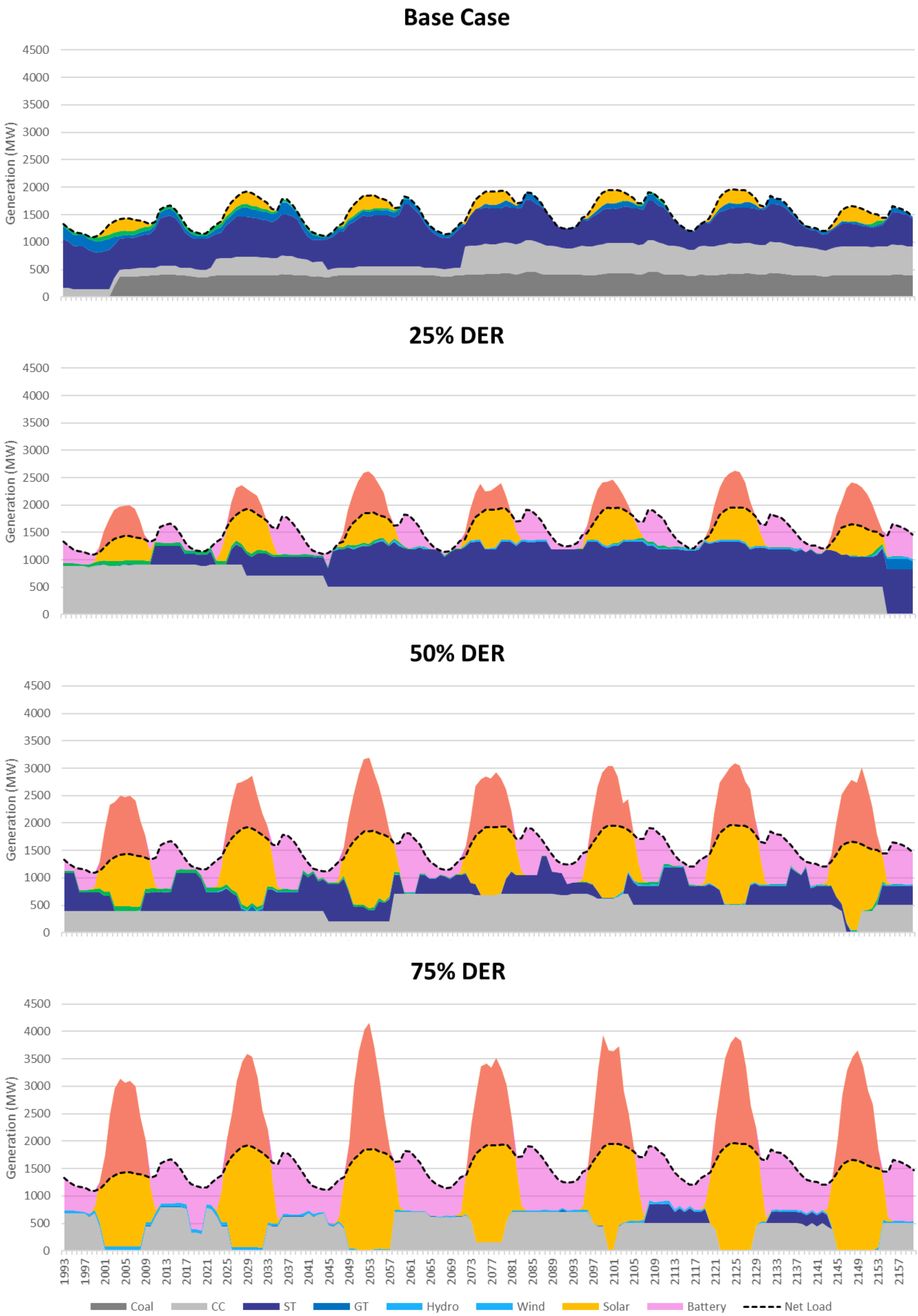

Figure 19: Dispatch Diagram, Maximum Renewables Generation Week (Mar 25)

The overall trends visible in the dispatch diagrams are also apparent when looking closer at hours online and unit cycling across the entire study year, not just one day as the dispatch diagrams focus on. Figure 20 shows the average starts per year (left) and average number of hours online per unit for each unit type (right) across the four scenarios. From these figures, the following observations can be made:

- Due to the retirement of AES in all but the Base Case its average hours drop to zero.
- Similar to trends highlighted in the dispatch diagrams, both the hours and starts of GT and ST units drop with increased penetration of DER. GT units experience their biggest drop between the Base Case and 25% DER case.
- Combined Cycle units are the only unit type that experiences as noticeable uptick in number of starts and hours online. This is because the CC fleet takes on much of the cycling duty (turning off and on) in the higher DER scenarios and most other generation is displaced entirely.
- The chart illustrates the increased flexibility required by the fossil fleet, especially for the CC units, which will be expected to cycle on and offline more often and run for fewer hours per year. This may change the maintenance requirements, cycling costs, and reliability of these generators in the future.

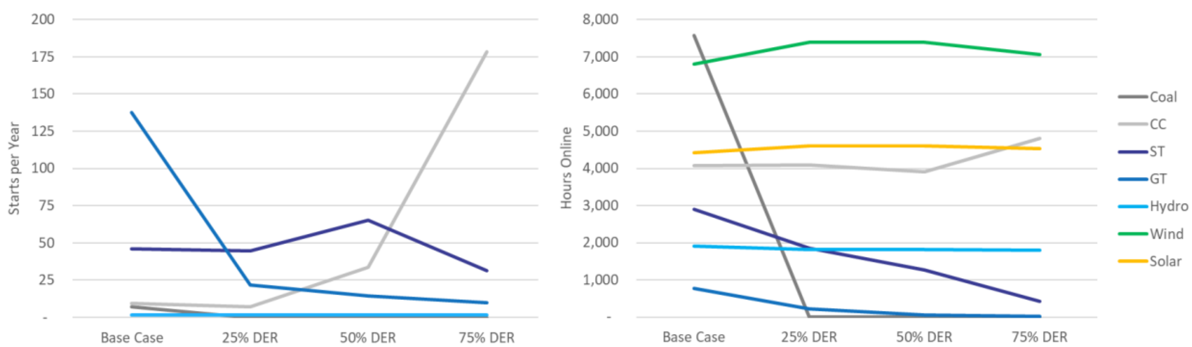

Figure 20: Average Starts (left) and Hours Online (right) per Year by Unit Type

It is not only the generation of the fossil fleet that is displaced. In addition, the DER also provides the grid's spinning reserves. These reserves represent generation that is held back in reserve by generators to meet unexpected drops in generation (contingency reserves) or normal fluctuations of load and solar resources. As discussed in Section 3.5, this study assumed that DER did not require additional reserves because it was added with battery storage and thus does not add net-variability to the system. It was also assumed that DER could be aggregated and provide grid services in a controllable manner.

Despite considerable changes in how the grid operates as the penetration of DER is increased there were no challenges associated with meeting reserve requirements. In fact, reserve shortfalls are eliminated in scenarios with DER integration. For example, the Base Case does experience a shortage of spinning reserves that amount to about 0.2% of total risk and occur during 4.1% of all hours. Many grids currently rely on fossil fuel-based generation to meet reserve requirements but with the addition of large amounts of storage to the grid, these new resources can begin to play a larger role in the provision of grid services.

5.2 Avoided Fuel, Emissions, and Generation Cost

The changes to generation and displacement of fossil fuels presented in Section 5.1, leads directly to reduced fuel consumption and fuel expenditures. This is an important benefit of DER, as it reduces reliance on imported fuels, emissions, and expenditures that flow out of Puerto Rico. The metrics presented in this section also provided valuable benchmarks to measure the *benefits* of DER integration, including avoided generation cost and avoided emissions. These avoided costs represent a shift from variable expenses (largely fuel) to fixed costs (mostly capital cost and maintenance for new DER equipment).

Changes in fuel consumption closely mirror the changes in generation discussed in the previous section. Table 8 shows the annual fuel consumption by fuel type in terms of MMBtu and the more fuel specific unit (i.e. barrels, bbls, for oil). Coal consumption ends with the retirement of AES and oil consumption declines with the addition of more DER. While gas experiences an increase versus the Base Case in the 25% DER scenario, which can be met by existing facilities, as gas-powered generation increases to replace generation once coming from AES. But gas consumption then declines as it is displaced by solar + battery in later cases. Overall, oil and gas both experience more than a 50% decline in consumption by the 75% DER scenario in addition to the 100% decline in coal consumption that all DER scenarios include. As a result, Puerto Rico would be less susceptible to fuel price volatility and would become more energy independent with increased DER adoption. This reduction in fuel consumption also translates to a more than 70% reduction in carbon dioxide emissions by the 75% DER case.

Table 8: Annual Fuel Consumption and Emissions by Scenario

		Base Case	25% DER	50% DER	75% DER
Consumption (MMBtu)	**Coal**	30,095,500	-	-	-
	Oil	28,868,900	24,086,510	19,235,470	12,613,700
	Gas	58,462,330	65,887,810	44,084,710	27,454,930
Consumption (fuel type units)	**Coal (short tons)**	1,544,151	-	-	-
	Oil (bbls)	4,884,857	4,146,285	3,326,911	2,182,950
	Gas (BCF)	58.46	65.89	44.08	27.45
Carbon Dioxide Emissions (tons)	**Total**	8,892,978	5,806,914	4,131,259	2,623,456
Change from Base Case					
Consumption (MMBtu)	**Coal**		(30,095,500)	(30,095,500)	(30,095,500)
	Oil		(4,782,390)	(9,633,430)	(16,255,200)
	Gas		7,425,480	(14,377,620)	(31,007,400)
Carbon Dioxide Emissions (tons)	**Total**		(3,086,064)	(4,761,719)	(6,269,522)
Percent Change from Base Case					
Consumption (MMBtu)	**Coal**		-100%	-100%	-100%
	Oil		-17%	-33%	-56%
	Gas		13%	-25%	-53%
Carbon Dioxide Emissions (tons)	**Total**		-35%	-54%	-70%

Overall, as DER is integrated the total production costs decline across the cases evaluated. Production costs, also referred to as variable costs, measure fuel expenses, variable operations and maintenance (VO&M) costs, and startup/shutdown costs. Production costs do not include fixed costs, including capital costs, fixed operations and maintenance (FO&M) costs, or costs to build and maintain the transmission and distribution network. It should be noted that this report does not evaluate the additional costs but defers that discussion to a subsequent report provided by Energy Futures Group which was developed in conjunction with this analysis.

As shown in Table 9 total production costs decrease significantly as DER is integrated on the system. The vast majority of the cost reductions come from decreased fuel costs, while VO&M cost is also reduced. Start costs, which were included to estimate both the startup fuel, as well as increased maintenance and degradation, increase slightly in the 25% and 50% DER scenarios, but start to decrease in the 75% DER scenario. System-wide start costs were calculated by categorizing each unit's starts as hot, warm, or cold depending on its unit type and applying the respective capital and maintenance costs, startup fuel costs, and auxiliary power and operations costs from NREL.[14]

The savings from introducing more DER onto the grid while also retiring fossil fuel-based generation are considerable. Table 9 shows that the savings range anywhere from roughly $97 million to $613 million per year.

However, these savings – in addition to other benefits like avoided capacity costs, potential transmission and distribution deferral, avoided emissions, and resiliency benefits - would have to be used to offset the capital costs associated with new capital expenditures for the DER PV and battery capacity, as well as associated distribution upgrades.

These savings can also be viewed as not only absolute dollars but also from the perspective of savings per additional total available solar measured as ($/MWh). To calculate this, divide the savings from Table 9 by the additional total available solar energy in MWh for each respective case versus the Base Case. The results show that there is a savings of between $43 and $75/MWh per additional solar on the system.

Table 9: Total Production Costs and Avoided Energy Costs (all costs are in real 2020 dollars)

	Base Case	25% DER	50% DER	75% DER
Fuel Cost ($000)	1,002,788	926,212	677,269	432,365
VO&M Cost ($000)	59,143	32,059	20,756	12,890
Start Cost ($000)	23,899	30,886	33,510	27,739
Total Production Cost ($000)	**1,085,830**	**989,158**	**731,534**	**472,994**
Difference to Base Case ($000)	N/A	96,672	354,296	612,836
Savings per Additional Solar ($/MWh)	N/A	43.27	68.23	75.27

[14] National Renewable Energy Lab, Power Plant Cycling Costs, https://www.nrel.gov/docs/fy12osti/55433.pdf

On a unit type basis the majority of the savings between the Base Case and DER cases is from reduced costs on coal, ST, and GT units, as shown in Figure 21. While CC units have an increase in costs from the Base Case to the 25% DER scenario as these units replace much of the generation from coal and take on a larger baseload role.

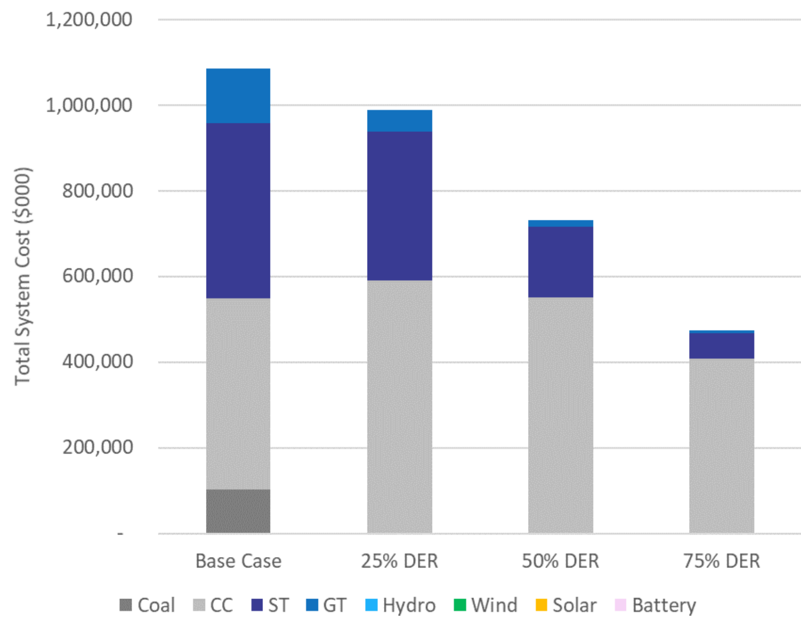

Figure 21: Total System Cost (2020 real $000) by Unit Type

5.3 Regional Flows

Another benefit of DER integration is that the resources are sited directly at the loads, reducing the total amount of energy that flows across the transmission network. This yields reliability, resiliency, and avoided transmission loss benefits. Currently Puerto Rico's generation is predominately located on the south-side of the island and is transferred via high-voltage transmission to the load centers in San Juan and Bayamón. This makes the system susceptible to outages due to transmission failures caused by weather and line outages.

The annual regional flows between the eight PREPA regions are provided in Figure 22, where positive numbers represent net exports and negative numbers represent net imports. In the Base Case both Ponce ES and Ponce OE are the only net exporters among the eight regions. However, with the retirement of AES beginning in the 25% DER case Ponce ES becomes a net importer. The overarching trend from the Base Case to the 75% DER case is that net flows decrease as each individual region becomes more self-sufficient with the increase in DERs located within that respective region. Despite individual regions becoming less reliant on neighboring regions for power the general imbalance of the southern part of the island, particularly Ponce OE, sending power to the northern regions continues, but to a much lesser extent. San Juan even becomes a small net exporter, predominately to neighboring loads in Bayamón, as the large increase in commercial solar flows back to neighboring regions.

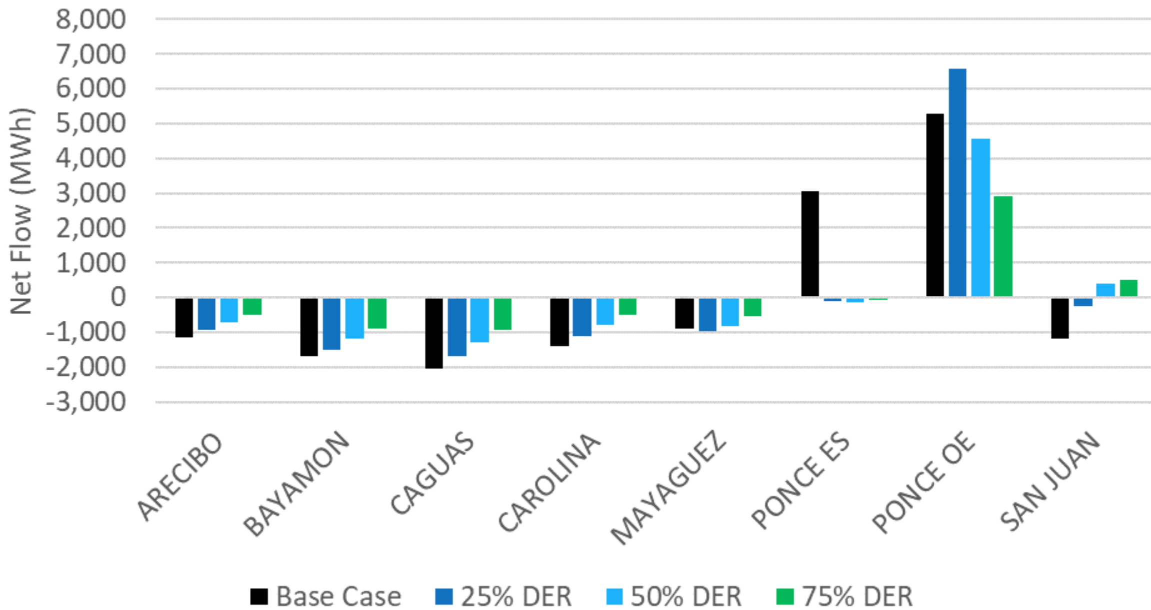

Figure 22: Annual Net Flows by Regions

The annual net flows shown in Figure 22 align with the hourly net flow duration curves highlighted for each region in Figure 23. The duration curves sort the hourly flows from each region from highest (exporting) to lowest (importing). This illustrates that most regions will see changes in the net transmission flows over the course of the year. From this chart, the following observations can be made:

- Arecibo, Bayamón, Caguas, Carolina, Mayagüez, and San Juan all see an increase in the number of hours with positive net flows out of their respective region.
- Ponce ES experiences a steep decline in net flows from the Base Case to the higher DER cases, largely due to the retirement of AES.
- Ponce OE shows a different trend, with much of the island's fossil fuel-based capacity located in Ponce OE it remains a strong exporter to other regions. Whereas once there are further retirements of fossil fuel-based generators and increased DER Ponce OE begins to follow the same trend as the other regions.
- The change in flows are most pronounced for about half of the year, which represents changes brought about by solar generation during daylight hours.

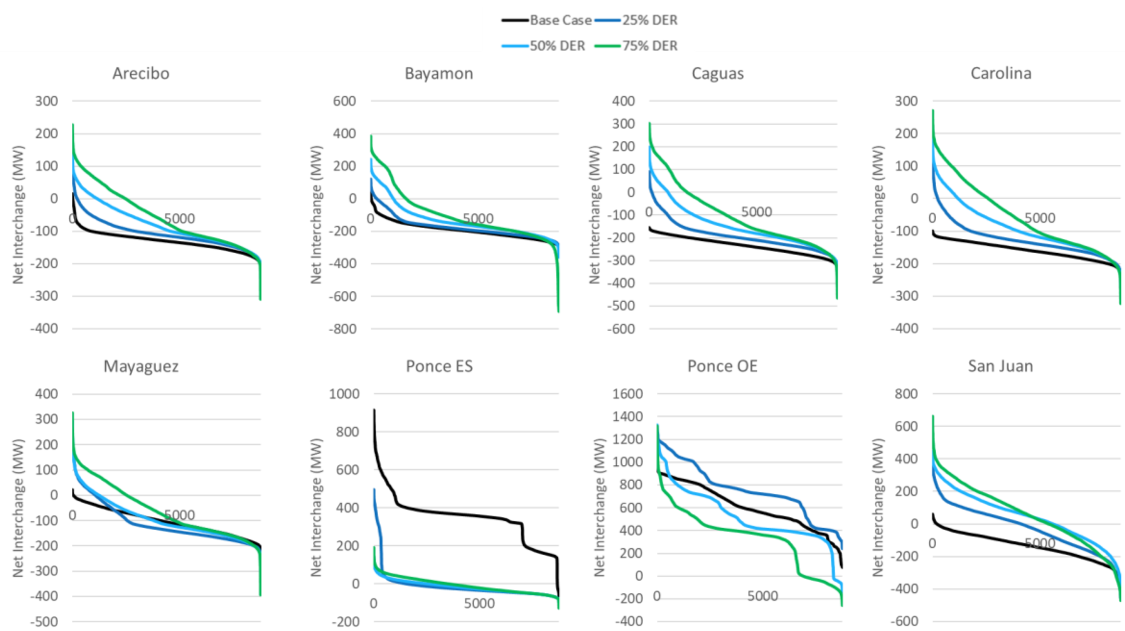

Figure 23: Duration Curves of Hourly Net Flows (MW)

5.4 Operations of Solar and Battery Storage

While the previous section focused on the total system dispatch and changes to the fossil fleet, it is also important to evaluate the utilization of the solar and storage resources. One important metric is the overall curtailment, which represents the amount of variable renewable generation that cannot be delivered to the grid due to oversupply and flexibility constraints. This can occur for both wind and solar resource and is often presented as a percentage of total available generation based on weather conditions.

With the coincident rise of battery storage the increase in solar DER curtailment is effectively mitigated, despite solar PV exceeding total load in many hours of the day. Figure 24 provides the annual curtailment of wind and solar resources, as a percentage of available energy. This figure shows that curtailment of solar resources is always quite low and is highest (on a relative basis) in the Base Case before any storage is added. This same relationship holds true for wind power that is curtailed. It is highest in the Base Case with no curtailment during the 25% and 50% DER cases but experiences a slight resurgence in the 75% DER case. Wind curtailment is higher than solar (on a relative basis) for two reasons; for one it is not paired with battery energy storage and thus is less likely to be shifted to later time periods, and second the DER is given “priority” to generate because it represents customer-sited generation. From a total renewable energy perspective, curtailment is limited to no more than 1% in all the DER scenarios.

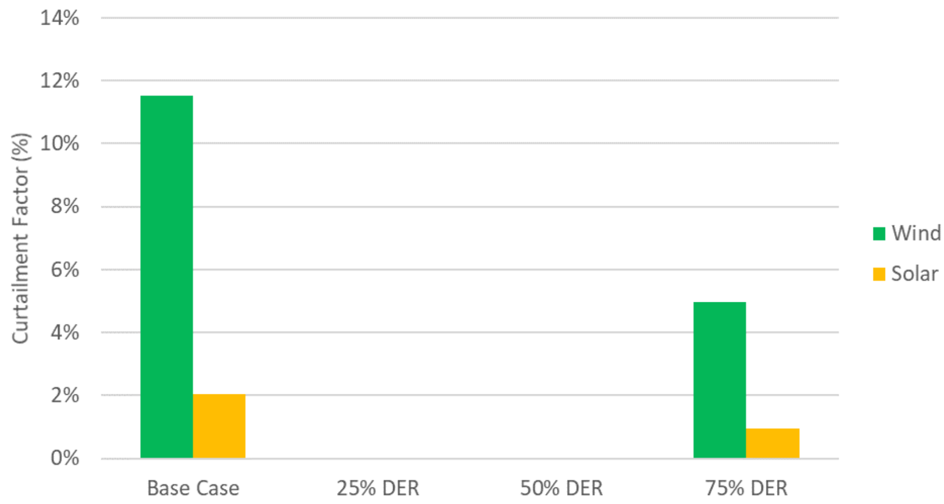

Figure 24: Curtailment Factor by Unit Type

This low level of curtailment is primarily due to the amount of battery storage that is also added to the hybrid systems. The impact of battery storage is clear when looking at Figure 25, which shows the net-generation of the battery storage fleet for the average day across the year. Positive numbers represent battery discharge and increased generation on the grid, and negative numbers represent charging (or increase in load). On the x-axis there are 24 hours starting with 0 and going to 23.

The chart shows the batteries on average discharge during evening peak load hours after sunset (hours 17 to 23) and early morning load hours before sunrise (0 to 6). Charging occurs predominately in the middle of the day, in line with the solar generation profile. This is also in line with the behavior shown in Figure 17. The net-generation changes highlight why we see minimal curtailment of solar while adding storage. As DER increases from 25% to 75%, the amount of generation charging the batteries in the middle of the day increases markedly, from just above 500 MW in the 25% DER case to more than 1,500 MW in the 75% DER case.

Figure 25: Average Battery Net Generation (left) and State of Charge (right) by Hour of Day

While looking at net-generation data is helpful it is also worthwhile to look at total energy, or MWh, of storage during an average day, as shown in Figure 26. This represents the amount of energy, on average, that is stored in the battery for use at a later time. The same profile is visible with the batteries charging during the day (increasing the battery storage to higher levels) and discharging in the morning and evening hours (depleting the battery storage to lower levels). From the 25% DER case to the 75% DER case there is more than twice as much energy stored in batteries going into the evening peak hours. Despite the 75% DER case starting from this higher level the batteries on average draw down to a very similar point across the three cases. This is due to the fact that batteries are also able to provide valuable grid services and some energy is stored during overnight periods so that the batteries can provide reserves in case they are needed unexpectedly.

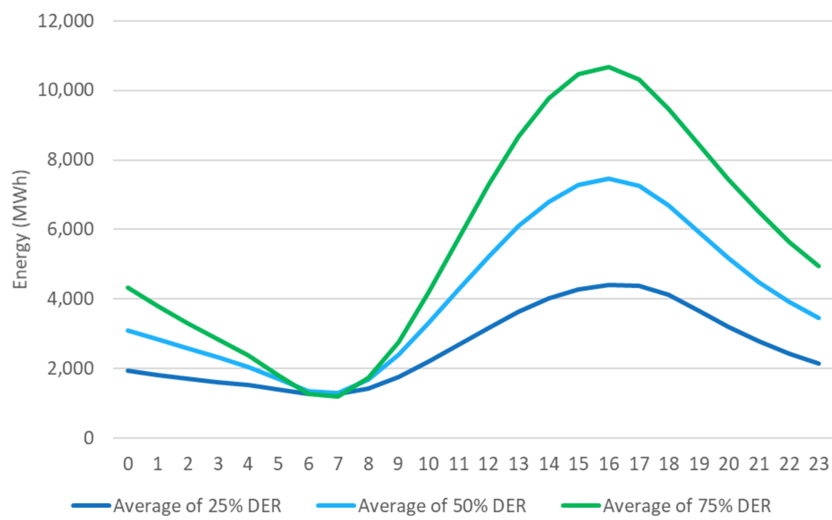

Figure 26: BESS Energy for the Average Day per Year

Another useful measure for battery utilization is the number of cycles that are accrued over the course of the year. It measures the total energy throughput of the battery, where one full charge and one full discharge is one cycle. Partial cycles can also be accrued, where two 50% charge and discharge events equal to one cycle. The total number of cycles provides an indication of how much the storage is utilized and is also important to measure expected degradation. There are multiple reasons why batteries may not be cycled fully each day:

- The solar resource is low and does not provide enough energy to charge the batteries and grid charging may not be economic nor necessary,
- The battery is not fully discharged because it is being utilized to provide contingency reserves,

The round-trip efficiency losses of charging the battery storage may not make it economic to charge all of solar energy when it can be delivered to the grid during the time of generation. This is illustrated in Figure 27 where the 25% DER case is on average seeing its battery resources cycle roughly 270 times per year while the 75% DER case has about 325 cycles per year. Note that this does not take into account potential additional behind-the-meter use cases of storage, which may change battery utilization due to an individual customer's use case. For example, any individual battery system may have output that is considerably different than the system-wide average, but on net the system would see battery utilization that generators during evening peak load hours and charges during the middle of the day.

`

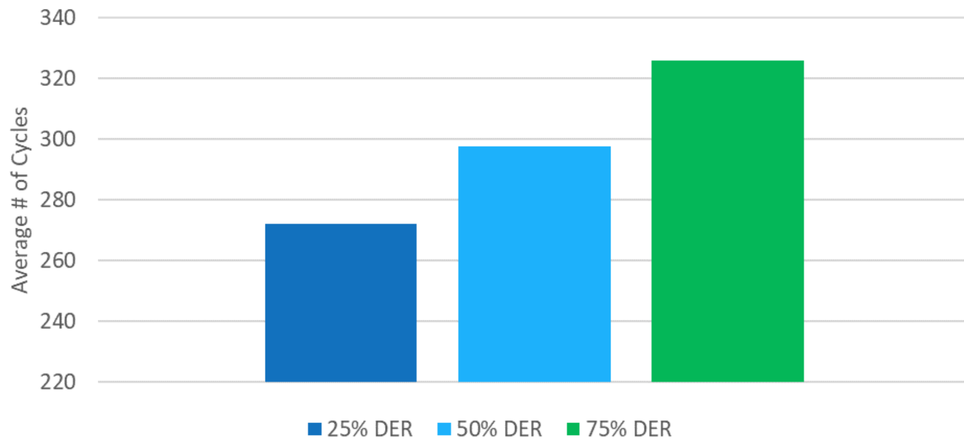

Figure 27: Annual Number of Battery Cycles by Scenario

5.5 Instantaneous Generation from Inverter-Based Resources

While the previous section covers the annual generation and utilization of DERs, it is critical to also evaluate the instantaneous operation of these resources across the entire year. This is because both solar and batteries (as well as wind) resources are inverter-based resources (IBR). IBR rely on a suite of power electronics, including the inverter, that help these units properly regulate their performance to meet grid conditions at any given time. As these resources take on a larger role in the grid there could be operational challenges, which are discussed in detail in Section 6. It is important to note that because solar and wind resources are variable they may, at times, reach very high levels of penetration (as a percentage of the grid's total resource mix) even if their annual generation levels are relatively modest.

Figure 28 shows that as more IBR is added with each scenario all hours have a greater total generation and percentage of IBR providing generation. Of particular note is that in the 50% DER and 75% DER case there are hours with 100% of generation coming from IBR, even after using storage to shift much of the surplus generation. Since inverter technologies needed to manage these conditions are still under development, reliability will need to be addressed through operational changes to mitigate challenges as well as consideration for synchronous condensers in higher penetration cases. In the 50% DER case only 4 hours across the entire year have all their energy coming from IBR – suggesting that this challenge could be mitigated with operational changes. However, in the 75% DER case nearly 1,250 hours have 100% of generation coming from IBR, this is just over 14% of all hours of the year. One could expect inverter technology advancing in the upcoming years to mitigate these situations, but if not the introduction of synchronous condensers could provide needed stability.

It is also helpful to see this data from an absolute MW perspective in the left plot. IBR generation often exceeds peak load (2,120 MW) in both the 50% DER and 75% DER cases due to the fact that much of the generation goes directly into the battery storage systems.

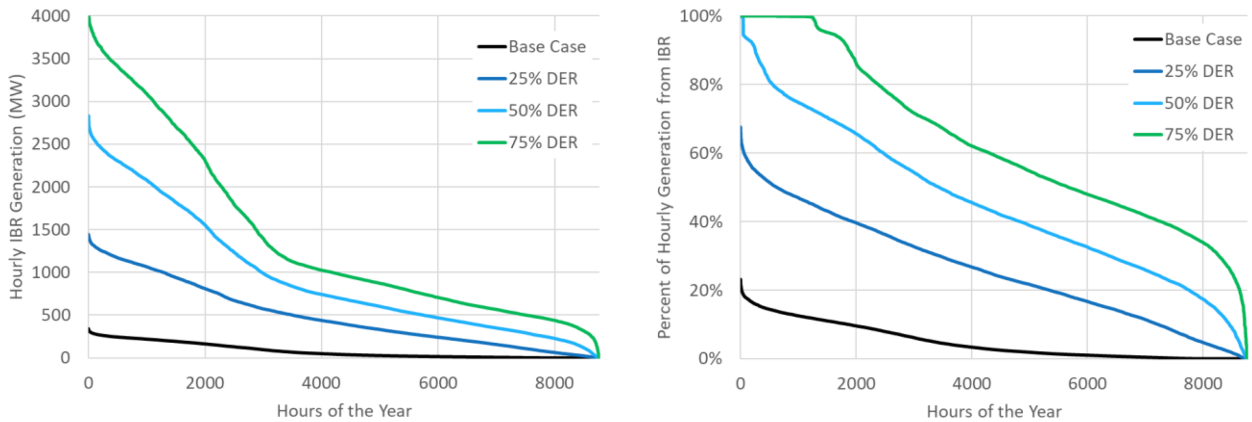

Figure 28: Duration Curve of IBR Generation (left) and Percent of Total Generation (right)

As mentioned above, the peak load is only 2,120 MW so it is clear there are hours when solar is generating much more than load. Although this surplus energy could be curtailed, Figure 24 shows this rarely happens. Instead this surplus is being used to charge batteries. Figure 29 highlights how even in the 25% DER case there are hours where solar is approaching 100% of load. By the time the system achieves 50% DER and 75% DER the system is experiencing times when solar is generating more than 200% of system load. This chart highlights the large role battery storage has on the system and the sheer scale of the resource mixes evaluated in this study.

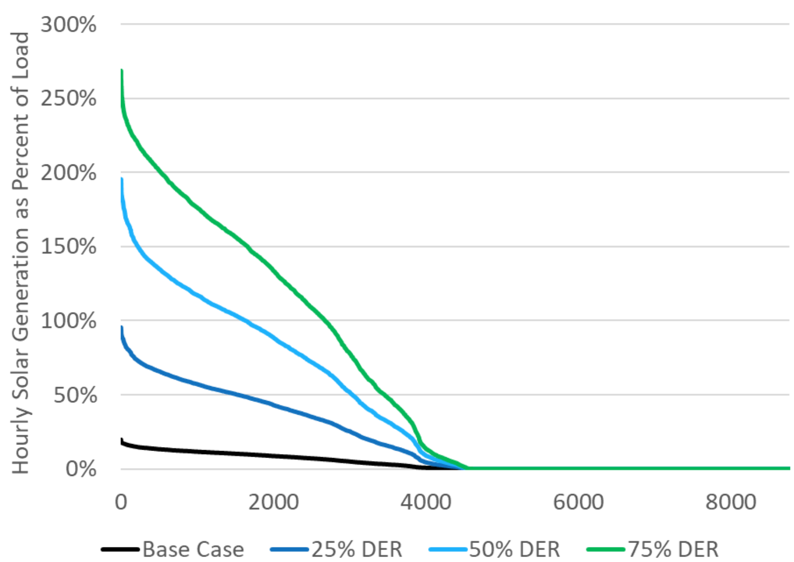

Figure 29: Duration Curve of Hourly Solar Generation as Percent of Load

Another way to view the impact of increased IBR on the system is to look at the number of fossil fuel-based units online across each hour of the year. This directly relates to the amount of synchronous inertia online (discussed more in Section 6). A system is generally more stable with a larger number of units online as there is more inertia and ability to maneuver the system to compensate for either a loss of any given generator or other unexpected changes to grid operations. In Figure 30 the Base Case has anywhere from 20 to 6 units online at any given hour, whereas the cases with an increased amount of

DER rarely have more than 8 units online. Both the 50% DER and 75% DER cases almost always have less than 6 units online, the minimum number of units online during any hour of the Base Case. The hours during which there are fewer fossil fuel units online correspond to periods of higher solar generation in the DER scenarios. The units that stay online during these periods are those providing more baseload like power, even if they are often forced to cycle themselves, which in the DER scenarios are the combined cycle units. This behavior is illustrated in the dispatch diagrams included in Figure 17 and Figure 18. The number of fossil units online does not represent a problem in and of itself, but it is a key metric to watch. Especially as the system spends an increasing amount of time operating in the range of 2 to 0 units as experienced in the 75% DER case.

And as above, the percentage of generation from fossil fuel-based units is a helpful way to see the impact that increased DER penetration has on the system. In Figure 31, the Base Case is almost entirely reliant on fossil fuel-based generation while there is a marked decrease on its reliance as the DER buildout increases. This is also apparent when looking at the absolute amount of generation from fossil fuel-based units, as shown in Figure 32. Although the reliance on fossil fuel-based units decreases with the integration of more DER capacity, they are still needed during more than a third of the year to cover more than 50% of load in even the 75% DER scenario. These are hours where there is either low solar output and/or high load.

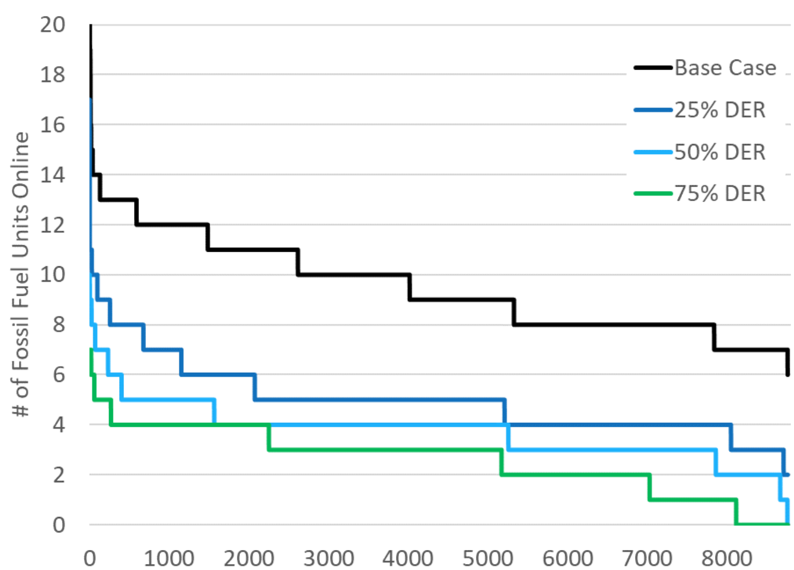

Figure 30: Duration Curve of Number of Fossil Fuel Units Online

`

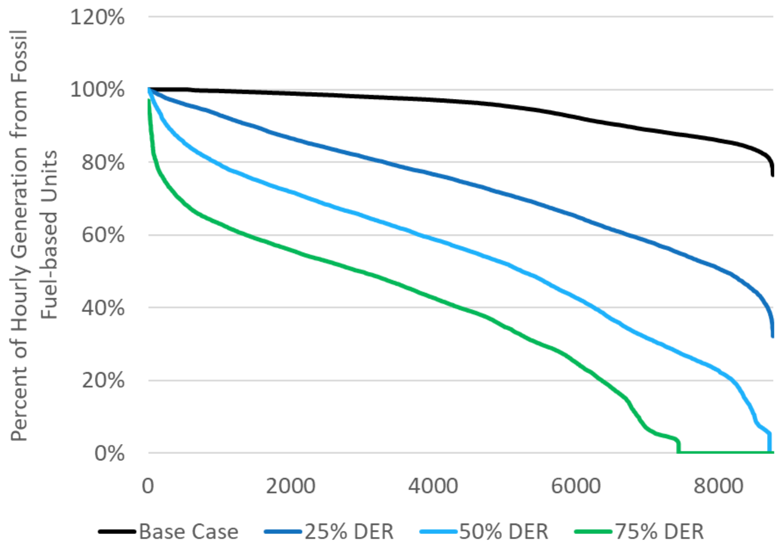

Figure 31: Duration Curve of Percent of Hourly Generation from Fossil Fuel-based Units

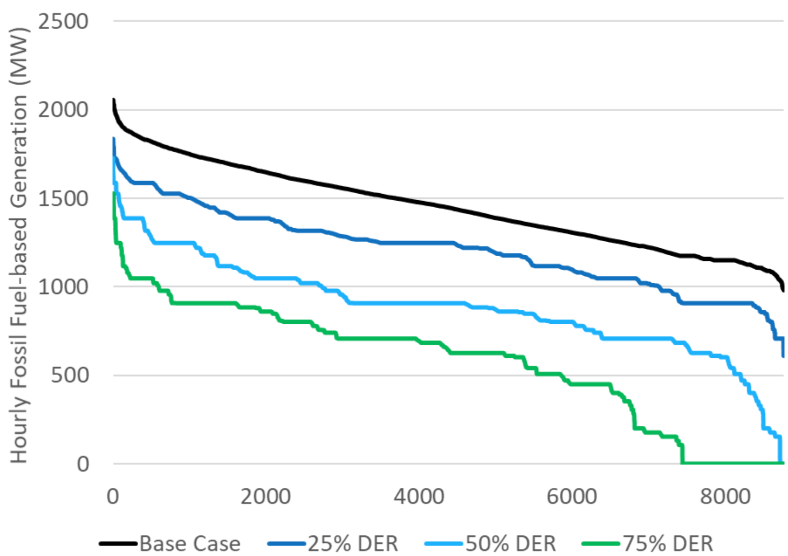

Figure 32: Duration Curve of Hourly Generation from Fossil Fuel-based Units

6 Grid Stability Analysis and Results

6.1 Introduction

All electric power grids must be analyzed to ensure stable operation under a large variety of operating conditions, environments, and grid disturbance events. This is true regardless of the level of renewables on the grid. However, grids with very high levels of renewables face more acute technical challenges because of the high-levels of inverter-based resources (IBR) like PV and battery systems and the displacement of conventional power plants with synchronous machine technology. However, these new resources also offer new benefits for supporting the grid in ways that were not previously available with a conventional power plant technology. These benefits are primarily due to the flexibility and speed of the inverters that form the interface between the resource (solar or battery) and the grid. The flexibility is because of a programmable response of inverters to different grid conditions and grid events. The speed refers to the faster rate at which IBRs are capable of responding to changing grid conditions. While a fast or faster response is not always desirable, it can be useful in certain circumstances. These advantages, coupled with an energy reservoir as in the case of battery storage, makes for a powerful combination (as shown through simulations of the grid in this section) that can help support a future grid with a dramatically different generation mix than the one that exists today.

6.2 Technical Challenges Assessed

To assess the stability of the grid under the proposed high-renewable scenarios, the following aspects of grid dynamic stability have been evaluated by simulating the response of the grid to disruptive events or grid disturbances. When studying a grid at such high levels of inverter-based generation, it is important to acknowledge the limitations of the simulation tools and to differentiate between challenges posed by the simulation tools and challenges posed by the operation of the physical grid itself. An overview of these challenges is presented in Table 10.

Table 10: Overview and Differentiation of Challenges for High-Renewable Grids

Grid Stability Challenges (Physical)	Analysis Challenges (Simulation Model)
Frequency Stability (i.e. low inertia)	Numerical solution divergence
Fault Recovery (i.e. ride-through)	Insufficient inverter detail represented
Inverter control stability	Insufficient grid detail represented

Grid Stability Challenges

The frequency stability challenge refers to the ability of a grid to maintain a frequency near its nominal value, in this case, 60Hz. Large deviations in system frequency from the nominal value (greater than about 1Hz) trigger emergency protection schemes like load-shedding, while very large deviations in frequency (greater than about 2Hz) push the grid close to its limit and often result in a grid-wide collapse or blackout.

Grid frequency is maintained close to 60Hz by maintaining a balance between generation and load. If generation exceeds load (for instance, due to a sudden loss of load), then grid frequency rises and generation must be reduced to bring frequency back to nominal. If generation drops below load (for instance, due to a sudden loss of generation), then grid frequency decreases and additional power must be injected to the grid, or load must be reduced or shed, in order to restore grid frequency.

These corrective actions must be taken quickly, within a few seconds or less, in order to be effective. This is because grid frequency will continue to deviate further and further from its nominal value until the power balance is restored. Providing the corrective power too late will result in a grid blackout if the grid frequency has already reached a point beyond which there is no return due to the excessive disconnection of other generators for self-protection reasons. Furthermore, the window of time in order to restore power balance after the initial loss of generation event is dependent primarily on the size of the initial power imbalance (MW of power generation being produced by the generator that suddenly disconnects or "trips") and the number and size of remaining synchronous machines (conventional generating units) online. Each synchronous machine online provides an "inertia" to the grid that opposes sudden changes in grid frequency, just as a car driving down the road continues to coast even if accelerator pedal is suddenly not depressed. More synchronous machines and physically larger synchronous machines contribute higher amounts of inertia, which helps provide a longer window of time to correct the power imbalance. However, as more renewable generation comes online and fewer synchronous machines are needed, the inertia of the grid decreases and the window of time to respond to a loss of generation, particularly a large loss of generation, shrinks.

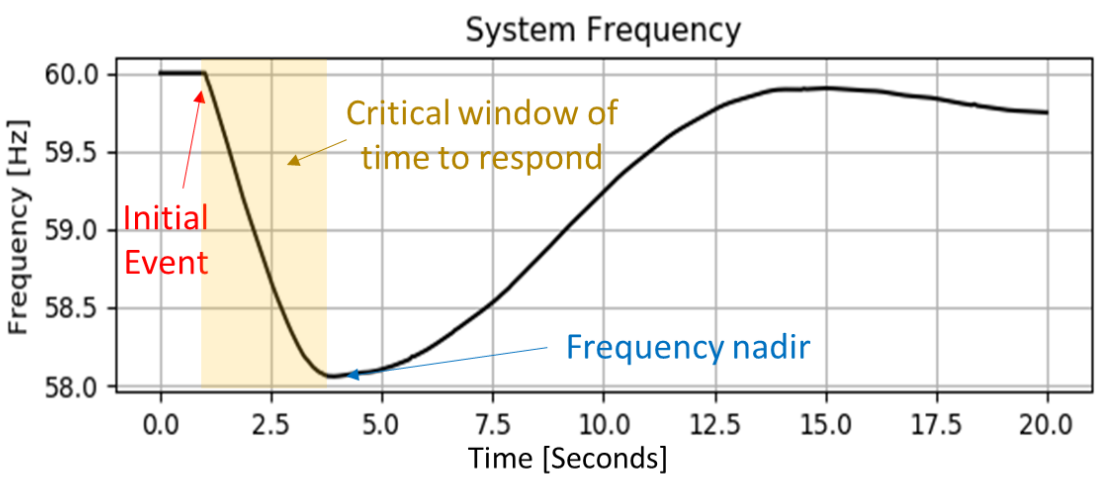

Figure 33 : Illustration of a Loss of Generation Event on Grid Frequency

In this analysis, the focus is on a loss-of-generation event because it is generally more difficult to quickly increase generation power than it is to quickly reduce power from existing generation, as would be needed for correct a loss of load event. In this analysis, it is assumed that the auxiliary load of a generating unit remains online even if the generator itself is lost, which is typical as the pumps, fans, and control systems of a power plant are designed to remain connected to the grid even if the generator disconnects.

Another group of challenges is termed "Fault Recovery," which is the ability of the grid to recovery from a fault event, or a short-circuit on the grid. Grid faults may be causes by obstructions like trees falling on transmission lines, lightning strikes of lines or towers, the collapse of transmission towers, etc. When such a fault occurs, the grid is designed to quickly remove the faulted transmission line from service, thereby "clearing" the fault from the grid, as shown in Figure 1. The intention is that the grid continues to operate without the line in-service until a crew can be dispatched to repair the line.

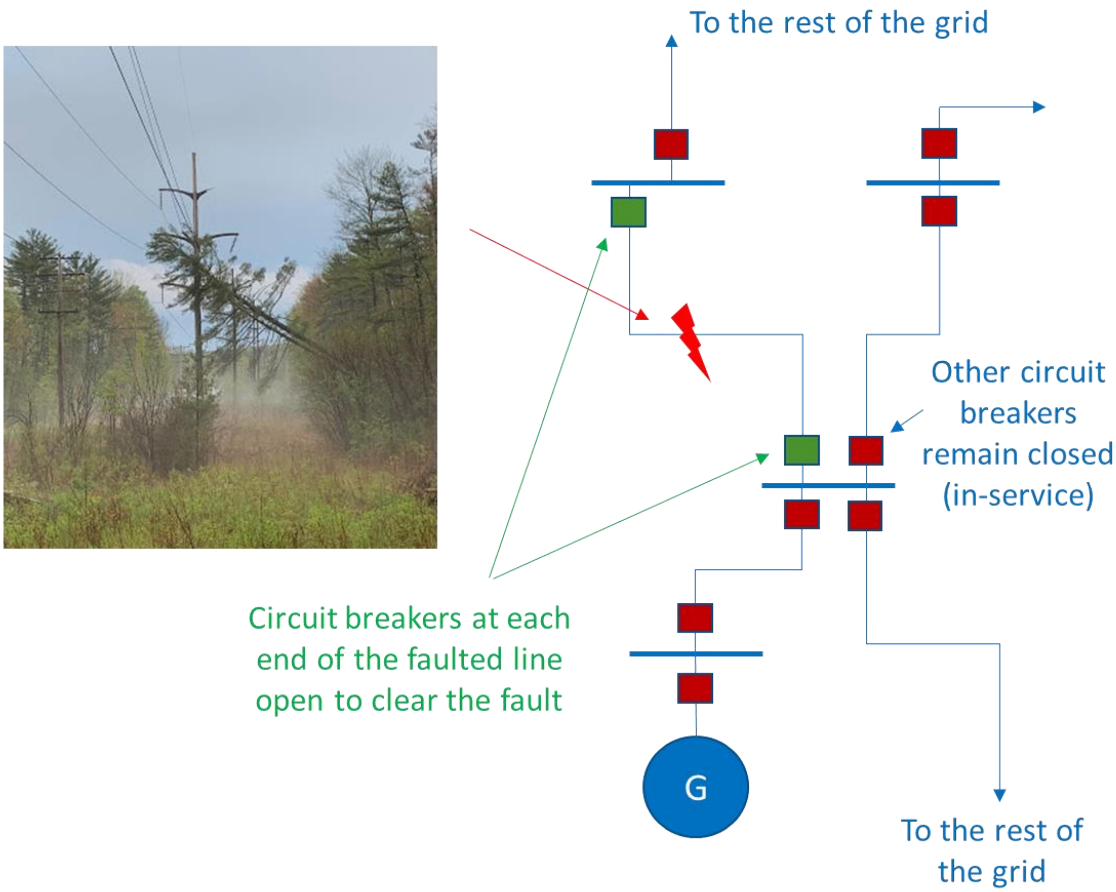

Figure 34: Illustration of a Grid Fault Event

In the brief period of time between the onset of the obstruction contacting the transmission line and the time when the circuit breakers on either end of the line open, the voltage on the line is severe depressed from a normal voltage of near 1.0 per-unit (pu) to near 0.0 pu, as shown in Figure 35.

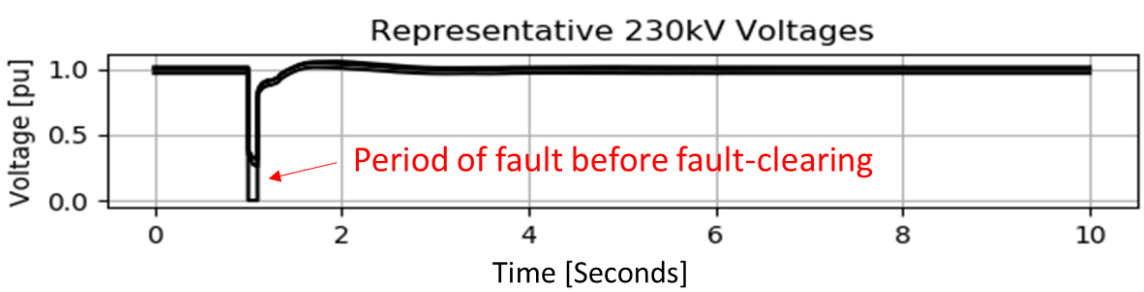

Figure 35: Illustration of a Fault Event Simulation

During a fault event where voltages are severely depressed, the ability of the transmission system to transmit power is very limited, such that generators cannot deliver the power they are generating and load suddenly stop receiving power. The impact this has on the grid is highly dependent on the type of generation (synchronous or inverter-based), the configuration of the generator's controls, the types of loads (i.e. electric lighting loads behave very differently from electric motor loads in air-conditioners), and the depth of voltage depression as seen by each generator and load. Furthermore, grid response to a fault depends on the duration of the fault (the time before the fault is cleared) and the number of phases involved in the fault. For this analysis, faults are assumed to be 100msec in duration, involving all three phases, and have zero fault impedances; assumptions which are aligned with PREPA's transmission planning practices. It is important to note that three-phase faults are the most severe type of fault and also the rarest type of fault in reality. Therefore, these assumptions are considered conservative.

The final group of challenges considered are inverter control stability challenges. These refer generally to the behavior of an inverter to respond in a stable manner to grid events like the loss-of-generation events and fault events described. Examples of unstable behavior includes oscillatory behavior to a failure to ride-through and recover from the disturbance without causing voltages or currents that are damaging to the inverter or other equipment. While time oscillatory behavior may be acceptable for brief periods of time (well-damped behavior), sustained or growing oscillations are not acceptable. Such oscillations may be the result of improper tuning of inverter controls for the grid conditions, or they may be the result of interactions among various inverters and/or synchronous machines on the system. These unstable behaviors are often initiated by a fault or loss-of-generation event, and therefore, the simulated disturbances are also testing for inverter control stability.

This analysis is intended to be an initial foray into analyzing ambitious and challenging set of proposed scenarios that shows a viable path forward by identifying challenges, potential mitigations, and where more attention is warranted. It is acknowledged that this analysis does not cover every aspect of grid stability. For instance, transmission protection systems are a critical part of operating a reliable grid as they are responsible for quickly identifying faults on the transmission system and clearing them with minimal impact. The industry has recognized that high levels of IBR present new challenges in the correct identification and discrimination of grid faults by some transmission protection schemes. While this analysis considers basic transmission system protection (voltage and frequency deviations), it does not consider the detailed inner workings of actual transmission line protection relays on the grid, which should be considered at some point along the journey to realizing the proposed scenarios.

Analysis Challenges

The simulation tools and models used in this analysis are widely used across the industry for transmission studies and stability analysis, and these models have been found to work well for grid with low to moderate levels of inverter-based equipment relatively to the levels of synchronous machine-based equipment on the grid. As the collective rating of IBRs approaches the collective rating of synchronous machines on the grid model, or even in a region of the grid model, several problems in the analytical domain can arise:

- The simulation tools struggle to find a numerical solution or converge. While a failure to converge can be indicative of an infeasible operating condition in reality, this is not necessarily the case. Other tools or methods must be applied to confirm that such a conclusion is valid. To mitigate this challenge, the parameters of the solution engine have been adjusted to improve the convergence characteristics of the model.
- The simplifying approximations made during inverter model development of actual inverter equipment and controls may no longer be valid in an inverter-dominant model. For instance, the

simplification or omission of special control functions and features may become more pronounced such that the model is no longer representative of the actual equipment. In general, the industry intends to develop models that are conservative such that inaccuracies due to simplifications made to the model cause the model to behave worse in simulation than in the field. Therefore, poor model performance is not always reflective of poor equipment performance. To mitigate this, the industry's best-in-class models have been applied and tuned to achieve good performance.

- The simulation tool, being a fundamental-frequency positive-sequence solution engine, is limited in its ability to capture all of the physical reality of the real world. Very fast transient events, transient responses, phase imbalances, harmonics, and non-sinusoidal phenomena are not captured in such a model. Other tools like electromagnetic transient (EMT) analysis tools have been developed to capture more completely these details as well as to facilitate full representation of inverter hardware and controls. However, these models require an order-of-magnitude more detail and complexity, which makes them more appropriate for subsequent detailed study work and not for initial study work.

It can be difficult to differentiate between a true grid stability problem and a modeling and analytical tool problem when analyzing dynamic simulation results with very high levels of inverter-based generation. In some cases, the simulation model may fail and appear to result in a loss of the grid when the grid operation would have been feasible in reality, resulting in a false-negative. It may also be possible to have false-positive results where the model predicts stable operation for what would be unstable in reality, but these cases are rare as the models are generally designed to be conservative and avoid producing false-positive results. Through experience and probing of the simulation tools, an engineering judgment is made on the results of the simulations presented in this analysis to determine at what point the PSSE models are to be believes and at what point other tools and models are needed for drawing conclusions.

6.3 Case Selection

The grid stability simulations capture the dynamic response of the grid over the course of 10 to 20 seconds following a grid event like a loss of generation or a fault event. Because it is impractical to simulate the dynamic response of the grid over the course of an entire year, as was evaluated in the production cost analysis, a selection of "snapshots" in time from each of the scenarios was selected for simulation of dynamic grid stability. The selection of these "snapshots" is very important as they must be chosen to be representative of a range of grid operations and not "cherry-picked" as worst-case or best-case operations, which would skew the conclusions drawn from the results.

To guide selection of representative snapshots for dynamic simulation, two important factors are defined and quantified for every hour of the year for each of the four scenarios. These are:

- **System Inertia**, H_{sys} [MW-s]: System inertia is a measure of the total inertia contribution from all online synchronous machines. Lower values of system inertia are associated with fewer synchronous machines online and result in the grid frequency moving faster after a disturbance, which makes a successful recovery of the grid more difficult.

$$H_{sys} = \sum_{0}^{i} MVA_i H_i$$

`

Where:
i is the i^{th} synchronous machine online in the grid, and
H_i is the inertia of the individual synchronous machine in per-unit on its MVA base

- **Synchronous Ratio** [-]: The synchronous ratio is defined as the ratio of the total rating (MVA) of synchronous machines online to the net generation (MW) of IBR at the time. Lower values of synchronous ratio indicate that the grid is becoming more inverter-dominant, which makes fault recovery and inverter control stability more difficult and also challenges the numerical methods used in the simulation tools.

$$Sync\ Ratio = \frac{\sum MVA_{sync\ machines\ online}}{\sum MW_{IBR\ generation,net}}$$

To see how these two important factors behave for the scenarios evaluated, a time-series of the first week of grid operations is shown in Figure 36. The top two windows show the total thermal generation and the total IBR generation in MW, respectively. The bottom two windows show the system inertia (H) and the synchronous ratio, respectively. In examining the inertia time-series, its shape is stepped as synchronous machines are brought online or taken offline. In the current scenario (black), the reduced inertia period tends to occur during overnight (early morning) periods where load is reduced and there is less need for power plants to be online, as would be expected. Examining the synchronous ratio time-series, the current scenario (black) shows generally high values (off the chart) indicating that there are far more synchronous machines online than MW production of IBR, as would be expected. During mid-day periods when there is more solar generation, the synchronous ratio dips into the 10-15 range, as would be expected.

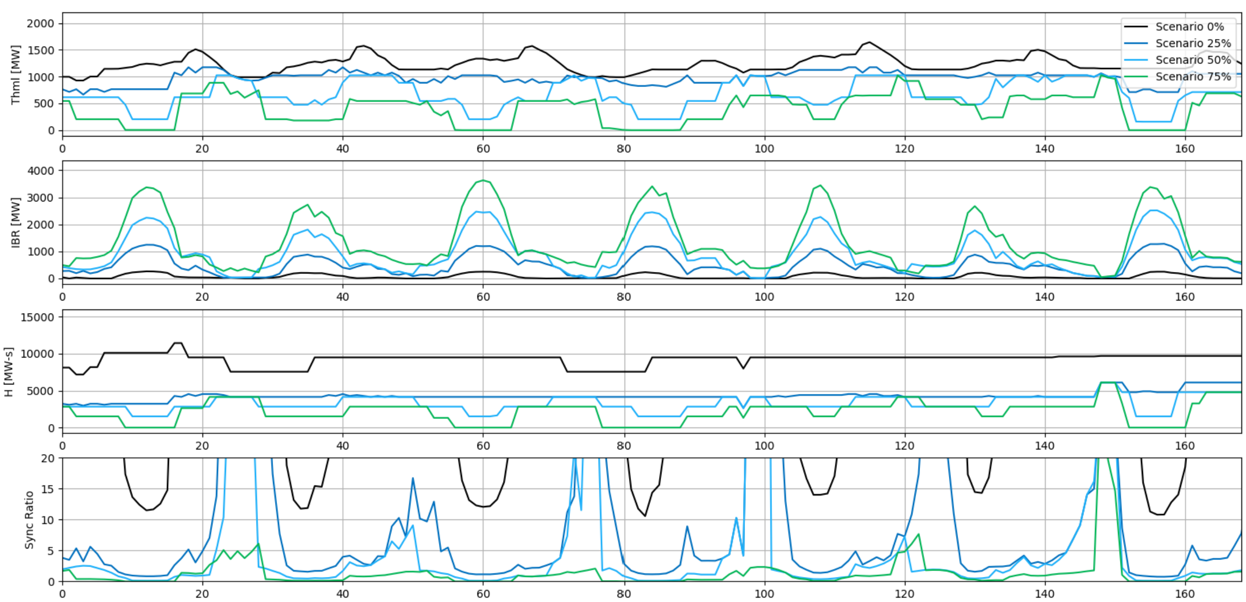

Figure 36: One-Week Time-Series of Grid Operations and Key Stability Factors

To examine the system inertia and synchronous ratio over an entire year of operation, the values of the time-series are sorted to form a duration curve for each factor and each scenario, which is plotted in

Figure 37. As expected, the scenarios with higher levels of renewables appear as lower values on the chart, indicating that those scenarios contain more hours of operation that are challenging to grid stability. Also note the extremely low values where system inertia and synchronous ratio both drop to zero, indicating that the production cost simulation anticipates time of an all-inverter-based grid. In the 50% scenario, this is expected for a small handful of hours in a year, which could be managed with relatively small operational changes to maintain a minimum number of synchronous machines online. In the 75% scenario, a fully inverter-based grid would be expected for over 1000 hours in a year, which would require advanced inverter technology like grid-forming inverters and/or the use of existing technologies like synchronous condensers, both of which are discussed in more detail in Section 6.6 .

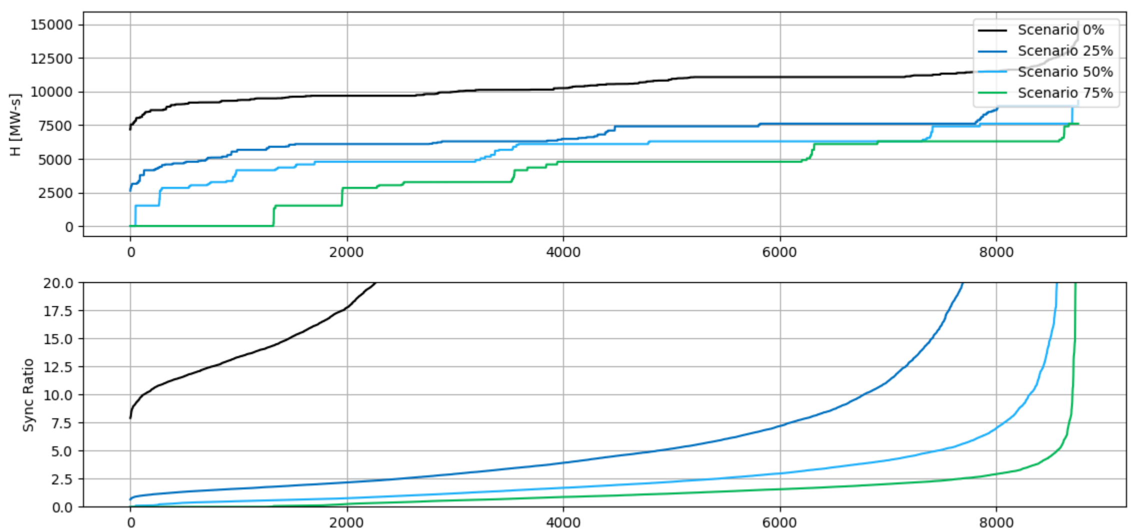

Figure 37: Duration Curve of Key Grid Stability Factors

Next, the specific hours or snapshots of grid operation are selected for dynamic simulation, which are shown on the duration curves as red dots in Figure 38. The selection criteria included that each scenario be evaluated, but with a focus on higher renewable scenarios. It is important that a range of system inertia values be evaluated (different "stair steps" on the plots) as well as to capture a range of synchronous ratios, with a focus on lower values where IBR generation is higher.

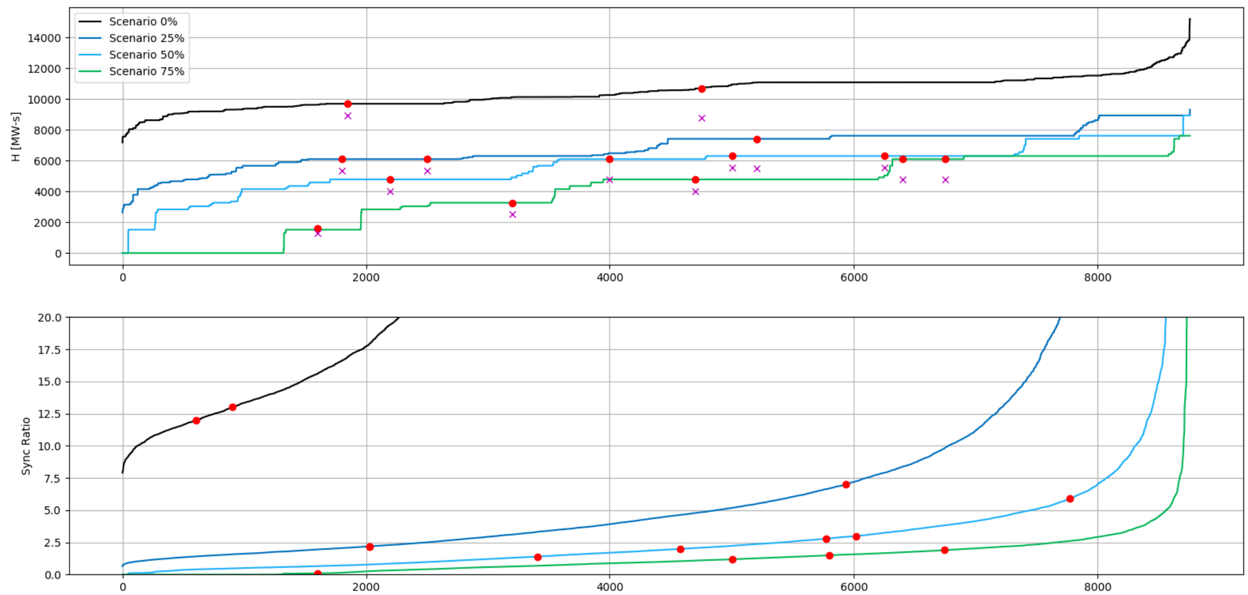

Figure 38: Case Selection for Dynamic Stability Simulations

Furthermore, it is important to consider for the loss-of-generation events, conditions where there is high levels of generation from the largest unit because the loss of a very large generator is more devastating to the grid than the loss of a small or minimally-dispatched generator, even if the system inertia in that case was slightly lower. Table 11 shows the highest dispatch of the largest single generators on the system for each scenario; the red text highlights the value and unit with a maximum dispatch for the scenario.

The cases that include the maximum dispatch shown in red have been included in the analysis for loss-of-generation events as they challenge grid stability in ways not necessarily captured by the system inertia and synchronous ratio factors alone. A magenta "X" on the system inertia plot shown in Figure 38 is used to mark the system inertia level remaining on the grid after a loss of the largest unit. To provide more context for these, the last row of Table 11 shows the percentage of hours over a year of operations where the unit with maximum generation is within 90% of its annual maximum dispatch.

Table 11: Highest Single Unit Dispatch Generation Values for Each Scenario

Generator Unit	Pmax (MW)	Base Case	25% DER Peak MW	50% DER Peak MW	75% DER Peak MW
AES (1 or 2)	227	155	0	0	0
Eco Electrica ST	181	178	181	181	181
Costa Sur ST (5 or 6)	410	360	410	**410**	**410**
Aguirre ST (1 or 2)	450	**367**	**450**	0	0
Palo Seco ST (3 or 4)	216	156	0	0	0
% of hours red unit is within 90% of Peak MW		0.3%	1.2%	13%	3.8%

It is noted that the loss of the entire Eco Electrica combined-cycle power plant (507MW total) is not considered in the loss-of-generation scenarios, but only loss of the largest individual unit of Eco Electrica

– the steam-turbine generator (STG). It is acknowledged that Eco Electrica is connected to the remainder of the grid by a single 230kV transmission line. While this line is short and its right-of-way well-managed, a loss of this line would result in a loss of the entire Eco Electrica plant, and potentially a system-wide blackout.

For each of the selected cases evaluated, faults were analyzed on 6 different transmission lines across the system, which is shown in Table 12 and Figure 39. As previous discussed, all faults are analyzed as three-phase, zero-impedance, six-cycle fault-and-clear events. The double-circuit transmission line from Aguirre to Aguas Buenas is modeled as both circuits being simultaneously faulted and cleared.

Table 12 : Summary of Transmission Fault Locations Evaluated

From Bus	To Bus	Circuit Voltage	Number of Circuits
Aguirre	Aguas Buenas	230	2
Costa Sur	Manati	230	1
Costa Sur	Maya TC	230	1
Costa Sur	Dbocas Fase	230	1
Cayey	Caguas	115	1
Guanica	San German	115	1

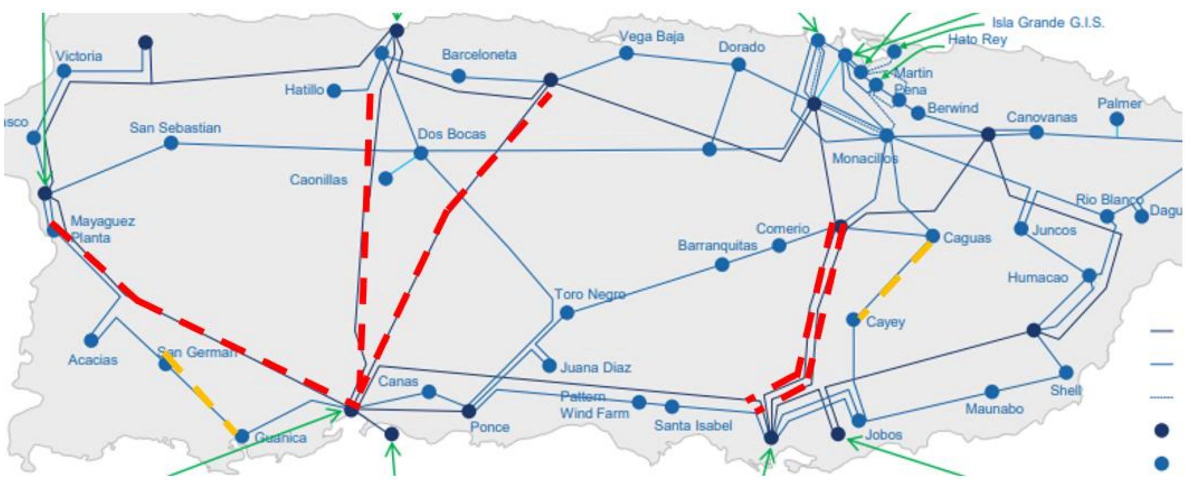

Figure 39: Transmission Fault Locations Evaluated

6.4 Loss of Generation Results

There are a few typical indicators used to evaluate grid performance for a loss-of-generation event, including frequency nadir and the amount of under-frequency load-shedding (UFLS). In addition, other indicators of performance include the rate-of-change-of-frequency (RoCoF), damping, system voltage excursions, and the quality of the recovery of the system. It is important to note that the Puerto Rican grid uses a sophisticated UFLS scheme that does not simply monitor grid frequency but also monitors the dynamics of grid frequency when decided whether or not to shed load. Such a system intends to minimize load shedding. In this case, the frequency nadir is a less meaningful metric because both severe and moderate grid events result in approximately the same frequency nadir. Therefore, the amount of UFLS is used instead as a primary indicator of system stress and margin from blackout.

First, the simulated response of the grid is shown in Figure 40 for a case in the current scenario with a loss of Aguirre STG2, where there is ample system inertia and a generally good recovery to the loss of generation. System frequency immediately begins to drop at 1.0 second when the generator is tripped. Three seconds later, the grid frequency has reached its lowest point and returns to a new steady-state point slightly below the nominal frequency, as would be expected until grid operator actions return the frequency to nominal. System voltages, of which a few 230kV buses are shown in the second window, indicate that voltage is well-controlled and after an initial loss of voltage support, voltages quickly recover, albeit with some relatively small oscillations due to the interaction of the remaining synchronous machines on the system. Figure 41 shows the collective response of the thermal generation fleet and the DER, which consists only of distributed PV. Thermal power generation decreases first due to the loss of the Aguirre unit, and then remain low due to the combination of load-shedding and a lack of governor response from the remaining thermal fleet. The DER power also drops in two large chunks, first at 3.5 seconds and again just after 7.5 seconds. This occurs for the portion of DER that is behind the UFLS scheme, such that as some load is shed to help the grid recover, some portion of the DER is shed. While not desirable, this is an expected result for most UFLS schemes operating on grids with significant levels of DER. A total of 255 MW is shed of a starting 1840 MW of total load.

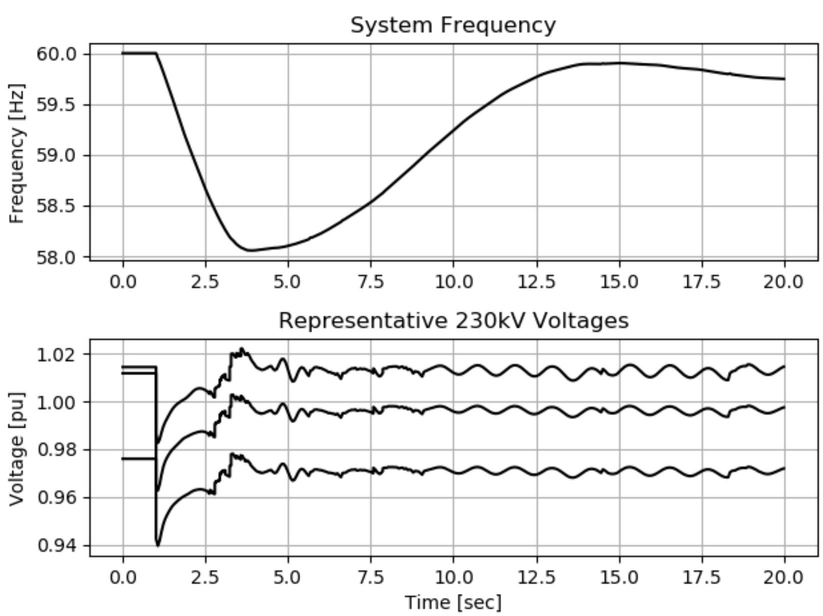

Figure 40: System-Level Response to a Loss-of-Generation Event, Current Scenario

`

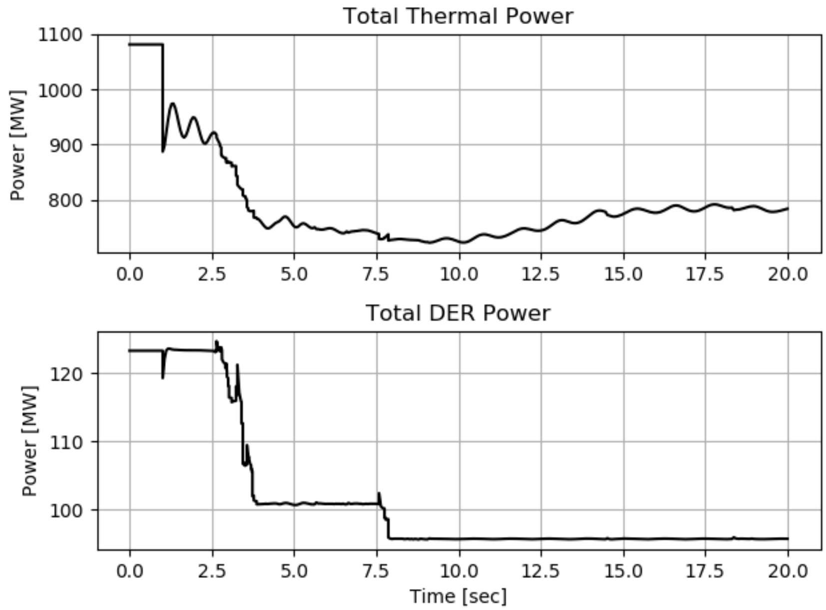

Figure 41: Generation Response to a Loss-of-Generation Event, Current Scenario

Looking at the 50% scenario in Figure 42, a snapshot is evaluated for stability that considers the loss of the Eco Electrica STG at a time when there is 200MW of DER net generation online. Figure 42 shows the response of the grid for 3 different variations. First, in the dotted traces, the generator is tripped and frequency declines as we saw in the previous graphs. The UFLS is activated, shedding load as well as over 100MW of DER that is integrated with the load. However, system frequency continues to decline, ultimately leading to a system-wide blackout because there is insufficient power injection from other resources to restore the grid to a stable equilibrium.

To mitigate this, fast-frequency response (FFR) functions are applied to the DER. The dashed trace of Figure 42 shows the response of the grid assuming that the DER has 50MW of FFR available and appropriately tuned to be deployed in 1 second. The UFLS is still activated (255MW) and 100MW of DER is disconnected from the grid by the UFLS. However, about 100MW of DER remains connected to help the grid survive, albeit with little margin. Grid frequency in the dashed trace stabilizes, but at a very low value near 58Hz. In the third variation, it is assumed that 150MW of FFR is available within the DER to be deployed over the course of 2 to 3 seconds. This fast and substantial injection of active power from DER is sufficient to stop grid frequency from falling past 59 Hz, where the grid stabilizes until subsequent grid operator actions can be taken to restore the grid frequency to 60Hz. Furthermore, no load is shed in this event. This demonstrated the power of properly configured FFR in not only saving the system from a blackout condition, but also potentially avoid load-shedding completely.

When the UFLS operates during an emergency event on the grid, one or more pieces of the distribution system are suddenly disconnected from the transmission system, typically at a 38kV substation. Each piece of the now-disconnected distribution system forms a separate and much smaller “islanded” grid. These small, islanded distribution grids would likely be comprised of different levels of DER (both solar and BESS) and load (residences and commercial/industrial centers without DER). The viability of an islanded distribution system to sustain itself and continue serving load as a microgrid or minigrid is complex and requires detailed study and specific design decisions that are beyond the scope of this analysis.

Most DER inverters are configured with "anti-islanding" detection logic that is designed to quickly detect a disconnection from the larger grid and shut down the DER, preventing an island from forming. This behavior has been historically desired for several reasons including safety of personnel and equipment, but this is changing. Even if the anti-islanding logic was disabled and even if there was sufficient battery energy and inverter power capabilities from all DER to cover the demand, today's inverters are not capable of sustaining a small, all-inverter grid, nor is the distribution system (specifically its voltage regulation and protection systems) designed to operate in this manner. In order to enable islanded microgrid operation, specific design and analysis is required for both the DER and the distribution system.

However, it is possible and relatively simpler to achieve a resiliency benefit from DER at the individual building. In the event of a loss of grid service, a building equipped with appropriately configured DER and sufficient inverter power rating and battery energy charge to cover essential loads for a period of time could disconnect from the grid at the building's electric service entrance and initiate islanded operation of the building alone. This is a simpler option because it does not require coordination of multiple DER or use of the distribution system in a way for which it was not designed. This approach could be used widely across the island in the 50% and 75% scenarios, given the number of households and DER ratings contemplated in this study.

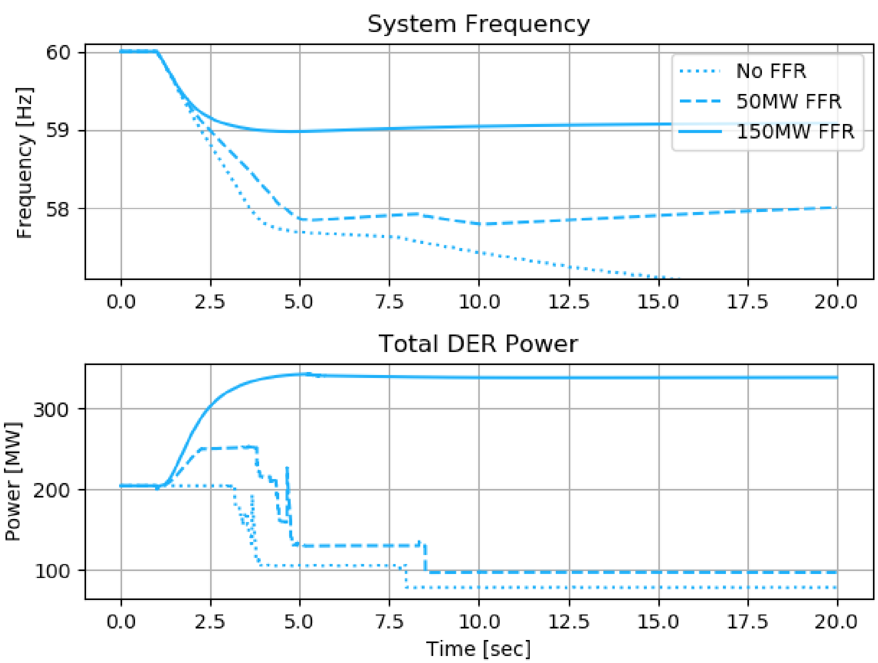

Figure 42: Grid Response to a Loss-of-Generation Event with Varying DER FFR, 50% Scenario

In the 75% scenario, Figure 43 shows the results of a case that considers a loss of the Costa Sur unit 6 dispatched at 410MW, leaving a system inertia level of 4780 MW-s remaining on the grid, which constitutes a very challenging condition. A total of 234MW of UFLS is activated in this case, which sheds a portion of the DER that was helping in the recovery of the grid. Ultimately the grid stabilizes with a peak deployment of nearly 250MW of FFR from DER and a sustained response of nearly 150MW of FFR from DER. However, it is noted that more than 250MW of total FFR are needed prior to the event to achieve this result because a portion of the DER is shed with the UFLS activation.

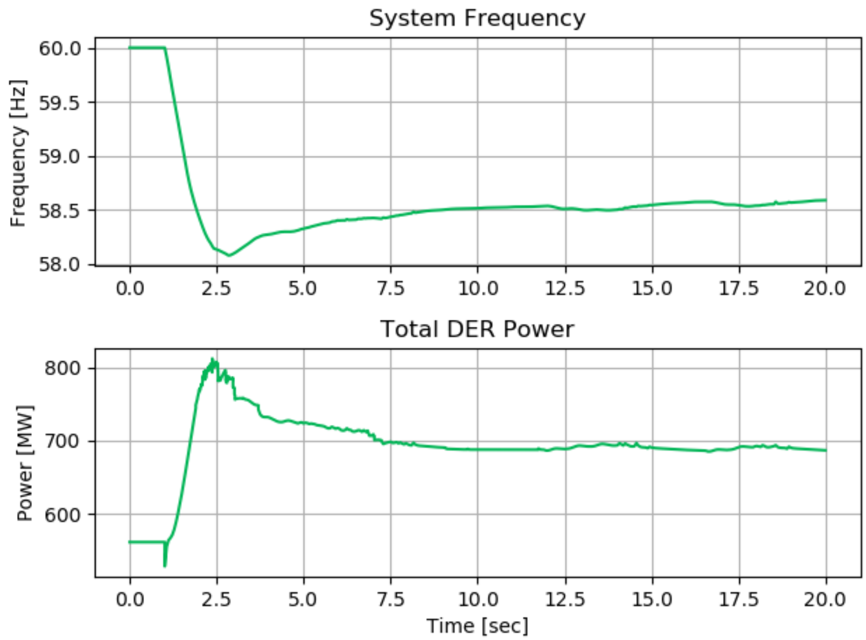

Figure 43: Grid Response to a Loss-of-Generation Event with DER FFR, 75% Scenario

The simulation of the remaining selected cases across all of the scenarios has been performance and the results are summarized and trends are highlighted in Figure 44. On the x-axis, the system RoCoF is plotted, which includes the impact not only of decreasing system inertia but also the MW dispatch of generator tripped, according to the equation:

$$RoCoF = \frac{\Delta P_{generation}}{2H_{sys}}$$

The stability of the system is challenged more for larger losses of generation as well as for lower levels of system inertia, both of which are captured in the RoCoF calculation, so that higher RoCoF values are indicative of more challenging loss-of-generation events. On the y-axis, the maximum deployed FFR is plotted. Each simulation is plotted as a point on the graph that is further color-coded according to the response of the grid in terms of whether the grid survives, and if so, how much UFLS was activated. Finally, the shaded regions of the plot are similarly color-coded to highlight the trends shown by the simulated cases, where the red region shows blackouts expected, the white region shows grid survival with no UFLS, and the yellow and orange regions show the survival with varying levels of load shedding.

As IBRs increase on the grid and conventional generation is displaced, the grid spends more time operating on the right half of the plot shown in Figure 44. If no mitigations were applied, it would be expected that blackouts would occur more frequently for loss of generation events. However, if FFR (note this is only one of many types of mitigation) is applied, it can not only enable the grid to survive loss-of-generation events, but also reduce or eliminate the need for load shedding. It is important to note that correctly applying FFR is not trivial. If the FFR is tuned to be too slow, it will not be effective and the grid may fail to survive the event. However, if the FFR is tuned to be too fast, it may over-react and/or result in oscillatory behavior and participate in adverse interactions with other grid equipment, destabilizing the grid and ultimately leading to a failure to survive the event.

It is also important to note that this graph and these results are based having some synchronous machines online. These results do not necessarily apply to an all-inverter based system, as will be discussed in more detail in Section 6.6.

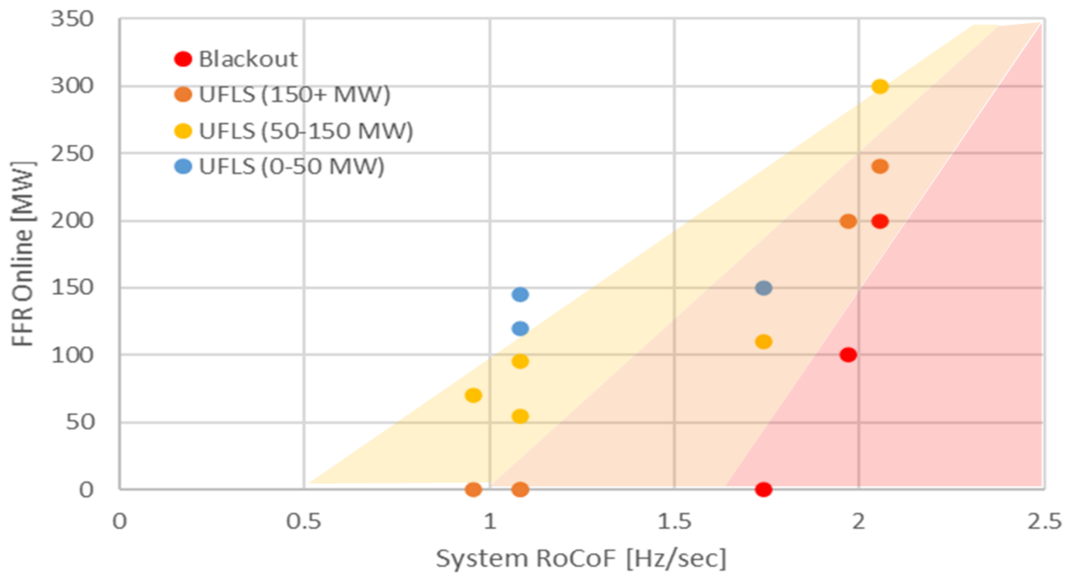

Figure 44 : Summary and Trends Identified from Loss-of-Generation Events

6.5 Fault-and-Clear Scenarios

A grid fault simulation result is shown first for the current scenario with a fault on the Costa Sur – Mayagüez 230kV transmission line in Figure 45 and Figure 46. At the onset of the fault, which is applied at 1.0 seconds, the voltage on the 230kV system is pull down below 0.5pu across the island. As a result, the electrical power being transmitted drops and there is an acceleration of the synchronous generators which results in an increase in grid frequency. As the fault is cleared, voltage quickly recovers, as does active power, which contains some damped oscillations due to the interaction of synchronous machines on the grid.

As shown in Figure 46, the DER also see very low voltages, which causes a reduction in active power. The DER are configured to provide voltage support for large voltage excursions, which can be seen by the attempt to increase reactive power output while voltages are low. After the fault is cleared, voltage return to a normal range and reactive power returns to its pre-fault level. Active power also decreases briefly due to the FFR functions acting to correct the over-frequency event. This performance is expected and is generally considered good.

`

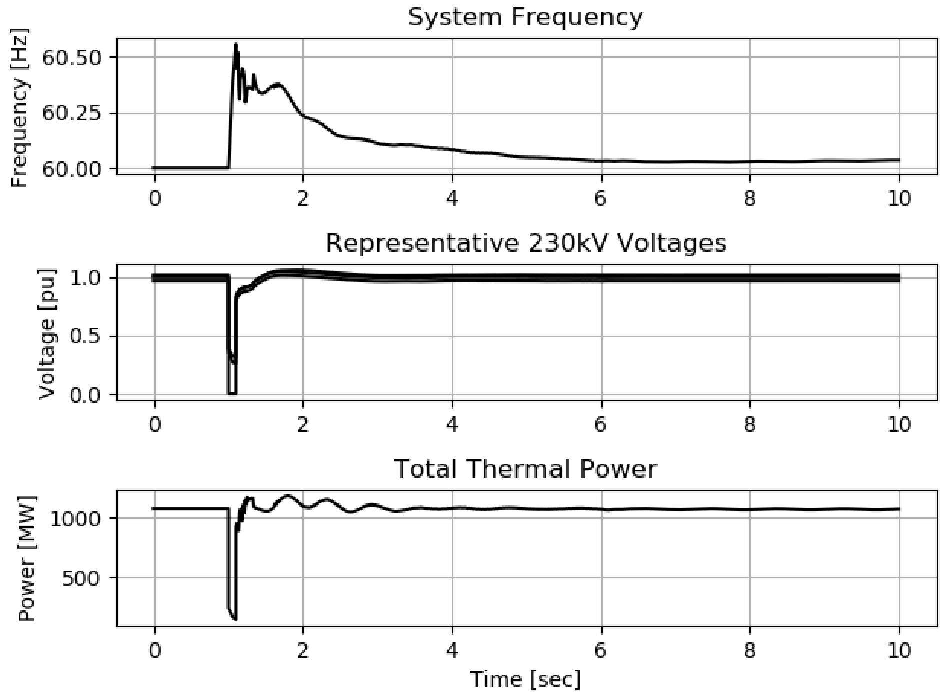

Figure 45: System-Level Response to a Fault Event, Current Scenario

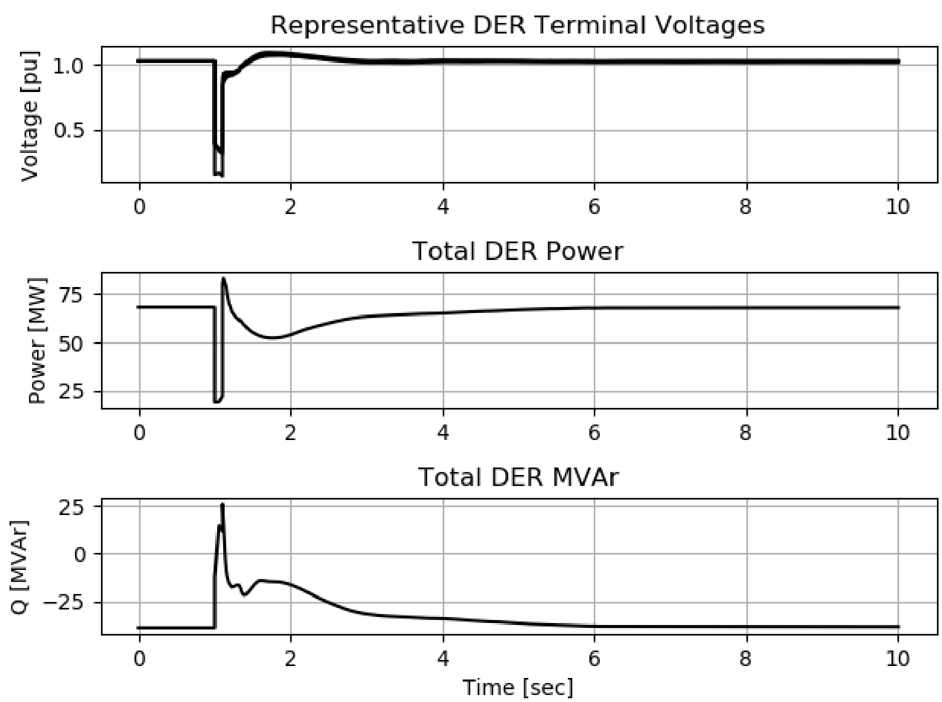

Figure 46: DER-Level Response to a Fault Scenario, Current Scenario

Next, the 50% scenario is assessed for two variations in DER configuration, which is shown in Figure 47, where the magenta trace shows the results from the same fault (Costa Sur – Mayagüez) and same DER configuration that was used in the current scenario shown in Figure 45 and Figure 46. This DER configuration already included FFR and volt-var response as well as ride-through protection settings consistent with modern values like California's Rule 21 and Hawaii's Rule 14H. However, this DER configuration reaches its limits for this 50% scenario case.

Unlike with the current scenario case where the synchronous ratio was 12.0, this 50% scenario case has a synchronous ratio of 2.0, meaning there is a significantly reduced presence of synchronous machines online, which is broadly in the direction of creating "weak grid" conditions. The weak grid conditions mean that there is less fast-acting voltage support typically provided by synchronous machines. This reduced support is manifested by the delayed recovery of voltage following fault clearing, as shown between 1 and 3 seconds in the simulation in Figure 47. This delayed voltage recovery is due to the stalling and re-starting of induction motor loads like residential air conditioners, which are represented by the dynamic composite load model. As the voltage gradually recovers, it achieves a level where the motor loads re-start, which results in a reduction in reactive power consumption and an increase in system voltage. The increase in voltage is seen across the system, including at the DER voltage levels. Despite the DER's attempt to control large voltage excursions (outside a +/- 5% of nominal) with their volt-var control functions, the high voltages persist above 1.1pu for over one second, causing most of the DER to trip. The sudden loss of power generation from the DER appear to the grid like an extremely large loss-of-generation event where there is no FFR from the DER available to arrest the decline in system frequency, resulting in a grid blackout.

However, by further increasing the volt-var response provided by the DER and expanding the over-voltage protection settings to tolerate 1.19pu voltage at the DER terminals for up to 4 seconds, the DER are able to ride-though and continue providing essential support to sustain the grid and its recovery, as shown in the solid blue traces of Figure 47.

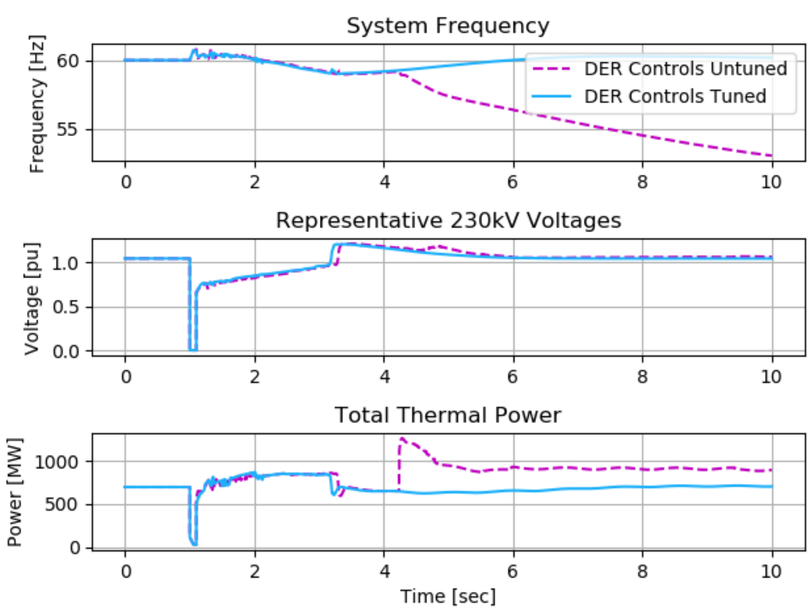

Figure 47: Grid Response to a Fault Event, Varying DER Controls, 50% Scenario

A fault on the double-circuit 230kV transmission line is evaluated for the same case of the 50% scenario as shown in Figure 47, where the results are plotted in Figure 48. Both traces of simulation utilize the best DER controls configuration, informed by the results of prior simulations. However, the difference between the magenta simulation, which shows a dramatic problem, and the blue simulation which shows reasonable response and survival of the system is the simulation time-step applied to the dynamic simulation in PSSE. The typical ¼ cycle time step used in most fundamental frequency dynamic simulation tools has been applied throughout these simulations and is used for the magenta simulation. For the blue simulation, a 1msec time step is used. The results of a model should not vary for small changes in time-step, and the fact that the result changes so dramatically indicates that these simulated grid conditions are beyond the capability of the simulation tools. While a more capable and detailed model may corroborate the survival shown in the blue trace, this cannot be assumed.

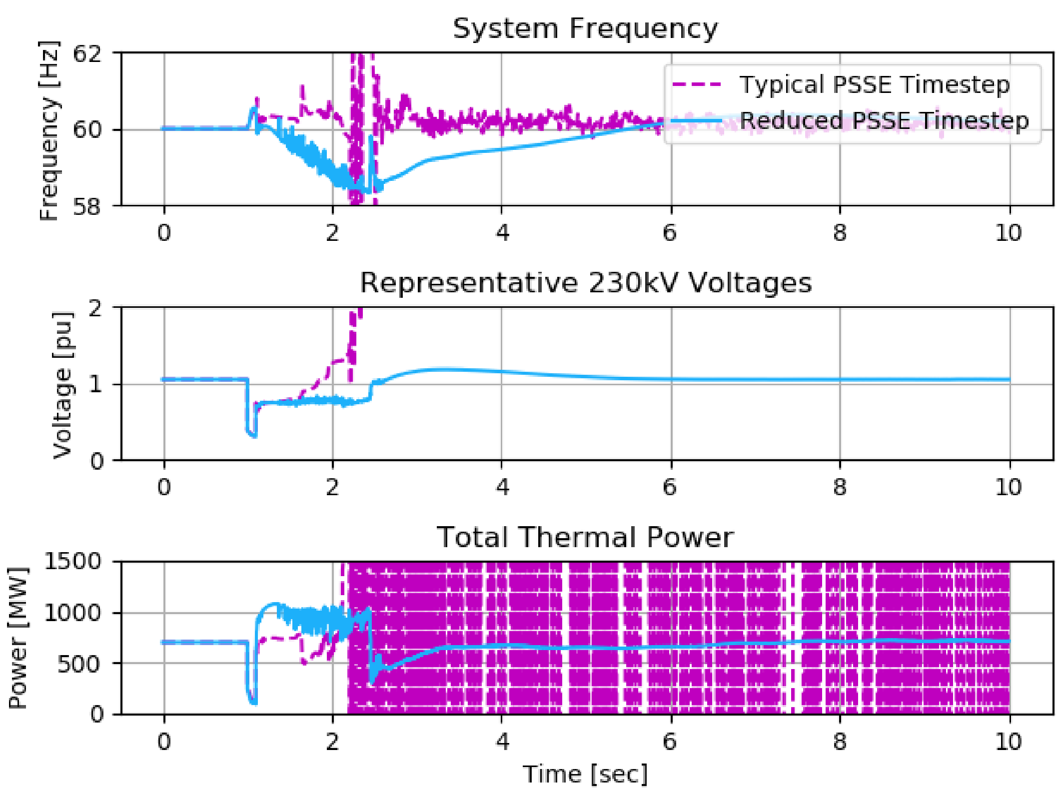

Figure 48: Grid Response to a Fault Event, Varying Simulation Time Step, 50% Scenario

The simulation of a case from the 75% scenario with a synchronous ratio of a mere 0.1 as shown in Figure 49 for both a typical time-step and a reduced time-step both show divergent numerical behavior, indicating that such scenarios are simply beyond the capability of the positive-sequence fundamental-frequency simulation tools, a result that was expected. Therefore, the stability of the grid for fault conditions for the very high IBR cases common in the 75% scenario cannot be evaluated in PSSE. Alternative methods for evaluating these cases are discussed in Section 6.6.

`

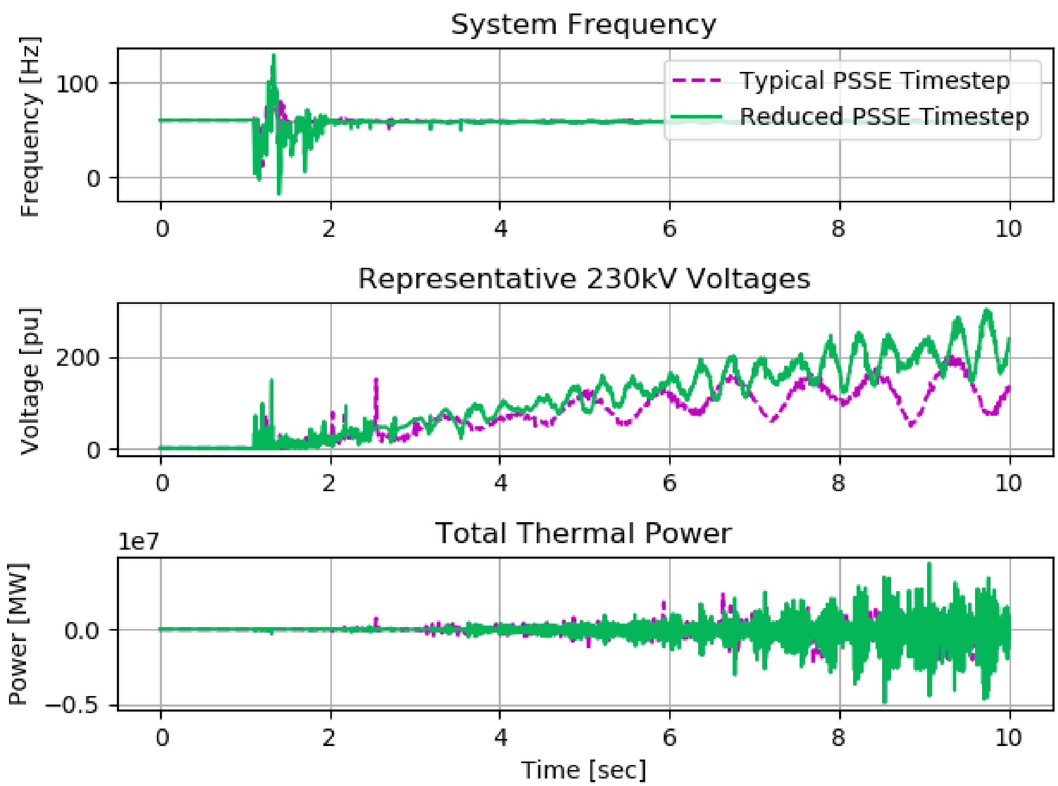

Figure 49: Grid Model Response to a Fault Event, Varying Simulation Time Step, 75% Scenario

A large set of simulations was performed for six different grid faults across cases from each scenario with various DER configurations in order to capture a broad range of operating conditions and identify the most effective DER control settings. The results are simplified and summarized in the following figures, which are color-coded as follows:

- Green cells for in cases where performance is considered good, similar to that shown in the current scenario in Figure 45.
- Orange is used for marginal performance where the grid survives but with some loss of DER and/or loss of load.
- Red is used for cases in which the system does not survive the fault event.
- Brown is used for cases in which there is evidence that the simulation tool is not capable of accurately simulating the event, as in Figure 49.

The following summaries including Figure 50, Figure 51, and Figure 52 show the evolution of DER controls and the resulting improvement in performance of the grid in response to transmission fault events. Beginning with basic implementation of “smart-inverter” functions and ending with tuned smart-inverter functions and reasonably expanded protection settings, the performance can be greatly improved.

Line | Scenario	Current	25%	50%	75%
Costa Sur-Manati 230kV				
Costa Sur-Mayaguez 230kV				
Costa Sur-Dbocas Fase 230kV				
Aguirre-Agubuena 230kV				
Cayey-Caguas 115kV				
Guanica-San German 115kV				

Figure 50: Performance Summary for Grid Faults with Basic DER Functionality

Line | Scenario	Current	25%	50%	75%
Costa Sur-Manati 230kV				
Costa Sur-Mayaguez 230kV				
Costa Sur-Dbocas Fase 230kV				
Aguirre-Agubuena 230kV				
Cayey-Caguas 115kV				
Guanica-San German 115kV				

Figure 51: Performance Summary for Grid Faults with FFR and Improved Volt-Var DER Functionality

Line | Scenario	Current	25%	50%	75%
Costa Sur-Manati 230kV				
Costa Sur-Mayaguez 230kV				
Costa Sur-Dbocas Fase 230kV				
Aguirre-Agubuena 230kV				
Cayey-Caguas 115kV				
Guanica-San German 115kV				

Figure 52: Performance Summary for Grid Faults with FFR and Improved Volt-Var and Expanded Over-Voltage Protection from DER

6.6 Very High Penetration Scenarios

Very high penetration of inverter-based resources like solar PV, battery energy storage, wind and whether or not they are distributed or utility-scale resources are challenging to grid operations for reasons of grid stability and resource adequacy. For resource adequacy, long-duration (multi-day) storage would be needed to cover outlier weather events where wind and solar resources may be very low for consecutive days or weeks. While there is plenty to be discussed on resource adequacy, this section will focus on the challenges due to grid stability.

High penetrations of IBR challenge grid stability because it typically implies that there are relatively few conventional synchronous-machine-based resources online, which provide important stabilizing benefits to the grid. The primary stabilizing characteristic of synchronous machine technologies is that they provide short-term (fractions of a second) storage of energy with a very high capability to release the energy (maximum currents that are multiples of their rated currents). The short-term energy reservoir in synchronous machines comes in two forms: the rotational energy of the spinning rotor and drivetrain and the magnetic field energy in the steel core of the generator. The rotational energy, typically described as inertia, acts to stabilize grid frequency during sudden changes in the power balance on the grid, like for loss-of-generation events. The magnetic field energy helps to provide a constant "voltage anchor" for the grid.

Today's inverter-based resources are designed to expect the grid to have these characteristics of inertia and "voltage anchors," and therefore, they rely on a certain level of synchronous machine technology to be connected to the grid with the IBRs. If today's IBR are connected to a grid that does not exhibit enough of these characteristics (ie. because there are too few synchronous machines online), then disturbances like a loss-of-generation will cause the grid to "move" or change state too quickly for the IBR to respond in a stabilizing way to support the grid. The result is typically a disconnection of the IBR and a lack of support to the grid that ends is partial or complete blackout.

There are two general approaches for enabling very high levels of IBRs on a grid. One approach is to improve the design and behavior of the IBRs such that they provide the inertia and "voltage anchor" characteristics that support the grid similar to the way synchronous machines do. This concept has been termed "grid-forming" inverter technology by in the industry. The second approach is to maintain the inertia and "voltage anchor" characteristics of the grid by keeping a sufficient number of synchronous machines online. Both approaches are briefly discussed.

Grid-forming inverter technology is in its infancy as of this publication. The primary thrust is in re-writing the inverter's software-defined controls so that the inverter provides the instantaneous inertial response and voltage support that synchronous machines do. However, this task is not easy for inverter manufacturers. Not only is it a fundamentally different control strategy than what has typically been used, but the response – and therefore, the effectiveness on the grid – is still subject to the inverter's hardware limitations in terms of current-handling capability and access to short-term energy reserves. On the grid operations and planning side, there is the challenge of specifying the technical needs from advanced grid-forming IBR in order to have a system that is stable and can achieve higher levels of renewable penetration. The inverter technology and application development is a journey. It will not simply be flipping a switch over to grid-forming inverter technology and going straight to 100% inverter-based grid operation. But in the time-frames discussed, it is achievable.

The second approach of utilizing synchronous machine technologies to provide the needed grid-stabilizing characteristics can be done a few ways. One way is to maintain a minimum level of conventional resources online when committing and dispatching conventional generation. This is often described as designating some conventional units as "must-run" units. This approach almost always costs more to run the grid because units that would be economically decommitted are now forced to run, causing the remaining units or less expensive units to be run at lower outputs or at less efficient operating points. This approach is evaluated in Section 7.1 as a production cost sensitivity.

Another method is to use synchronous condensers to provide the synchronous machine characteristics and not modify the dispatch and commitment decisions, which can be left economically optimized. A synchronous condenser is essentially a synchronous generator without a turbine attached that is connected to the grid and rotating synchronously with the grid. Without a turbine attached, it cannot generate power and it does not burn fuel. But it does provide inertia and "voltage anchor" support to stabilize the grid, as well as steady-state reactive power support. Synchronous condensers have some relatively small losses, which must be provided by the grid, so they consume some power any time they are operating. Synchronous condensers can be procured and commissioned as new units, or existing power plant generators can be converted to synchronous condensers, often for substantial cost savings. However, synchronous condensers can introduce their own stability challenges and cause power system swings, which should be studied and understood in advance.

6.7 Summary

The grid stability analysis shows that as the penetration of inverter-based resources increases, the challenges to maintain grid stability, especially in the face of significant disturbance events like a loss-of-generation or a grid fault, become more acute. To make this more concrete, the grid stability challenges have been distilled into two factors: (1) system inertia or "H" [MW-s] and (2) Synchronous Ratio. The duration curve of inertia and the synchronous ratio are plotted for each of the four scenarios evaluated in Figure 53. As expected, higher-penetrations of IBR are associated with lower values of inertia and lower synchronous ratios, and are therefore more challenging to the stability of the grid.

In Figure 53, three levels of grid stability risk are shown color-coded as white, yellow, and red. In the white region, risk is considered low as this is a region where conventional power plants dominate the grid and conventional planning and operating practices are effective in maintaining stability. The current scenario has nearly all hours of operation in this low-risk region.

The next risk region is yellow, indicating higher levels of risk to grid stability and a significant change to traditional grid planning and operating practices. This analysis finds that through utilization of advanced inverter functions (like FFR and volt-var) and careful configuration of DER protection and response characteristics, the grid can be stable in the yellow region. This region is where the 25% and 50% scenarios have the bulk of their operating conditions.

Finally, the highest risk for grid stability is indicated by the red regions. This region is characterized by inverter-dominant grid operations and requires new methods, approaches, utilization of technologies, and analytical tools to achieve acceptable levels of stability and reliability. These may include dynamic and probabilistic planning and stability assessments, use of emerging inverter technologies like grid-forming technology, and the use of detailed electromagnetic transient simulation tools. In addition, conventional synchronous machine-based technologies like synchronous condensers can be deployed in conjunction with the other new technologies to help serve as a bridge to the new future grid.

`

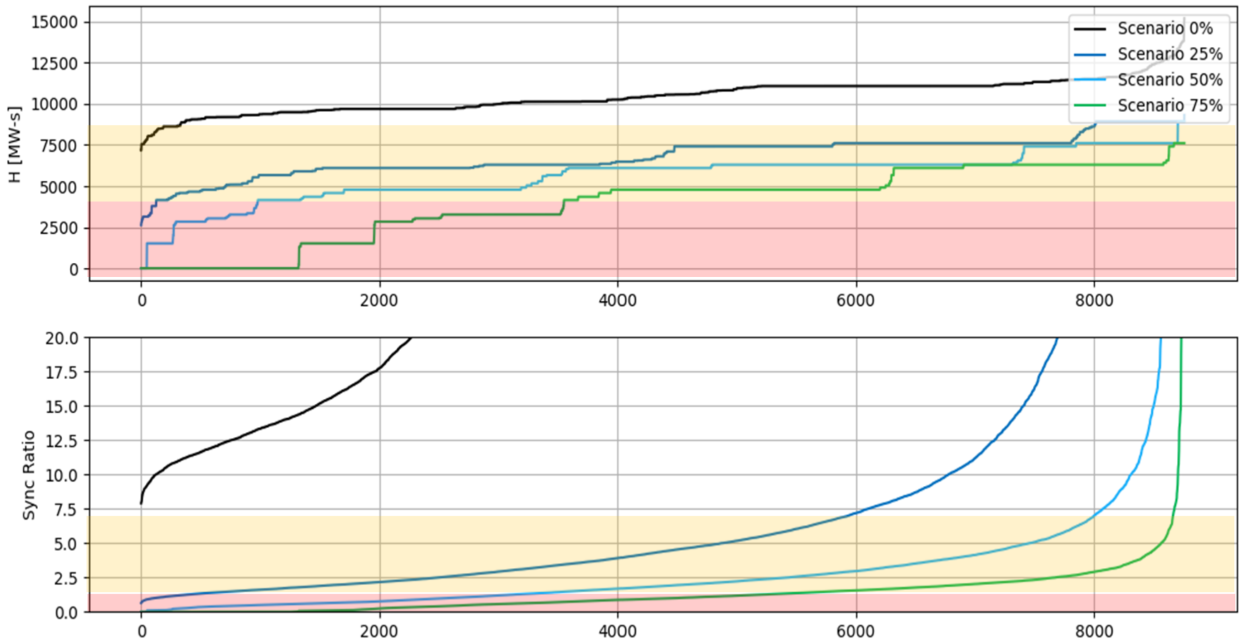

Figure 53: Summary of Risk Considering the Maturity of Inverter Technologies in 2020

`

7 Sensitivity Analysis

7.1 Grid Stability Sensitivity

As Section 5.5 indicates, the DER scenarios quickly reach periods of very high instantaneous inverter-based generation. This would represent some of the highest levels of IBR integration seen anywhere in the world today and could pose a reliability risk if unmitigated. To operate reliably at these levels would require one of three options:

- Grid-forming inverter technology that does not require synchronous generation to operate, but is currently being developed and is in commercial infancy,
- The addition of synchronous condensers, a mature technology commercially available today,
- Operational changes that commit additional synchronous generators to maintain a minimum inertia level, which would lead to solar curtailment.

Each of these mitigations comes at cost, and preference is given to grid-forming inverter controls because would not require significant capital expenditures like synchronous condensers, or increased fuel consumption and curtailment like operational changes. However, a sensitivity was evaluated to simulate the effects of grid stability constraints. This provides a clear example that reliability can be maintained even at very high DER integration if grid-forming technologies are not made available and synchronous condensers are not installed. This is especially useful to show the effects of grid stability constraints on near-term DER integration.

The Grid Stability Sensitivity is built around implementing two separate constraints within the PLEXOS model. These system constraints are informed by the initial results of the grid stability analysis conducted in PSSE (see Section 6). The first constraint requires unit commitment to maintain system inertia above 4,000 MW-s. The second constraint requires system dispatch to maintain a synchronous ratio of greater than 1.5. The synchronous ratio is measured as the relative difference between the thermal units' MVA contribution and the net-generation of inverter-based resources (IBR). These constraints will work together to put bounds on the operation of the system that ensure a greater level of reliability without relying on the introduction of grid forming inverters or synchronous condensers, as assumed across all Base Cases.

As discussed in the grid stability analysis the 75% DER is the most effected case. The high penetrations of IBR results in extended periods of low system inertia. Figure 54 shows that in the 75% DER Base Case the system inertia was less than 4,000 MW-s for more than 3,500 hours of the year. In the Grid Stability sensitivity all hours where above 4,000 MW-s and almost all were higher than the same hour from the Base Case even if it was already above 4,000 MW-s. This is primarily due to the inclusion of the synchronous ratio constraint which is shown in Figure 55. While the system inertia was below the target of 4,000 MW-s for roughly 3,500 hours in the base case, the synchronous ratio was less than 1.5 for close to 6,200 hours.

`

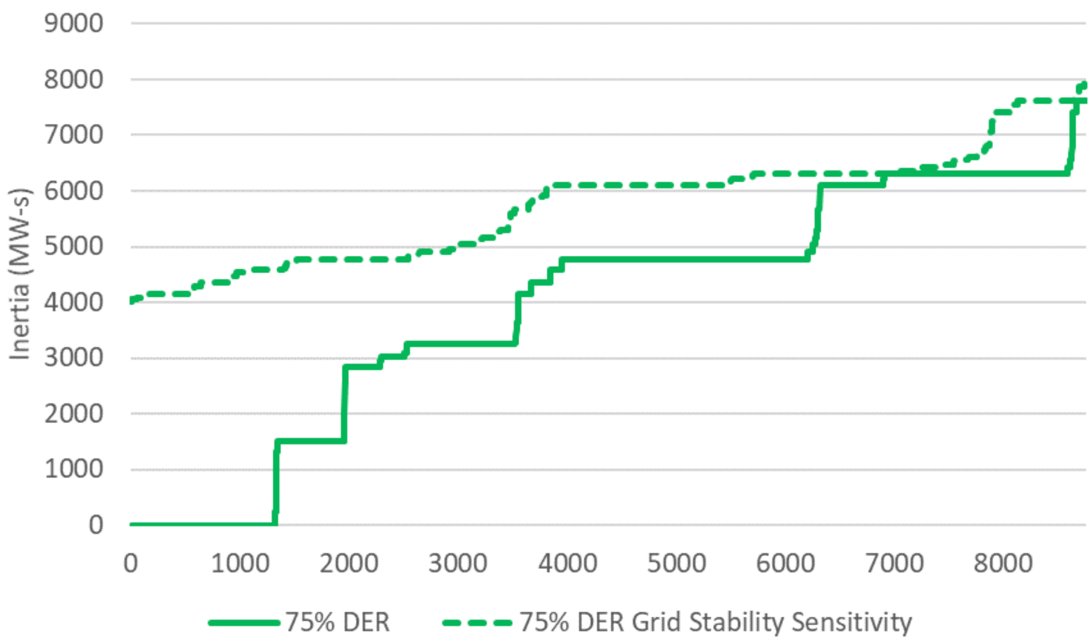

Figure 54: Duration Curve of System Inertia

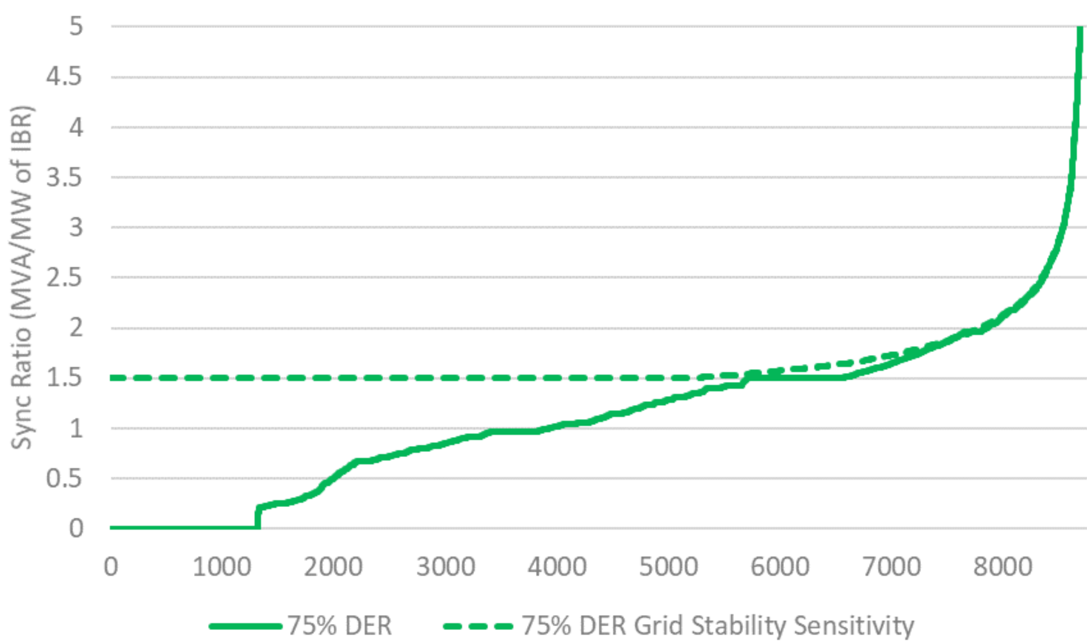

Figure 55: Duration Curve of Synchronous Ratio

These constraints had little impact on the Base Case, 25% DER, and 50% DER cases as can be seen from the little to no change in annual net generation between the cases in Figure 56. There are small changes in the 50% DER case but it is not until the 75% DER case that the Grid Stability sensitivity shows meaningful differences from the 75% DER Base case. There is an increase in generation from Combined Cycle, ST, and GT units in the Grid Stability sensitivity. This makes sense as these units are committed more often to ensure enough thermal generation is online to maintain adequate system inertia and synchronous ratio. With this increase in thermal generation there is a requisite decline in solar generation and an increase battery usage.

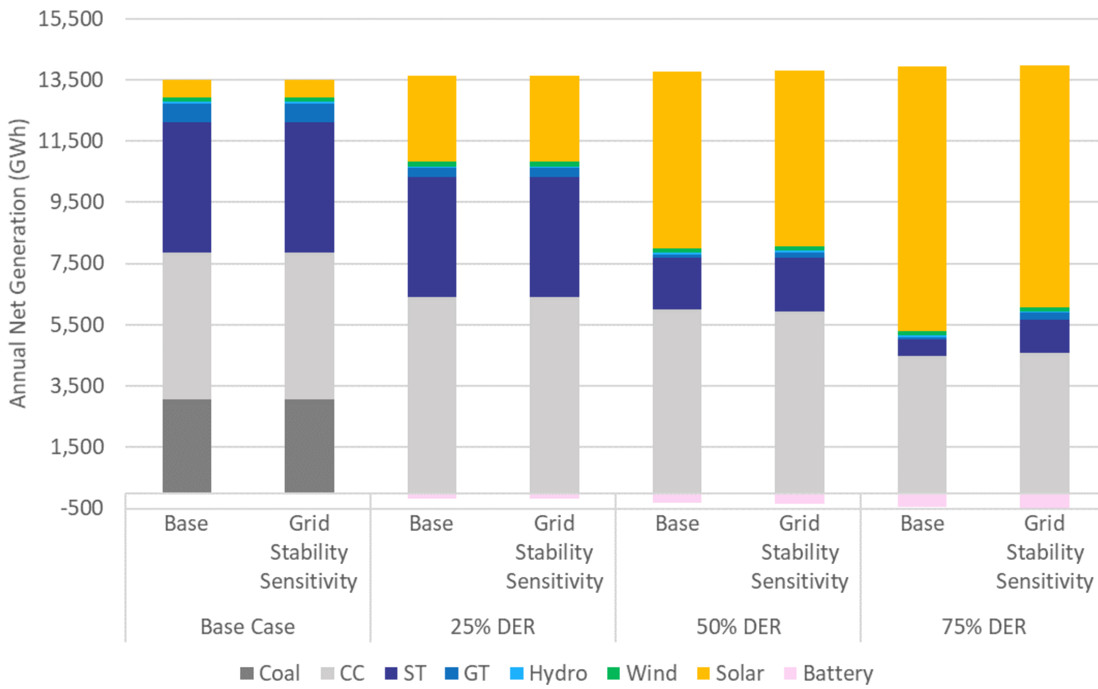

Figure 56: Annual Net Generation for Base cases versus Grid Stability Sensitivity

As more thermal generation is kept online during the peak hours of solar production to ensure grid stability there is an uptick in curtailment of IBR. Figure 57 shows that there is no difference in curtailment for the Base Case and 25% DER cases. While the 50% DER case has a slight increase from zero curtailment to less than 1%. The 75% DER case experiences a more significant increase in curtailment, going from roughly 1% to about 9.5%. Although this increase is more substantial than the other three cases the absolute amount of curtailment of only 9.5% is still reasonable for a system with 75% of its energy coming from renewable resources.

This increase in curtailment was lessened by more fully utilizing the battery resources on the grid. This can be seen by comparing the average number of cycles per year the batteries go through between the two case, as shown in Figure 58. Again the 25% DER case shows little to no change, but the 50% and 75% DER cases both have noticeable increases in the number of cycles the batteries go through per year. This is because the thermal generation is not backing down during the middle of the day as much in the Grid Stability sensitivity so the solar power is displaced and can no longer be consumed by the grid. Instead as much of it as possible is going into the batteries for use later in the evening.

`

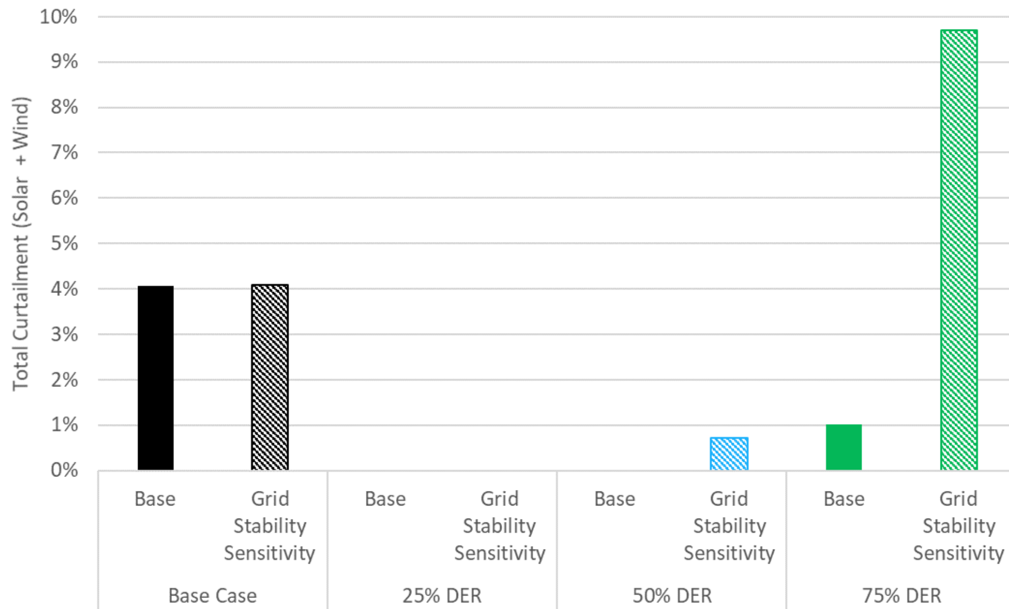

Figure 57: Total Renewable Curtailment

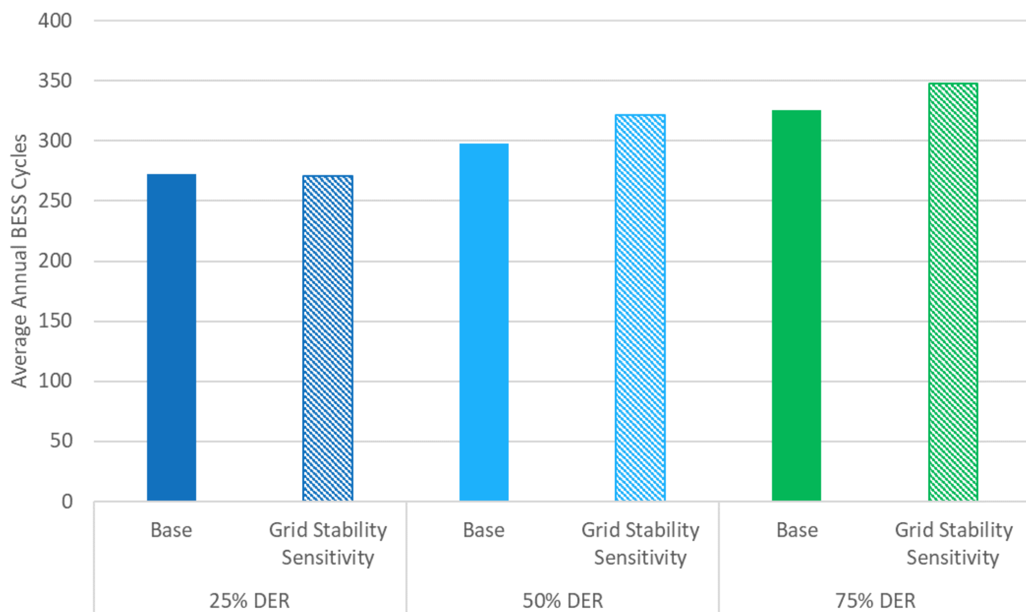

Figure 58: Average Battery Cycles per Year

These changes in operating behavior are apparent when comparing the dispatch of the two 75% DER cases for just a 3-day period, as shown in Figure 59. In the 75% DER case each of the three days experiences an extended period of little to no thermal generation in the middle of the day. However, in the Grid Stability sensitivity these periods are eliminated and an ample amount of thermal generation across multiple unit types remains online across all hours of the day. The increase in battery usage is also apparent as total generation in the Grid Stability sensitivity nears 4,000 MW each of the three days, whereas in the 75% DER Base case the peak is not much higher than 3,500 MW. This change is wholly from the battery being utilized more as Net Load remains unchanged between the two cases.

`

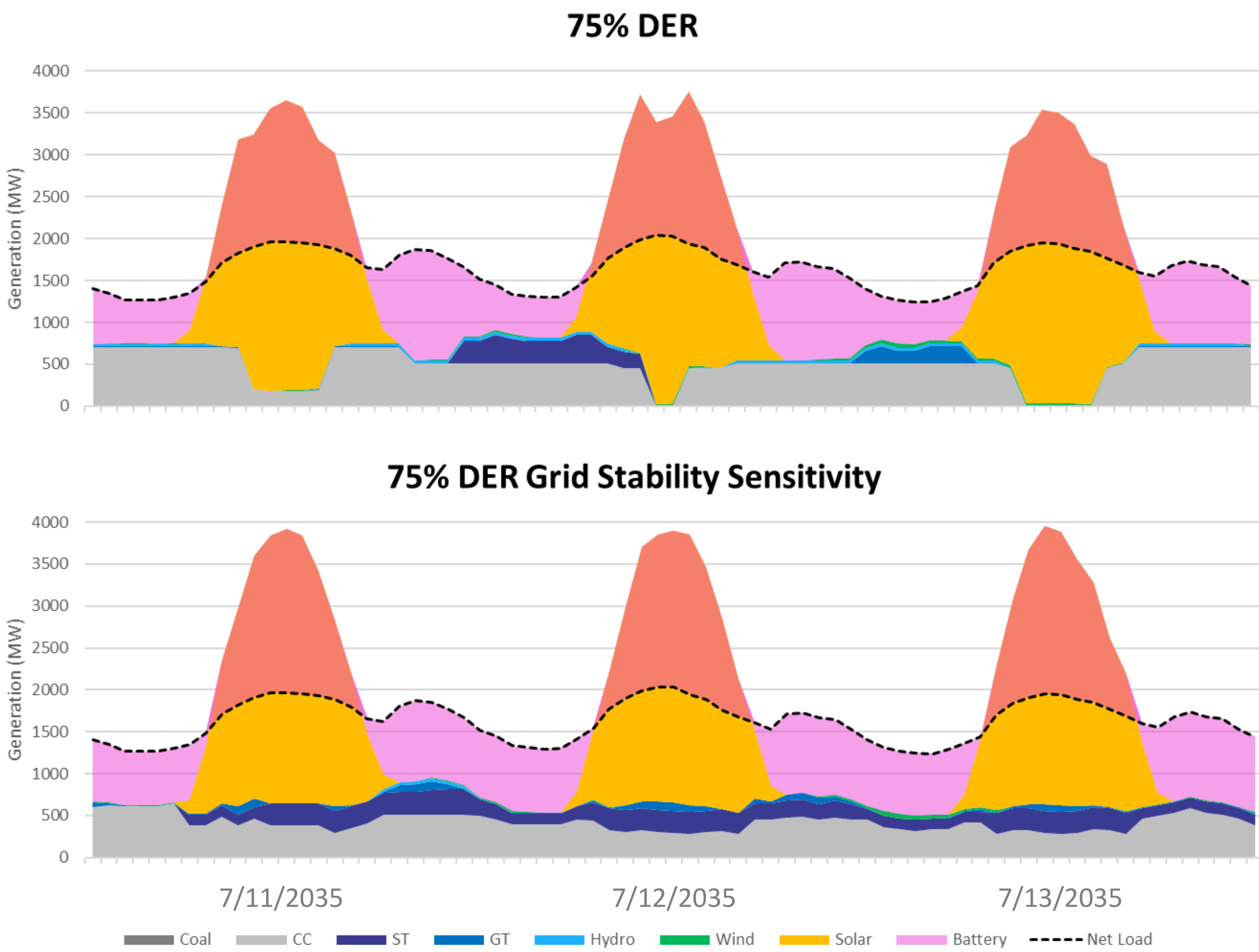

Figure 59: Dispatch Diagram of 75% DER cases from July 11th to July 13th, 2035

On a cost basis the trends discussed above continue to hold. When comparing the total system cost (fuel costs, VO&M costs, and start costs), as shown in Table 13 there is little change in the Base Case and 25% DER. In the 50% DER case the total system costs only increase about $11 million, but in the 75% DER case the costs increase more than $127 million per year. Although this is a significant increase from the 75% DER Base case it is important to note that even with that increase it is still a more substantial decline from any of the three other cases. In addition, this demonstrates that operational changes can be an effective – and economic -mitigation strategy for managing grid stability at lower DER integration levels.

Table 13:Total System Cost between the Base Cases and Grid Stability Sensitivity Cases

Scenario	Base Case		25% DER		50% DER		75% DER	
Sensitivity	Base	Grid Stability Sensitivity	Base	Grid Stability Sensitivity	Base	Grid Stability Sensitivity	Base	Grid Stability Sensitivity
Total (real 2020 $millions)	1,086	1,086	989	990	732	743	473	600

7.2 AES Accelerated Retirement Sensitivity

In addition to the Grid Stability Sensitivity, a sensitivity evaluating an accelerated retirement of AES was conducted. The study year for all previous cases has been 2035, but for the purposes of this sensitivity a study year of 2024 was chosen. On the basis of PV and storage deployment, this represents a realistic timeline for the retirement of both AES units from the system. Based on this view an updated load profile was created to reflect expected load in 2024. In Table 14 the total annual sales assumptions for the AES Accelerated Retirement Sensitivity is compared against the 2035 Load used in all other cases. The 2035 load includes reaching a 25% energy efficiency target by 2035. As the 2024 load is an intermediate step an energy efficiency target of 11% was used. For more discussion on this please refer to the subsequent report by EFG.

Table 14: AES Accelerated Retirement Sensitivity Load Assumptions

	2035 Load	AES Accelerated Retirement (2024) Load
Total Annual Sales (GWh)	11,736	13,932

Just as load was adjusted to match the updated study year of 2024 the buildout of DPV and batteries has been adjusted to reflect what can reasonably be assumed to be completed by 2024. The starting point for this intermediate DER buildout is the 25% DER case as it represents the most achievable buildout in the near term. The updated buildout is outline in Table 15. The AES Accelerated Retirement Sensitivity only evaluates the effects of AES 1 & 2 retiring from the system, unlike the other retirements outlined in Section 2.3.

Table 15: DER Buildout Assumptions for the AES Accelerated Retirement Sensitivity

	25% DER Base Case	AES Accelerated Retirement Sensitivity
Residential DPV (MW)	1,350	614
Commercial DPV (MW)	142	65
Battery (~4.5 hours) (MW)	1,179	442

For comparison purposes the sensitivity results also include an updated Base Case run which used the increased load from Table 14. This will allow for a direct comparison of how a system with today's composition compares with one that has added DER capacity and retired AES.

With the retirement of AES the AES Accelerated Retirement Sensitivity case shows a significant increase in generation by CC units, as shown in Figure 60. This is in line with what was seen in the main results in Figure 15. However, with only an intermediate buildout of DER capacity as compared with even the 25% DER base case there is also a significant increase in generation by ST units. With the retirement of AES the system lost 454 MW of capacity. This capacity was replaced with more than 500 MW of DPV and another 442 MW of ~4.5 hour batteries. However, even though a greater amount of capacity was added to the system than retired the capacity factor of the units added is much lower than that of AES. From a reliability standpoint each system evaluated below saw zero instances of unserved energy or reserve shortages, but the DER added to the system still does not produce enough energy to fully replace AES's generation. Therefore, ST units have taken a greater role in generation than in previous cases to fully replace the energy once provided by AES.

`

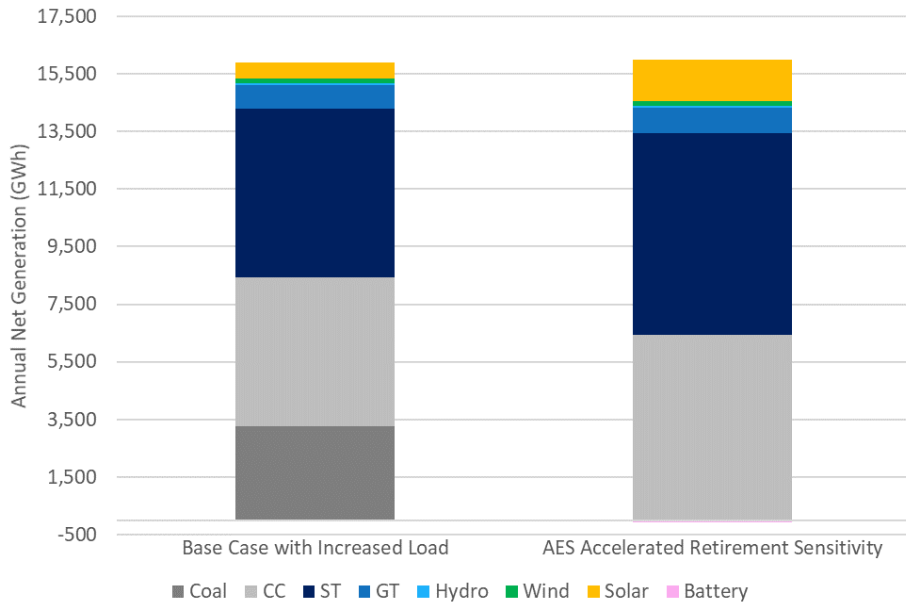

Figure 60: Annual Net Generation for the AES Accelerated Retirement Sensitivity

Total System Costs show a similar trend with the AES Accelerated Retirement Sensitivity resulting in roughly $68 million of increased costs, as shown in Table 16. This increase in costs is mostly from oil-fired (primarily ST units) generation replacing lower cost coal-fired generation.

Table 16: Total System Costs for the AES Accelerated Retirement Sensitivity

	Base with Increased Load	AES Accelerated Retirement Sensitivity
Total System Costs (real 2020 $millions)	1,349	1,417

Dispatch diagrams highlighting the same weeks as those shown earlier are included in Figure 61 and Figure 62. Please note that although these are the same weeks previously highlighted in Figure 18 and Figure 19 the load for the cases below was scaled higher to reflect the expected conditions for the study year 2024. As noted earlier, both CC and ST units are being dispatched more often with the retirement of AES. Even with less DER on the system than previously evaluated cases the presence of more solar and batteries is clear in the AES Accelerated Retirement Sensitivity. Unlike in the previous evaluated cases there are hours shown below where batteries are charging off of thermal generation instead of almost entirely off of solar. This shift is most likely due to the more limited amount of generation from solar in this case versus the three main DER cases. And ties back into why ST units play a more significant role in the system as discussed above.

Overall, the accelerated retirement of AES is feasible with an incremental buildout of DER to help replace lost capacity. The system will be able to properly operate and meet demand throughout the year.

`

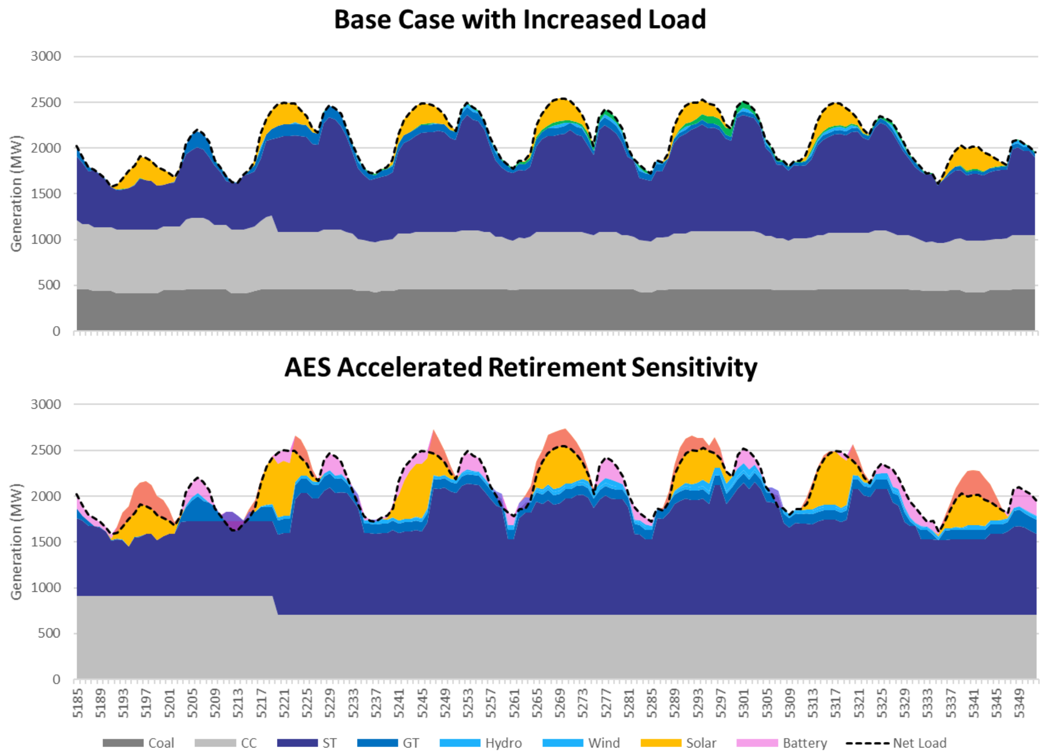

Figure 61: Dispatch Diagrams, AES Retirement Sensitivity, Peak Load Week (Aug 5)

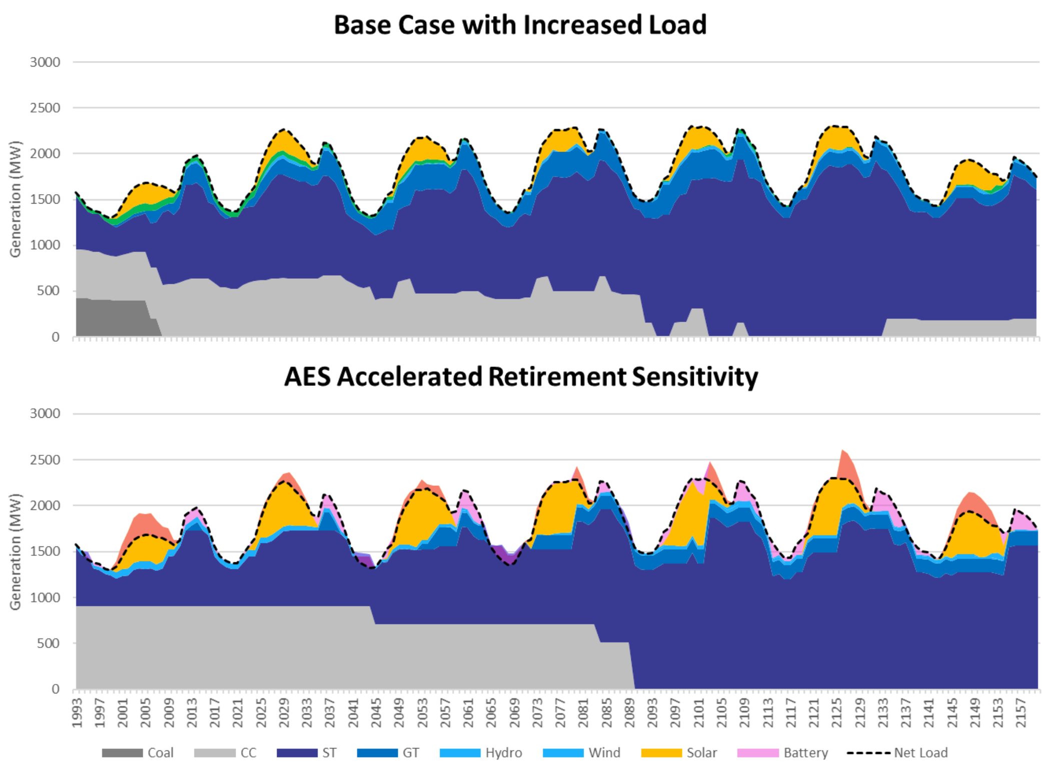

Figure 62: Dispatch Diagrams, AES Retirement Sensitivity, Max Renewable Week (Mar 25)

8 Mitigations and Recommendations

Integrating significant levels of distributed energy resources can be accomplished in an economic manner that improves reliability, resiliency, and grid stability. However, this transition will require changes to operational practices as well as investments in generation, transmission, distribution, and enabling technologies. Some of these mitigations are provided in the list below.

- Increased flexibility of the conventional fossil fleet will become increasingly important. Investments to increase flexibility, specifically part-load operation and cycling, should be evaluated to ensure reliable operation of the generators.
- Load flexibility will also be an important aspect of DER integration. Investments made to utilize loads for conventional demand response (reducing load during peak demand period) and grid services will be an important aspect of grid reliability with fewer fossil units available.
- To reach levels of DER integration evaluated in this study, increased visibility and control of DER resources will be important. This can be achieved either directly via centralized communications or control by the grid operator or with third-party aggregators. Investments in aggregation and DER monitoring would allow the system operator could consider expected generation from DER resources to commit and dispatch the system at least in part, based on system needs.
- The distributed battery storage in this analysis was assumed able to provide grid services like fast frequency response (FFR) autonomously. However, in order for the DER to have the capability (headroom) to respond quickly and autonomously when needed, the DER must be operated to maintain a minimum level of power and energy reserves. To augment the reserves from DER, it is also possible to use utility-scale BESS resources with FFR.
- It will be important to manage DER inverter configuration closely to have an accurate record of all DER control settings. This is a critical step for having an accurate model of the grid so it is possible to understand and mitigation challenges that arise.
- It is recommended to have the ability to adjust the response characteristics and protection settings as the grid evolves. The ability to update inverter settings remotely can go a long way toward mitigation "legacy inverter control" settings that are no longer appropriate for a future grid and end up hampering the grids ability to integrate higher levels of renewables.
- As significant levels of DER are integrated, it is recommended to revisit the under-frequency load-shedding scheme to coordinate it with downstream DER, which may be providing support to the grid during disturbances and should avoid being disconnected.
- It is recommended that grid stability analysis for very high penetrations of renewables be conducted with more appropriate models like electromagnetic transient (EMT) simulation models. Note that it is not considered necessary to represent the entire Puerto Rican grid in EMT, but representing reasonable-sized portions will provide tremendous insight to the inverter controls and behaviors that could inform detailed inverter specification documents.
- It is recommended to study emerging inverter technologies like grid-forming inverter technology and its potential benefits for stabilizing a high-renewable inverter-dominant Puerto Rican grid.
- It is recommended to review existing transmission protection schemes to check for schemes like line-distance protection that may be vulnerable to misoperation when high levels of inverter-based resources are present.

`

9 Key Findings

The results of this study are significant and clearly illustrate that Puerto Rico can radically shift its power system to one that is based on local, renewable, and resilient distributed energy resources. This can be done in a way that improves system reliability, grid stability, and resiliency for Puerto Rico's ratepayers. This transition will yield environmental benefits with reduced CO_2 emissions and other environmental pollutants and will considerably decrease fossil fuel consumption in Puerto Rico. This will make the power system, and the economy, less susceptible to the fuel price volatility of oil markets and more energy independent. In addition, the study results produced the following key findings:

- DER can be used as a tool to accelerate the retirement of Puerto Rico's aging fossil fleet replacing that capacity with more flexible, clean, and resilient technology. The AES coal plant, for example, could be retired by 2024 provided there is enough investment in DERs and energy efficiency.
- As solar integration increases across Puerto Rico it will be spread out across the island. While any individual solar site may have a large amount of variability due to cloud cover, the island-wide variability will be significantly reduced.
- Increased flexibility will be required by the fossil fleet, especially for the CC units, which will be expected to cycle on and offline more often and run for fewer hours per year. This may change the maintenance requirements, cycling costs, and reliability of these generators in the future.
- Renewable curtailment is quite low across all scenarios and is highest (on a relative basis) in the Base Case before any storage is added. Total renewable energy perspective, curtailment is limited to 1% even in the highest DER scenarios.
- Oil and gas both experience more than a 50% decline in consumption by the 75% DER scenario. As a result, Puerto Rico would be less susceptible to fuel price volatility and would become more energy independent with increased DER adoption. This reduction in fuel consumption also translates to a more than 70% reduction (over 6 million tons) in carbon dioxide emissions by the 75% DER case.
- The production cost savings (not accounting for capital cost of new resources) from introducing more DER onto the grid while also retiring fossil fuel-based generation are considerable, with savings range anywhere from roughly $144 million (25% DER) to $703 million per year (75% DER). This equates to an avoided energy cost of $64 to $86/MWh of additional solar energy.
- Another benefit of DER integration is that the resources are sited directly at the loads, reducing the total amount of energy the flows across the transmission network. This yields reliability, resiliency, and avoided transmission loss benefits. Across the scenarios analyzed, DER reduced net flows across the network as each individual region becomes more self-sufficient with the increase in DERs located within that respective region.
- In the 50% DER and 75% DER case there are hours with 100% of generation coming from IBR, even after using storage to shift much of the surplus generation. With current inverter technologies and the absence of synchronous condensers, this level of operation would not be reliable, but changes to operations can be made to ensure reliability if those mitigations are not available.
- DER inverter controls for grid-response is critical to achieving stable grid operation up through the 50% scenario. The use of DER inverter functions like frequency-watt response (FFR) and volt-

var response that are tuned for fast-response are effective in stabilizing the grid for significant disturbances. About 300MW of FFR is needed to enable the grid to survive generation-loss events through the 50% scenario.

- For very high penetrations of DER, more detailed analytical tools (like electromagnetic transient tools) are needed to assess the stability of the 75% scenario, particularly with higher-fidelity representation of the inverter-based resources.
- Reducing the maximum dispatch of the largest single generating unit, committing addition conventional generators, and utilizing synchronous condensers are effective approaches based on existing technology and traditional practices that can be used to mitigation grid stability challenges for very high penetration scenarios.

`

10 Next Steps

The power system evolution evaluated in this study is significant and should not be taken lightly. If implemented, these changes would make Puerto Rico one of the highest inverter-based renewable grids in the world, which industry leading DER integration. While this study was comprehensive, it was not exhaustive. There are unaddressed technical, economic, reliability, and organizational challenges that should be evaluated further. These include, but are not limited to the following:

- Further research should be conducted to better understand the role of forecasting, both for the solar resource and in the way DER is operated more generally. This study did not explicitly consider forecasting of the solar resource or battery utilization. Instead it was assumed that the battery storage additions could effectively manage the uncertainty in the solar resource.
- Further analysis could be conducted to evaluate the role of microgrids to provide both local resiliency benefits and grid benefits. This study did not evaluate specific DER systems or microgrids, but instead evaluated the bulk-system impact on the grid.
- This study assumed aggregated control and visibility of the DER. While this may be appropriate for long-term system planning several years in the future, DER aggregation has, as of yet, not been deployed at scale. Near-term analysis on DER integration should be evaluated to consider challenges of operations prior to aggregated control and visibility.
- Additional study work should be conducted to quantify reliability impacts of retiring generation in the appropriate manner, specifically using resource adequacy methods. The retirements analyzed in this study were selected conservatively but did not rely on detailed retirement and reliability analysis.
- More detailed analysis is required for assessing the stability of grid for inverter-dominant grid operations like those from the 75% renewable scenario. This would include electromagnetic transient (EMT) simulation tools with high-fidelity inverter models to better understand the stability of the grid with today's grid-following inverter technology and the emerging grid-forming inverter technology.
- The development of a DER inverter behavior specification is recommended to clearly define the performance, characteristics, and functions needed to enable a stable and reliable future grid that is reliant on DER.
- A review of existing transmission protection schemes to check for schemes like line-distance protection that may be vulnerable to misoperation when high levels of inverter-based resources are present.

Appendix

Additional Data and Assumptions

Table 17: Calculations of Resilient Homes, DER Capacity, and Renewable Energy by Scenario

Row	Formula	Property	25% DER	50% DER	75% DER
A	Assumed	Renewable Energy as % of Total Load	25%	50%	75%
B	Input Data	Total Number of Homes in Puerto Rico	1,500,000	1,500,000	1,500,000
C	Input Data	Owner Occupied # of Homes	986,165	986,165	986,165
D	Input Data	Active Residential Customers	1,340,652	1,340,652	1,340,652
E	Input Data	Percent of Non Apartment Houses	95%	95%	95%
F	Input Data	Number of Customers with home suitable for Rooftop PV	1,000,000	1,000,000	1,000,000
G	= F / D	Percent of Customers that have a home suitable for Rooftop PV	75%	75%	75%
H	Assumed	Percent of homes with a rooftop PV system by Load Year	50.0%	75.0%	100.0%
I	Assumed	Assumed average rooftop PV size (kW)	2.7	2.7	2.7
J	= (F * H * I) / 1000	Residential Installed rooftop PV (MW)	1,350	2,025	2,700
K	Input Data	NREL SAM Capacity Factor[1]	19.2%	19.2%	19.2%
L	= (J * K * 8760) / 1000	Total Generation of Rooftop PV (GWh)	2,271	3,406	4,541
M	Assumed	Gross Energy Sales before EE (GWh)[2]	15,648	15,648	15,648
N	= M * 25%	Energy Efficiency Assumption (GWh)[3]	3,912	3,912	3,912
O	= M - N	Gross Energy Sales after EE (GWh)	11,736	11,736	11,736
P	= A * O	Renewable Target (GWh)	2,934	5,868	8,802
Q	Input Data	Existing Renewable Generation from UPV and Wind (GWh)	423	423	423
R	= P - L - Q	Additional Renewable Generation from C&I (GWh)[4]	240	2,039	3,838
S	= (R * 8760) / (K * 8760)	Necessary Renewable Buildout from C&I (MW)	143	1,212	2,282
T	= J + S	Total PV Capacity (Residential Rooftop PV + C&I (MW)	1,493	3,237	4,982
U	= (J-172) * 4.5	Storage Buildout for Residential DPV (MWh)[5]	5,301	8,339	11,376

Notes

1. Based on data from NREL Puerto Rico Simulated High Resolution Dataset, National Solar Radiation Database
2. From PREPA IRP, Exhibit 3-11: Gross Energy Demand for Generation
3. Based on Queremos Sol's Energy Efficiency and Conservation Policy Objective of 25% by 2035
4. C&I refers to commercial and industrial customers, as well as carports and repurposed landfills
5. Assumed weighted average of solar PV and battery systems, ranging from 1.8 kW, 4.2 kWh to 4.2 kW, 21.6 kWh systems.
   172 nets out existing rooftop PV from battery calculations

Table 18: Retirement Priority Ranking

Unit Name	Type	Capacity (MW)	Generation Cost ($/MWh)	FO&M ($/kW-y)	Age (Yrs)	Emissions Rate (ton/MWh)	Flexibility	Forced Outage Rate	Location (0 = North, 1 = South)	Retirement Weight	Retirement Rank
AES 1	Coal	227	40	38.37	19	1.01	5	0.03	1	150	1
AES 2	Coal	227	40	38.37	19	1.01	5	0.03	1	150	2
Palo Seco Steam 3	ST	216	134	46.47	61	0.84	3	0.42	0	147	3
Palo Seco Steam 4	ST	216	134	46.47	60	0.84	3	0.42	0	147	4
Aguirre Steam 2	ST	450	131	32.04	46	0.84	3	0.2	1	140	5
Aguirre Steam 1	ST	450	130	32.04	46	0.83	3	0.2	1	140	6
Aguirre CCGT 1	CC	260	274	22.64	44	0.90	2	0.2	1	132	7
Aguirre CCGT 2	CC	260	274	22.64	44	0.90	2	0.2	1	132	8
Yabucoa GT12	GT	21	365	26.54	50	1.16	1	0.15	**1**	130	9
Yabucoa GT11	GT	21	365	26.54	50	1.16	1	0.15	**1**	130	10
Aguirre GT21	GT	21	365	26.54	49	1.16	1	0.15	1	129	11
Aguirre GT22	GT	21	365	26.54	49	1.16	1	0.15	1	129	12
Costa Sur GT11	GT	21	365	26.54	49	1.16	1	0.15	1	129	13
Costa Sur GT12	GT	21	365	26.54	49	1.16	1	0.15	1	129	14
San Juan Steam 7	ST	100	142	49.02	56	0.91	3	0.15	0	125	15
San Juan Steam 8	ST	100	142	49.02	52	0.91	3	0.15	0	123	16
Costa Sur Steam 6	ST	410	106	35.96	48	0.57	3	0.04	1	122	17
Costa Sur Steam 5	ST	410	106	35.96	49	0.57	3	0.02	1	120	18
Vega Baja GT11	GT	21	365	26.54	50	1.16	1	0.15	**0**	105	19
Vega Baja GT12	GT	21	365	26.54	50	1.16	1	0.15	**0**	105	20
Daguao GT11	GT	21	365	26.54	49	1.16	1	0.15	0	104	21
Daguao GT12	GT	21	365	26.54	49	1.16	1	0.15	0	104	22
Palo Seco GT12	GT	21	365	26.54	49	1.16	1	0.15	0	104	23
Palo Seco GT21	GT	21	365	26.54	49	1.16	1	0.15	0	104	24
Palo Seco GT11	GT	21	365	26.54	49	1.16	1	0.15	0	104	25
Jobos GT11	GT	21	365	26.54	48	1.16	1	0.15	0	104	26
Jobos GT12	GT	21	365	26.54	48	1.16	1	0.15	0	104	27
Palo Seco GT22	GT	21	365	26.54	48	1.16	1	0.15	0	104	28
Palo Seco GT31	GT	21	365	26.54	48	1.16	1	0.15	0	104	29
Palo Seco GT32	GT	21	365	26.54	48	1.16	1	0.15	0	104	30
EcoElectrica	CC	507	81	29.89	22	0.44	2	0.02	1	89	31
Cambalache GT 2	GT	83	159	24.44	44	1.00	1	0.1	0	81	32
Cambalache GT 3	GT	83	159	24.44	44	1.00	1	0.1	0	81	33
San Juan CCGT 6	CC	200	85	27.4	13	0.63	2	0.18	0	77	34
San Juan CCGT 5	CC	200	83	27.4	13	0.61	2	0.18	0	77	35
Mayaguez Plant 1	GT	50	119	26.54	12	0.75	1	0.09	0	60	36
Mayaguez Plant 2	GT	50	119	26.54	12	0.75	1	0.09	0	60	37
Mayaguez Plant 3	GT	50	119	26.54	12	0.75	1	0.09	0	60	38
Mayaguez Plant 4	GT	50	119	26.54	12	0.75	1	0.09	0	60	39

Table 19: Fossil Unit Average Heat Rate Curves

Category	Unit Name	Min Stable Level	Max Capacity	Heat Rate Coeff (ax^2)	Heat Rate Coeff (bx)	Heat Rate Coeff (c)	MW1	MW2	MW3	MW4	MW5	MW6	MW7	AHR1	AHR2	AHR3	AHR4	AHR5	AHR6	AHR7
Coal	AES 1	166	227	0.00896	6177	363	166	176	186	197	207	217	227	9,849	9,814	9,792	9,783	9,783	9,792	9,808
Coal	AES 2	166	227	0.00896	6177	363	166	176	186	197	207	217	227	9,849	9,814	9,792	9,783	9,783	9,792	9,808
CC	Aguirre CCGT 1	46	260	0.02546	-745	1379	46	82	117	153	189	224	260	30,404	18,220	13,995	12,164	11,368	11,114	11,179
CC	Aguirre CCGT 2	46	260	0.02546	-745	1379	46	82	117	153	189	224	260	30,404	18,220	13,995	12,164	11,368	11,114	11,179
CC	EcoElectrica	275	507	0.00879	-501	1810	275	314	352	391	430	468	507	8,496	8,025	7,731	7,563	7,486	7,478	7,523
CC	San Juan CCGT 5	106	200	0.02266	-510	726	106	122	137	153	169	184	200	8,741	8,214	7,889	7,702	7,616	7,605	7,652
CC	San Juan CCGT 6	106	200	0.02333	-525	748	106	122	137	153	169	184	200	9,003	8,460	8,124	7,933	7,844	7,833	7,881
ST	Aguirre Steam 1	143	450	0.00443	6057	705	143	194	245	297	348	399	450	11,618	10,547	10,016	9,747	9,624	9,591	9,617
ST	Aguirre Steam 2	143	450	0.00448	6120	712	143	194	245	297	348	399	450	11,739	10,656	10,121	9,849	9,725	9,691	9,717
ST	Costa Sur Steam 5	131	410	0.00494	6149	652	131	178	224	271	317	364	410	11,773	10,699	10,166	9,895	9,771	9,738	9,764
ST	Costa Sur Steam 6	131	410	0.00494	6149	652	131	178	224	271	317	364	410	11,773	10,699	10,166	9,895	9,771	9,738	9,764
ST	Palo Seco Steam 3	69	216	0.00935	6135	343	69	94	118	143	167	192	216	11,747	10,675	10,143	9,873	9,749	9,716	9,742
ST	Palo Seco Steam 4	69	216	0.00935	6135	343	69	94	118	143	167	192	216	11,747	10,675	10,143	9,873	9,749	9,716	9,742
ST	San Juan Steam 7	32	100	0.02180	6622	171	32	43	55	66	77	89	100	12,671	11,519	10,947	10,656	10,523	10,487	10,515
ST	San Juan Steam 8	32	100	0.02170	6590	170	32	43	55	66	77	89	100	12,609	11,462	10,893	10,603	10,471	10,435	10,463
GT	Aguirre GT21	13	21	0.00580	11180	65	13	14	16	17	18	20	21	16,260	15,802	15,424	15,106	14,835	14,602	14,400
GT	Aguirre GT22	13	21	0.00580	11180	65	13	14	16	17	18	20	21	16,260	15,802	15,424	15,106	14,835	14,602	14,400
GT	Cambalache GT 2	50	83	0.00118	8967	206	50	56	61	67	72	78	83	13,150	12,748	12,419	12,146	11,916	11,719	11,549
GT	Cambalache GT 3	50	83	0.00118	8967	206	50	56	61	67	72	78	83	13,150	12,748	12,419	12,146	11,916	11,719	11,549
GT	Costa Sur GT11	13	21	0.00580	11180	65	13	14	16	17	18	20	21	16,260	15,802	15,424	15,106	14,835	14,602	14,400
GT	Costa Sur GT12	13	21	0.00580	11180	65	13	14	16	17	18	20	21	16,260	15,802	15,424	15,106	14,835	14,602	14,400
GT	Daguao GT11	13	21	0.00580	11180	65	13	14	16	17	18	20	21	16,260	15,802	15,424	15,106	14,835	14,602	14,400
GT	Daguao GT12	13	21	0.00580	11180	65	13	14	16	17	18	20	21	16,260	15,802	15,424	15,106	14,835	14,602	14,400
GT	Jobos GT11	13	21	0.00580	11180	65	13	14	16	17	18	20	21	16,260	15,802	15,424	15,106	14,835	14,602	14,400
GT	Jobos GT12	13	21	0.00580	11180	65	13	14	16	17	18	20	21	16,260	15,802	15,424	15,106	14,835	14,602	14,400
GT	Mayaguez Plant 1	25	50	0.00158	7236	100	25	29	33	38	42	46	50	11,286	10,719	10,296	9,969	9,708	9,496	9,320
GT	Mayaguez Plant 2	25	50	0.00158	7236	100	25	29	33	38	42	46	50	11,286	10,719	10,296	9,969	9,708	9,496	9,320
GT	Mayaguez Plant 3	25	50	0.00158	7236	100	25	29	33	38	42	46	50	11,286	10,719	10,296	9,969	9,708	9,496	9,320
GT	Mayaguez Plant 4	25	50	0.00158	7236	100	25	29	33	38	42	46	50	11,286	10,719	10,296	9,969	9,708	9,496	9,320
GT	Palo Seco GT11	13	21	0.00580	11180	65	13	14	16	17	18	20	21	16,260	15,802	15,424	15,106	14,835	14,602	14,400
GT	Palo Seco GT12	13	21	0.00580	11180	65	13	14	16	17	18	20	21	16,260	15,802	15,424	15,106	14,835	14,602	14,400
GT	Palo Seco GT21	13	21	0.00580	11180	65	13	14	16	17	18	20	21	16,260	15,802	15,424	15,106	14,835	14,602	14,400
GT	Palo Seco GT22	13	21	0.00580	11180	65	13	14	16	17	18	20	21	16,260	15,802	15,424	15,106	14,835	14,602	14,400
GT	Palo Seco GT31	13	21	0.00580	11180	65	13	14	16	17	18	20	21	16,260	15,802	15,424	15,106	14,835	14,602	14,400
GT	Palo Seco GT32	13	21	0.00580	11180	65	13	14	16	17	18	20	21	16,260	15,802	15,424	15,106	14,835	14,602	14,400
GT	Vega Baja GT11	13	21	0.00580	11180	65	13	14	16	17	18	20	21	16,260	15,802	15,424	15,106	14,835	14,602	14,400
GT	Vega Baja GT12	13	21	0.00580	11180	65	13	14	16	17	18	20	21	16,260	15,802	15,424	15,106	14,835	14,602	14,400
GT	Yabucoa GT11	13	21	0.00580	11180	65	13	14	16	17	18	20	21	16,260	15,802	15,424	15,106	14,835	14,602	14,400
GT	Yabucoa GT12	13	21	0.00580	11180	65	13	14	16	17	18	20	21	16,260	15,802	15,424	15,106	14,835	14,602	14,400
Other	Landfill Gas	2	4	0.03047	11180	12	2	2	3	3	3	4	4	17,437	16,562	15,908	15,402	14,999	14,671	14,400

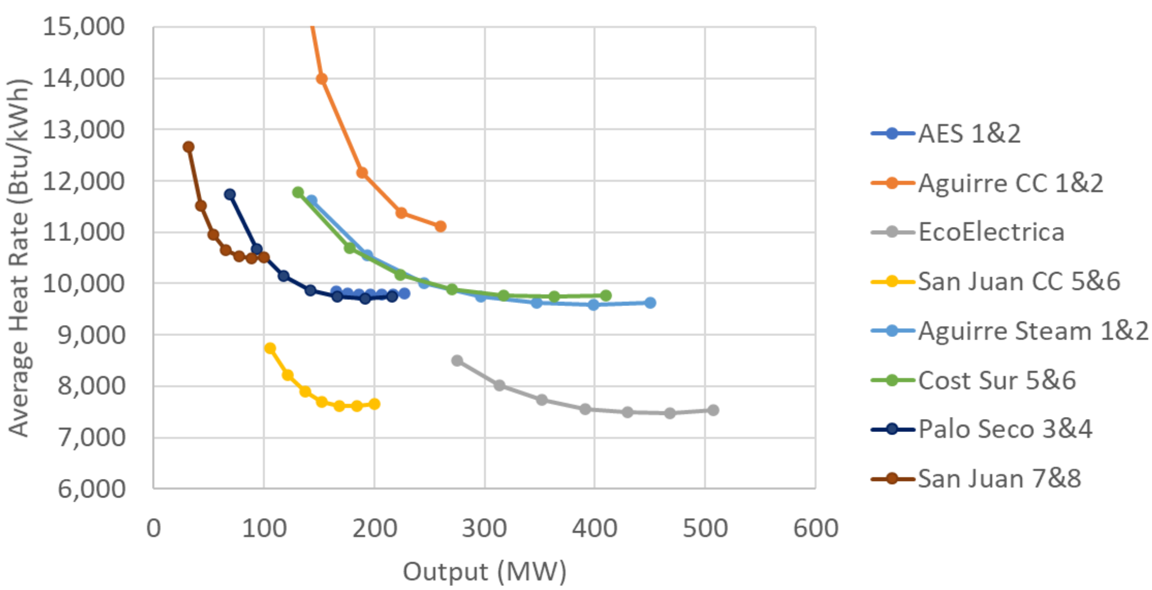

Figure 63: Fossil Unit Average Heat Rate Curves

`

Table 20: DER Capacity by Region, Customer Class, and Scenario

	DPV Capacity (MW)			Battery Capacity (MWh)		
	25% DER	50% DER	75% DER	25% DER	50% DER	75% DER
Residential	**1,350**	**2,025**	**2,700**	**5,301**	**8,339**	**11,376**
Arecibo	145	211	277	517	815	1,112
Bayamón	251	378	504	994	1,562	2,133
Caguas	221	331	440	860	1,350	1,841
Carolina	162	246	329	656	1,035	1,409
Mayagüez	152	227	302	590	923	1,260
Ponce ES	62	88	114	206	324	446
Ponce OE	118	176	234	459	720	981
San Juan	239	369	499	1,021	1,611	2,196
Commercial	**143**	**1,212**	**2,282**	**0**	**0**	**0**
Arecibo	12	102	191	0	0	0
Bayamón	12	106	199	0	0	0
Caguas	19	162	304	0	0	0
Carolina	13	110	207	0	0	0
Mayagüez	21	181	341	0	0	0
Ponce ES	5	41	76	0	0	0
Ponce OE	8	68	129	0	0	0
San Juan	52	443	834	0	0	0
Total	**1,493**	**3,237**	**4,982**	**5,301**	**8,339**	**11,376**
Arecibo	157	312	468	517	815	1,112
Bayamón	264	483	703	994	1,562	2,133
Caguas	240	492	744	860	1,350	1,841
Carolina	175	356	536	656	1,035	1,409
Mayagüez	174	408	643	590	923	1,260
Ponce ES	67	129	191	206	324	446
Ponce OE	126	245	363	459	720	981
San Juan	291	812	1,333	1,021	1,611	2,196

*Includes existing distributed rooftop PV

Table 21: Dynamic Load Model Parameters for PSSE CMLDBU Model

CON	Description	Param Set 1	Param Set 2	Param Set 3	Param Set 4
J+0	LOAD MVA BASE	-1	-1	-1	-1
J+1	SUBSTATION SHUNT B (PU OF MVA BASE)	0	0	0	0
J+2	Rfdr - Feeder R (pu of Load MVA base)	0.04	0.02	0.03	0.05
J+3	Xfdr - Feeder X (pu of Load MVA base)	0.04	0.02	0.03	0.05
J+4	Fb - Fraction of Feeder Compn at substation end	0.75	0.75	0.75	0.75

`

J+5	Xxf - Transformer Reactance - pu of load MVA base	0.08	0.08	0.08	0.08
J+6	Tfixhs - High side fixed transformer tap	1	1	1	1
J+7	Tfixls - Low side fixed transformer tap	1	1	1	1
J+8	LTC - LTC flag (1=active, 0=inactive)	0	0	0	0
J+9	Tmin - LTC min tap (on low side)	0.9	0.9	0.9	0.9
J+10	Tmax - LTC max tap (on low side)	1.1	1.1	1.1	1.1
J+11	Step - LTC Tstep (on low side)	0.0063	0.0063	0.0063	0.0063
J+12	Vmin - LTC Vmin tap (low side pu)	1.025	1.025	1.025	1.025
J+13	Vmax - LTC Vmax tap (low side pu)	1.04	1.04	1.04	1.04
J+14	TD - LTC Control time delay (sec)	30	30	30	30
J+15	TC - LTC Tap adjustment time delay (sec)	5	5	5	5
J+16	Rcmp - LTC Rcomp (pu of load MVA base)	0	0	0	0
J+17	Xcmp - LTC Xcomp (pu of load MVA base)	0	0	0	0
J+18	FmA - Motor A Fraction	0.201	0.221	0.201	0.221
J+19	FmB - Motor B Fraction	0.146	0.162	0.146	0.162
J+20	FmC - Motor C Fraction	0.064	0.062	0.064	0.062
J+21	FmD - Motor D Fraction	0.151	0.249	0.151	0.249
J+22	Fel - Electronic Device Fraction	0.145	0.108	0.145	0.108
J+23	PFel - PF of Electronic Load	1	1	1	1
J+24	Vd1 - Voltage at which electronic loads start to drop	0.7	0.7	0.7	0.7
J+25	Vd2 - Voltage at which all electronic load have dropped	0.5	0.5	0.5	0.5
J+26	PFs - Static Load Power Factor	-0.997	-0.997	-0.997	-0.997
J+27	P1e - P1 exponent	2	2	2	2
J+28	P1c - P1 coefficient	0.485	0.311	0.485	0.311
J+29	P2e - P2 exponent	1	1	1	1
J+30	P2c - P2 coefficient	0.515	0.689	0.515	0.689
J+31	Pfrq - Frequency sensitivity	0	0	0	0
J+32	Q1e - Q1 exponent	2	2	2	2
J+33	Q1c - Q1 coefficient	-0.5	-0.5	-0.5	-0.5
J+34	Q2e - Q2 exponent	1	1	1	1
J+35	Q2c - Q2 coefficient	1.5	1.5	1.5	1.5
J+36	Qfrq - Frequency sensitivity	-1	-1	-1	-1
J+37	MtypA - Motor type	3	3	3	3
J+38	LFmA - Loading factor (MW/MVA rating)	0.75	0.75	0.75	0.75
J+39	RaA - Stator resistance	0.04	0.04	0.04	0.04
J+40	LsA - Synchronous reactance	1.8	1.8	1.8	1.8
J+41	LpA - Transient reactance	0.12	0.12	0.12	0.12
J+42	LppA - Sub-transient reactance	0.104	0.104	0.104	0.104
J+43	TpoA - Transient open circuit time constant	0.095	0.095	0.095	0.095

`

J+44	TppoA - Sub-transient open circuit time constant	0.0021	0.0021	0.0021	0.0021
J+45	HA - Inertia constant	0.1	0.2	0.2	0.1
J+46	etrqA - Torque speed exponent	0	0	0	0
J+47	Vtr1A - U/V trip1 V (pu)	0.7	0.75	0.65	0.7
J+48	Ttr1A - U/V trip1 time (sec)	0.02	0.02	0.02	0.02
J+49	Ftr1A - U/V trip1 fraction	0.2	0.2	0.2	0.2
J+50	Vrc1A - U/V trip1 reclose V (pu)	1	1	1	1
J+51	Trc1A - U/V trip1 reclose time (sec)	99999	99999	99999	99999
J+52	Vtr2A - U/V trip2 V (pu)	0.5	0.6	0.55	0.45
J+53	Ttr2A - U/V trip2 time (sec)	0.02	0.02	0.02	0.02
J+54	Ftr2A - U/V trip2 fraction	0.7	0.7	0.7	0.7
J+55	Vrc2A - U/V trip2 reclose V (pu)	0.7	0.78	0.75	0.65
J+56	Trc2A - U/V trip2 reclose time (sec)	0.1	0.08	0.12	0.16
J+57	MtypB - Motor type	3	3	3	3
J+58	LFmB - Loading factor (MW/MVA rating)	0.75	0.75	0.75	0.75
J+59	RaB - Stator resistance	0.03	0.03	0.03	0.03
J+60	LsB - Synchronous reactance	1.8	1.8	1.8	1.8
J+61	LpB - Transient reactance	0.19	0.19	0.19	0.19
J+62	LppB - Sub-transient reactance	0.14	0.14	0.14	0.14
J+63	TpoB - Transient open circuit time constant	0.2	0.2	0.2	0.2
J+64	TppoB - Sub-transient open circuit time constant	0.0026	0.0026	0.0026	0.0026
J+65	HB - Inertia constant	0.5	0.3	0.4	0.4
J+66	etrqB - Torque speed exponent	2	2	2	2
J+67	Vtr1B - U/V trip1 V (pu)	0.6	0.5	0.65	0.7
J+68	Ttr1B - U/V trip1 time (sec)	0.02	0.02	0.02	0.02
J+69	Ftr1B - U/V trip1 fraction	0.2	0.2	0.2	0.2
J+70	Vrc1B - U/V trip1 reclose V (pu)	0.75	0.8	0.7	0.75
J+71	Trc1B - U/V trip1 reclose time (sec)	0.05	0.05	0.1	0.15
J+72	Vtr2B - U/V trip2 V (pu)	0.5	0.6	0.55	0.65
J+73	Ttr2B - U/V trip2 time (sec)	0.02	0.02	0.02	0.02
J+74	Ftr2B - U/V trip2 fraction	0.3	0.3	0.3	0.3
J+75	Vrc2B - U/V trip2 reclose V (pu)	0.65	0.75	0.7	0.8
J+76	Trc2B - U/V trip2 reclose time (sec)	0.05	0.1	0.08	0.15
J+77	MtypC - Motor type	3	3	3	3
J+78	LFmC - Loading factor (MW/MVA rating)	0.75	0.75	0.75	0.75
J+79	RaC - Stator resistance	0.03	0.03	0.03	0.03
J+80	LsC - Synchronous reactance	1.8	1.8	1.8	1.8
J+81	LpC - Transient reactance	0.19	0.19	0.19	0.19
J+82	LppC - Sub-transient reactance	0.14	0.14	0.14	0.14

`

J+83	TpoC - Transient open circuit time constant	0.2	0.2	0.2	0.2
J+84	TppoC - Sub-transient open circuit time constant	0.0026	0.0026	0.0026	0.0026
J+85	HC - Inertia constant	0.1	0.2	0.15	0.2
J+86	etrqC - Torque speed exponent	2	2	2	2
J+87	Vtr1C - U/V trip1 V (pu)	0.65	0.6	0.55	0.65
J+88	Ttr1C - U/V trip1 time (sec)	0.02	0.02	0.02	0.02
J+89	Ftr1C - U/V trip1 fraction	0.2	0.2	0.2	0.2
J+90	Vrc1C - U/V trip1 reclose V (pu)	1	1	1	1
J+91	Trc1C - U/V trip1 reclose time (sec)	9999	9999	9999	9999
J+92	Vtr2C - U/V trip2 V (pu)	0.5	0.6	0.55	0.55
J+93	Ttr2C - U/V trip2 time (sec)	0.02	0.02	0.02	0.02
J+94	Ftr2C - U/V trip2 fraction	0.3	0.3	0.3	0.3
J+95	Vrc2C - U/V trip2 reclose V (pu)	0.65	0.75	0.7	0.7
J+96	Trc2C - U/V trip2 reclose time (sec)	0.1	0.08	0.16	0.12
J+97	Tstall - Stall dealy (sec)	9999	9999	9999	9999
J+98	Trestart - Restart delay (sec)	0.3	0.5	0.4	0.6
J+99	Tv - Voltage input time constant(sec)	0.02	0.02	0.02	0.02
J+100	Tf - Frequency input time constant(sec)	0.05	0.05	0.05	0.05
J+101	CompLF - Compressor load factor, p.u. of rated power	1	1	1	1
J+102	CompPF - Compressor power factor at 1.0 p.u. voltage	0.98	0.98	0.98	0.98
J+103	Vstall - Compressor stall voltage at base condition (p.u.)	0.52	0.52	0.52	0.52
J+104	Rstall - Compressor motor res. with 1.0 p.u. current	0.1	0.1	0.1	0.1
J+105	Xstall - Compressor motor stall reactance - unsat.	0.1	0.1	0.1	0.1
J+106	LFadj - Load factor adjustment to stall voltage	0	0	0	0
J+107	Kp1 - Real power constant for running state 1	0	0	0	0
J+108	Np1 - Real power exponent for running state 1	1	1	1	1
J+109	Kq1 - Reactive power constant for running state 1	6	6	6	6
J+110	Nq1 - Reactive power exponent for running state 1	2	2	2	2
J+111	Kp2 - Real power constant for running state 2	12	12	12	12
J+112	Np2 - Real power exponent for running state 2	3.2	3.2	3.2	3.2
J+113	Kq2 - Reactive power constant for running state 2	11	11	11	11
J+114	Nq2 - Reactive power exponent for running state 2	2.5	2.5	2.5	2.5
J+115	Vbrk - Compressor motor "break-down" voltage (p.u.)	0.86	0.82	0.8	0.84

`

J+116	Frst - Fraction of motors capable of restart	0.2	0.2	0.2	0.2
J+117	Vrst - Voltage at which motors can restart (p.u.)	0.95	0.93	0.97	0.94
J+118	CmpKpf - Real power constant for frequency dependency	1	1	1	1
J+119	CmpKqf - Reactive power constant for frequency dependency	-3.3	-3.3	-3.3	-3.3
J+120	Vc1off - Voltage 1 at which contactors start dropping out (p.u.)	0.5	0.6	0.65	0.55
J+121	Vc2off - Voltage 2 at which all contactors drop out (p.u.)	0.4	0.45	0.5	0.4
J+122	Vc1on - Voltage 1 at which all contactors reclose (p.u.)	0.6	0.7	0.75	0.65
J+123	Vc2on - Voltage 2 at which contactors start reclosing (p.u.)	0.5	0.55	0.6	0.5
J+124	Tth - Compressor motor heating time constant(sec)	15	20	10	18
J+125	Th1t - Temperature at which compressor motor begin tripping	0.7	0.7	0.7	0.7
J+126	Th2t - Temperature at which compressor all motors are tripped	1.9	1.9	1.9	1.9
J+127	Fuvr - Fraction of compressor motors with undervoltage relays	0.1	0.1	0.1	0.1
J+128	UVtr1 - 1st voltage pick-up (p.u.)	0.6	0.5	0.55	0.65
J+129	Ttr1 - 1st definite time voltage pick-up (sec)	0.02	0.04	0.03	0.02
J+130	UVtr2 - 2nd voltage pick-up (p.u.)	0	0	0	0
J+131	Ttr2 - 2nd definite time voltage pick-up (sec)	9999	9999	9999	9999

Additional Results and Figures

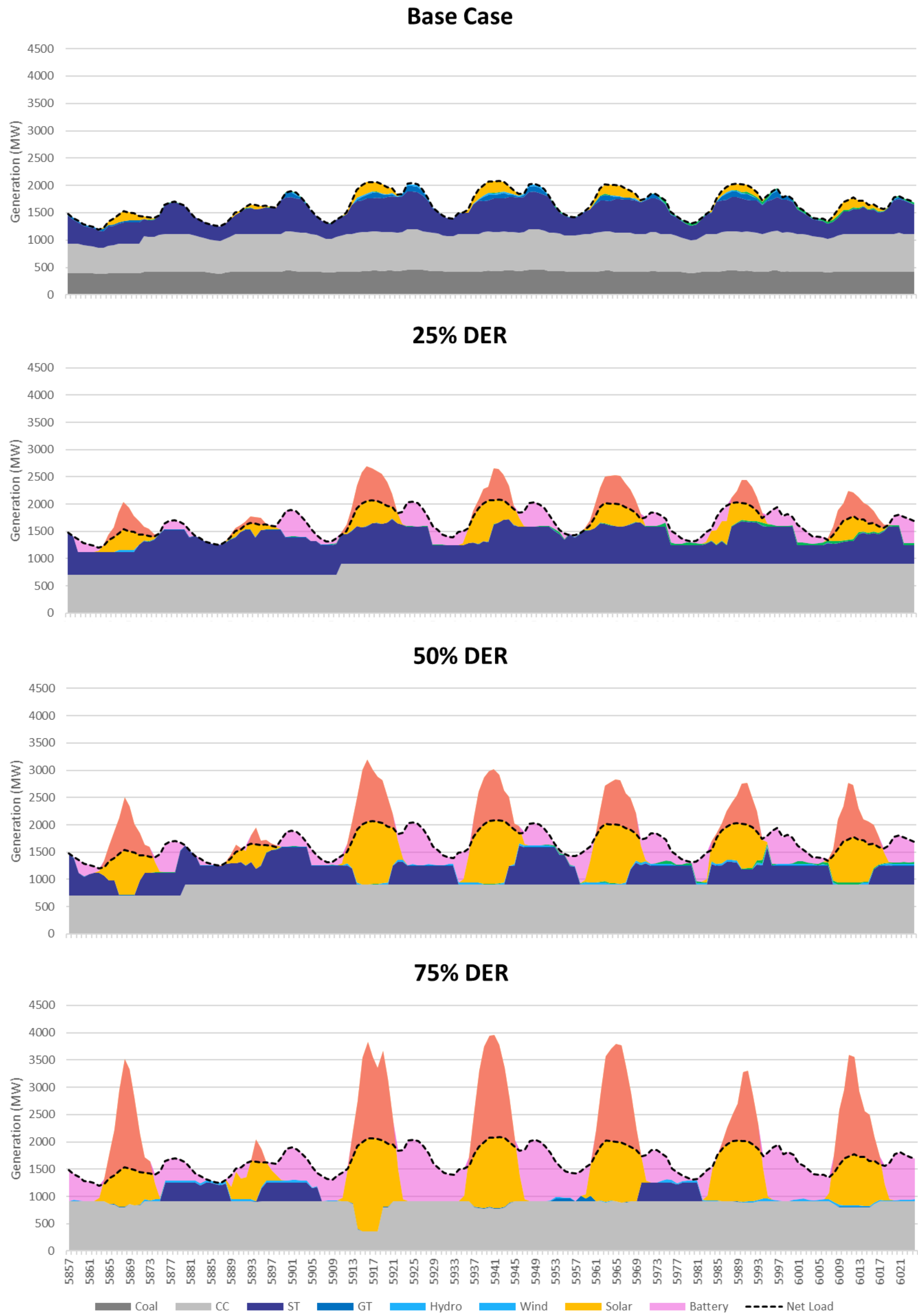

Figure 64: Dispatch Diagram, Minimum Renewables Generation (Sept 2)

`

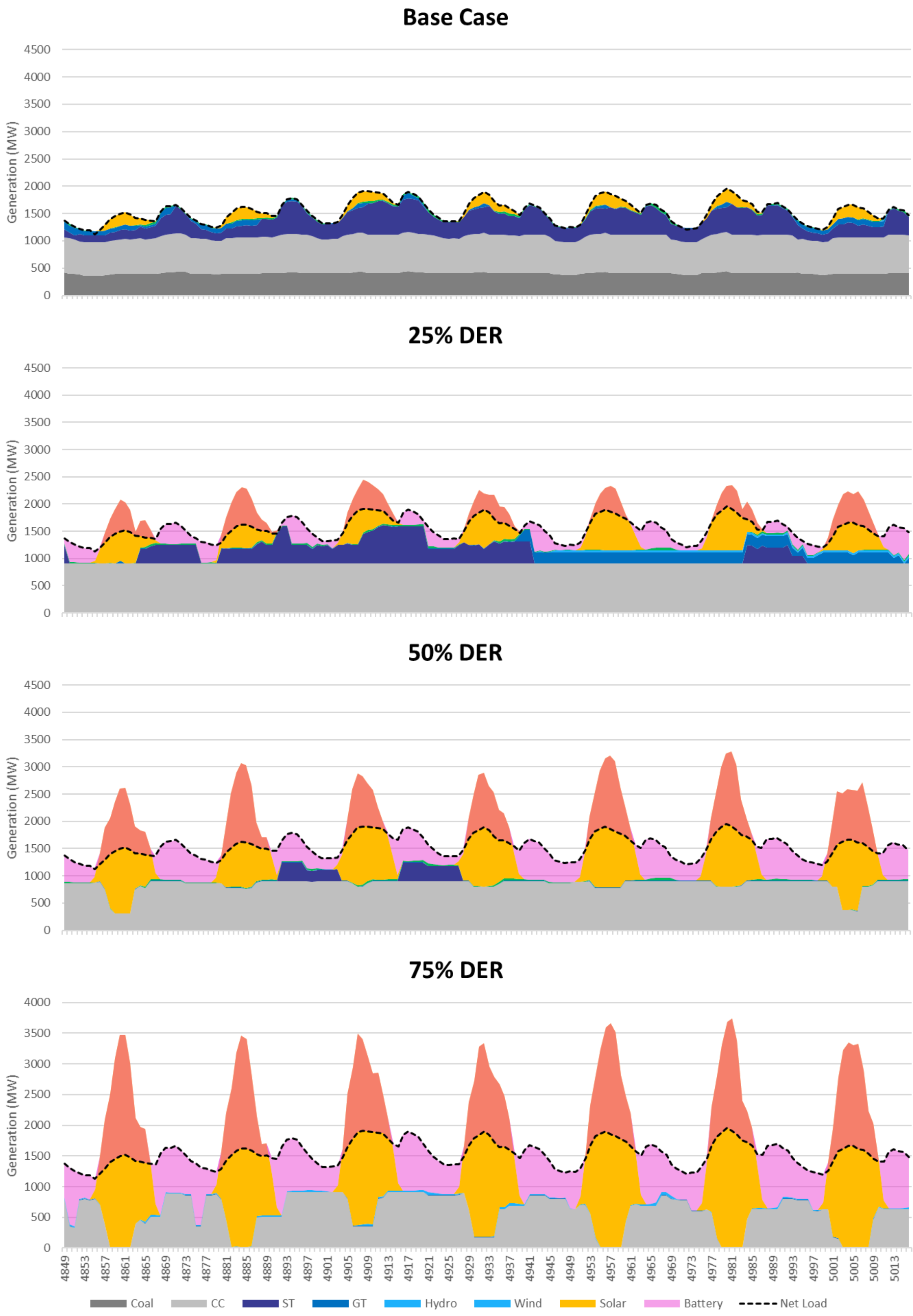

Figure 65: Dispatch Diagram, Representative Average Week (July 22)

`

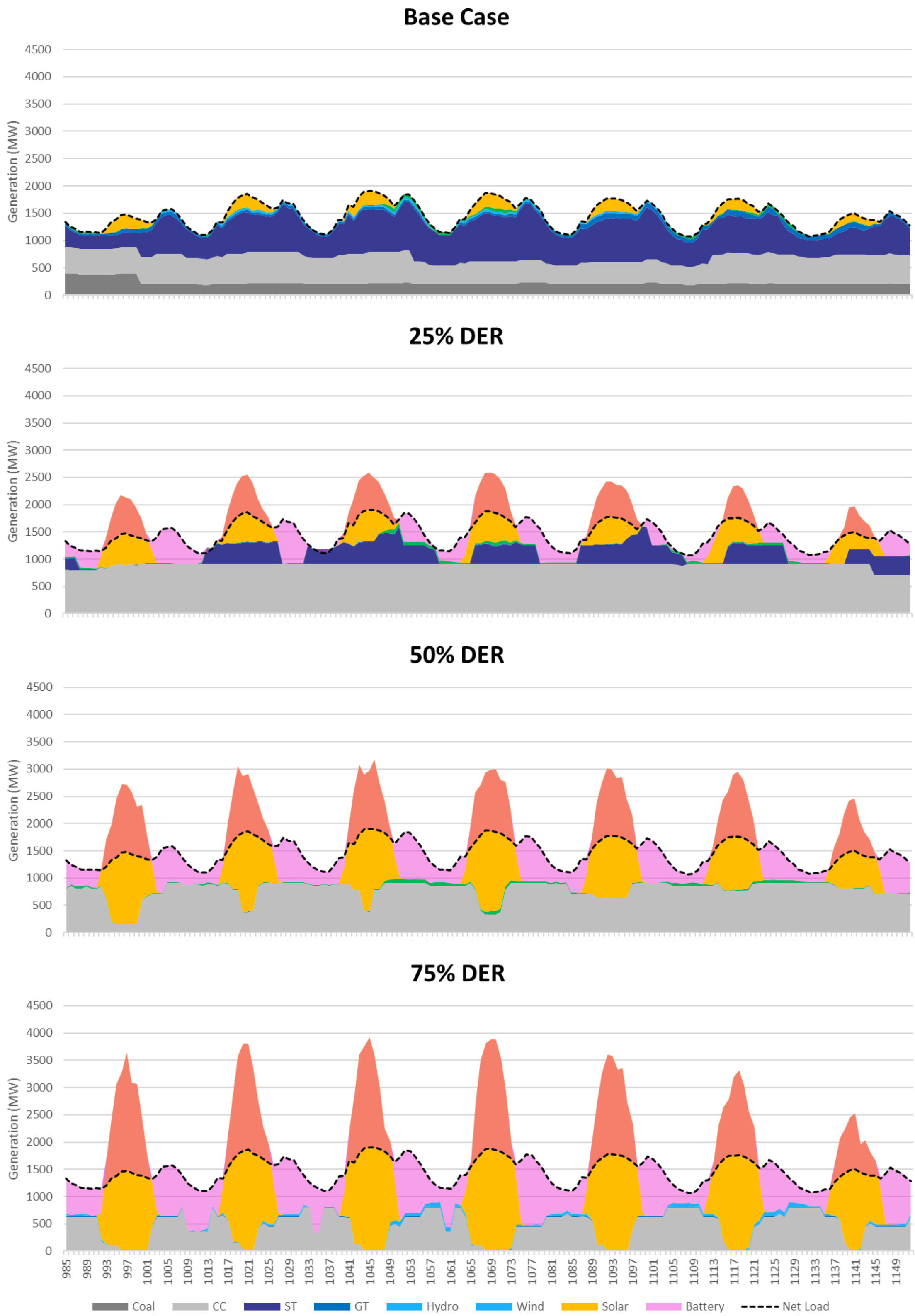

Figure 66: Dispatch Diagram, Minimum Demand (Feb 11)

`

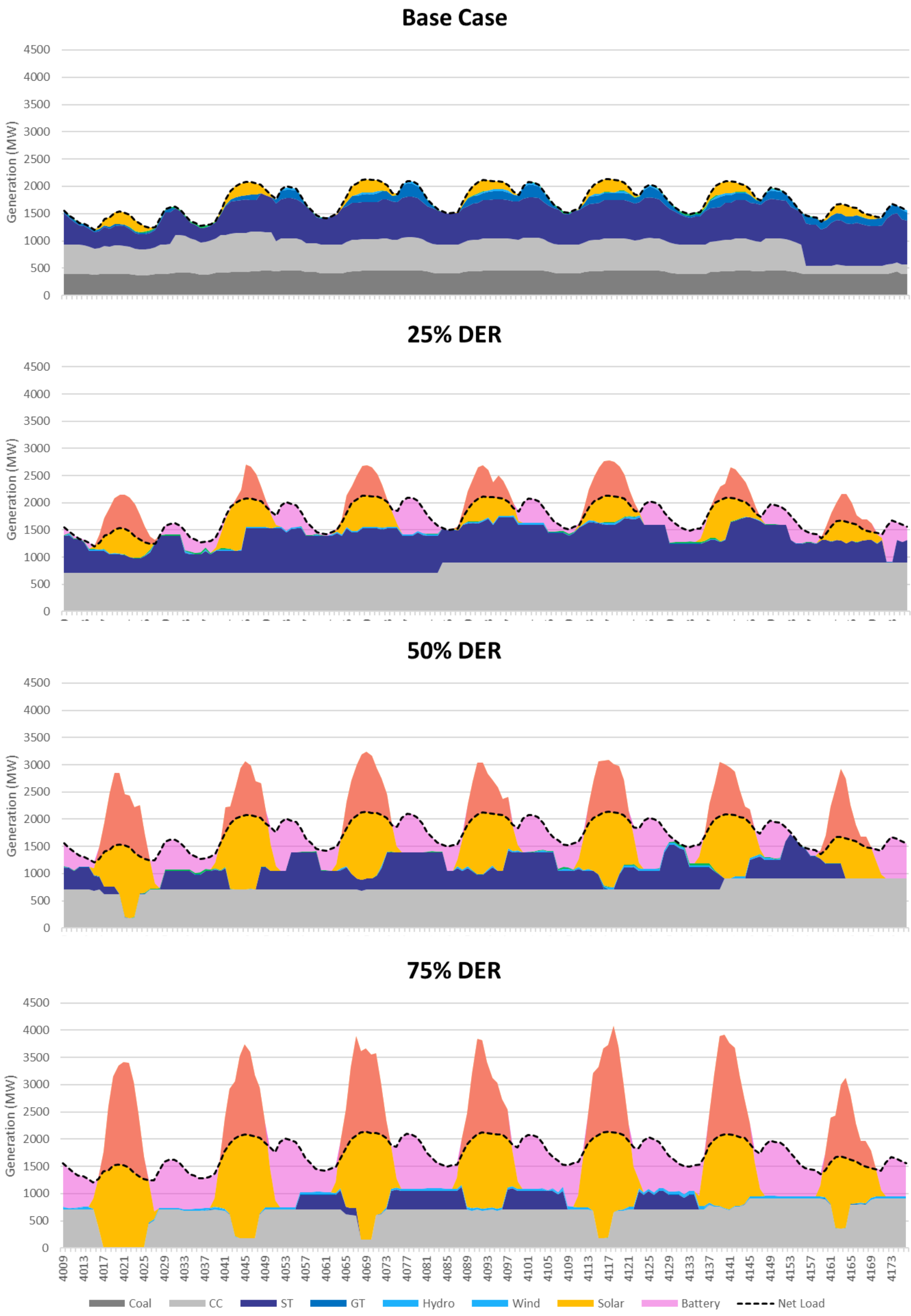

Figure 67: Dispatch Diagram, High Demand Period (June 17)

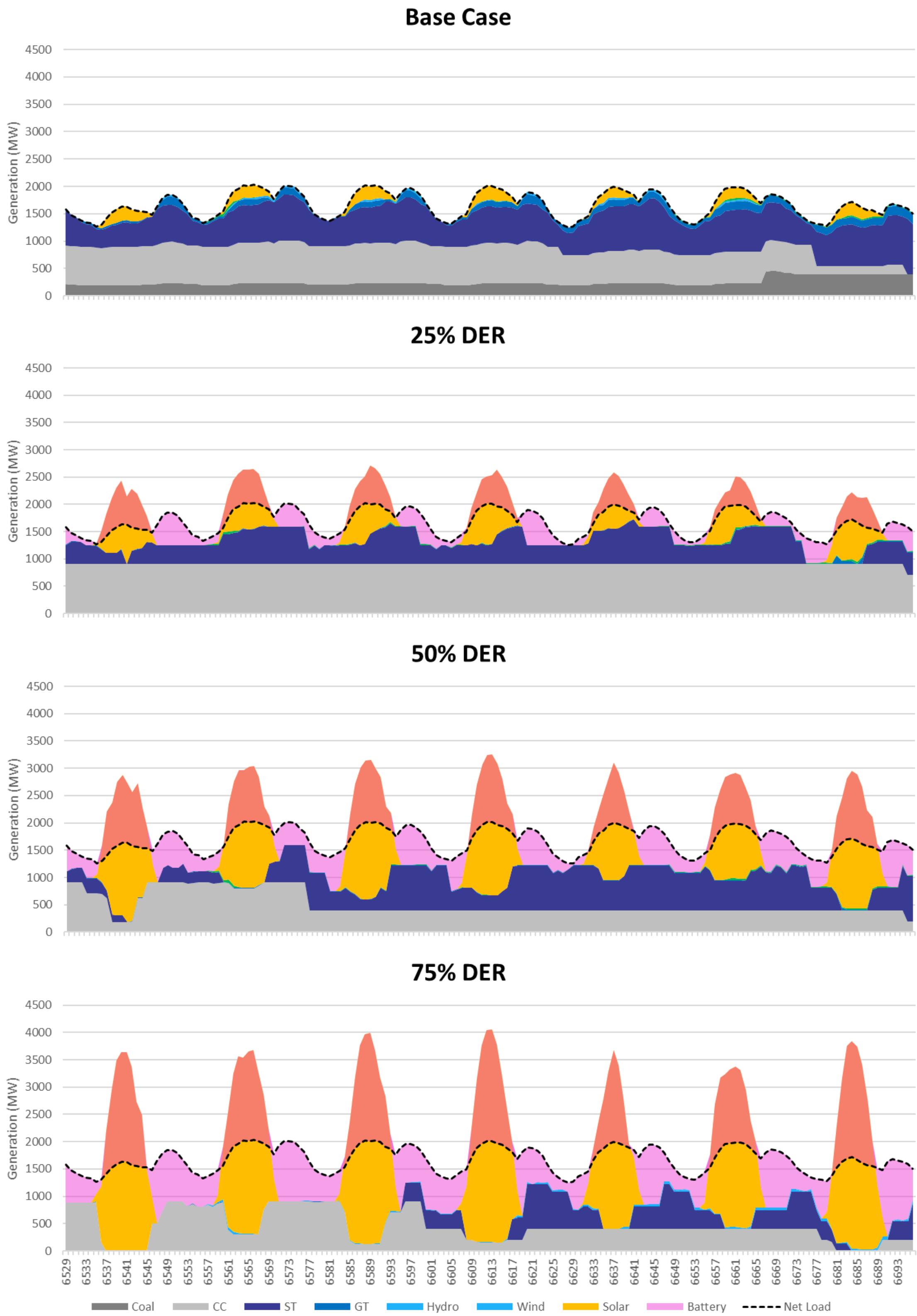

Figure 68: Dispatch Diagram, High Renewables Generation (Sept 30)

`

Table 22: Annual Fuel Consumption and Emissions

		Base Case	25% DER	50% DER	75% DER
Consumption (MMBtu)	Coal	30,095,500	-	-	-
	Oil	28,868,900	24,086,510	19,235,470	12,613,700
	Gas	58,462,330	65,887,810	44,084,710	27,454,930
Consumption (fuel type units)	Coal (short tons)	1,544,151	-	-	-
	Oil (bbls)	4,884,857	4,146,285	3,326,911	2,182,950
	Gas (BCF)	58.46	65.89	44.08	27.45
Carbon Dioxide Emissions (tons)	Coal	3,095,319	-	-	-
	Oil	1,916,469	1,454,400	1,129,674	738,118
	Gas	3,420,044	3,854,435	2,578,960	1,606,115
	Total	8,431,833	5,308,834	3,708,634	2,344,233
Change from Base Case					
Consumption (MMBtu)	Coal		(30,095,500)	(30,095,500)	(30,095,500)
	Oil		(4,782,390)	(9,633,430)	(16,255,200)
	Gas		7,425,480	(14,377,620)	(31,007,400)
Consumption (fuel type units)	Coal (short tons)		(1,544,151)	(1,544,151)	(1,544,151)
	Oil (bbls)		(738,572)	(1,557,946)	(2,701,907)
	Gas (BCF)		7	(14)	(31)
Carbon Dioxide Emissions (tons)	Coal		(3,095,319)	(3,095,319)	(3,095,319)
	Oil		(462,069)	(786,795)	(1,178,351)
	Gas		434,391	(841,085)	(1,813,929)
	Total		(3,122,998)	(4,723,199)	(6,087,600)
Percent Change from Base Case					
Consumption (MMBtu)	Coal		-100%	-100%	-100%
	Oil		-17%	-33%	-56%
	Gas		13%	-25%	-53%
Consumption (fuel type units)	Coal (short tons)		-100%	-100%	-100%
	Oil (bbls)		-15%	-32%	-55%
	Gas (BCF)		13%	-25%	-53%
Carbon Dioxide Emissions (tons)	Coal		-100%	-100%	-100%
	Oil		-24%	-41%	-61%
	Gas		13%	-25%	-53%
	Total		-37%	-56%	-72%